AN ABSTRACT OF THE DISSERTATION OF

Rex A. Cole for the degree of Doctor of Philosophy in Molecular and Cellular Biology presented on March 21, 2008

Title: An Emerging Role for the Exocyst: Plant Morphogenesis

Abstract approved:

_____

John E. Fowler

Plants develop a vast array of cell shapes and sizes by selectively modifying their surrounding cell walls to expand in some regions and not in others. This process of morphogenesis requires the delivery of secretory vesicles to specific locations at the cell periphery, where exocytosis adds new membrane and proteins to the plasma membrane, and secretes materials to build and modify the cell wall. In yeast and mammals, the process of localized exocytosis has been found to involve an eight protein complex, the exocyst. Prior to my work, genes encoding all eight components of the exocyst had been identified in sequenced plant genomes, but no function had yet been determined for any of them. Utilizing T-DNA insertion mutants of putative exocyst components in *Arabidopsis thaliana*, I demonstrated that one component, SEC8, is required for pollen germination and competitive pollen tube growth. Subsequently, through genetic analyses, phenotypic observation, and cell biological experiments, I provided evidence that, combined with biochemical studies by my collaborators, demonstrated that the putative exocyst components function together as a complex (or complexes) in plants. Multiple components of the exocyst all localize to the tips of growing pollen tubes, the site of localized exocytosis, and strong mutations in exocyst components result in the formation of pollen tubes that are shorter and wider than wild-type. Exocyst mutants also have both an etiolated hypocotyl elongation defect and a root growth defect in the vegetative plant. Unexpectedly, characterization of these mutant plants implicated the exocyst for a role in phytohormone signaling, specifically, in the efficient reception of brassinosteroid signals. This work firmly establishes that the exocyst complex functions

in plants to affect plant morphogenesis in at least three developmental processes: polarized growth in pollen tubes, cell elongation in etiolated hypocotyls, and both cell division and cell elongation in growing roots. It also links the exocyst with at least two brassinosteroid -mediated developmental pathways. Finally, it strongly suggests that the exocyst also has a role in defining the cell elongation zone in roots, with exocyst mutants showing that the establishment of this zone can be disconnected from establishment of the root meristem.

An Emerging Role for the Exocyst: Plant Morphogenesis

by
Rex A. Cole

A DISSERTATION
submitted to
Oregon State University

in partial fulfillment of
the requirements for the
degree of
Doctor of Philosophy

Presented March 21, 2008
Commencement June 2008

Doctor of Philosophy dissertation of Rex A. Cole

presented on March 21, 2008

APPROVED:

Major Professor, representing Molecular and Cellular Biology

Director of the Molecular and Cellular Biology Program

Dean of the Graduate School

I understand that my dissertation will become part of the permanent collection of Oregon State University libraries. My signature below authorizes release of my dissertation to any reader upon request.

Rex A. Cole, Author

ACKNOWLEDGEMENTS

The author expresses everlasting gratitude to his devoted and amazing wife, Cynthia J. Cole, who loved long, sacrificed often, complained little, and contributed much to his health, happiness, and sanity during the completion of this work. She is most certainly a partner in this effort, for it could not have been completed without her.

A special thanks to Zuzana Vejlupkova for friendship and tireless assistance in the lab; to Maria Ivanchenko for valuable discussions with the author on phytohormones, GUS staining, and the scheduling of lunch; and to a long list of hard-working undergraduate students who helped maintain, genotype, and harvest an endless number of Arabidopsis plants for the genetic studies that were integral to this research, including: J. McElravy, J. Hines, P. Staiger, M. Frederick, S. Ma, N. Snyder, L. Snyder, and H. Pham. Finally, thanks to my committee members, John Fowler, Theresa Filtz, Carol Rivin, Dahong Zhang, and Matthew Cannon; they were the nicest firing squad I could ever hope to face.

CONTRIBUTIONS OF AUTHORS

The author thanks Dr. John E. Fowler for his many ideas, thoughtful critiques, and helpful discussions which contributed to the completion of all aspects of this dissertation, and the author's survival of graduate studies. Chapter 2 of this dissertation is a published journal article for which I am first author, while Lukas Synek and Viktor Zarsky contributed the concept of Figure 1.1 and provided useful critiques of the manuscript for which they were listed as co-authors. The author shares first co-authorship with Michal Hala on the manuscript that composes Chapter 3 of this dissertation. Additional co-authors on this manuscript were Lukas Synek, Edita Drdova, Tamara Pecenkova, Alfred Nordheim, Tobias Lamkemeyer, Johannes Madlung, Frank Hochholdinger, John Fowler and Viktor Zarsky. Specifically, Michal Hala, Alfred Nordheim, Tobias Lamkemeyer, Johannes Madlung, and Frank Hochholdinger, provided all the biochemistry work reported in chapter 3, including Figures 3.4, 3.5, 3.6, and 3.7; Lukas Synek contributed the majority of the data related to exocyst localization in pollen, including Figure 3.3, although I assisted with the Sec8 immunolocalization; and Edita Drdova assisted with the collection of quartet pollen germination data. All collaborators provided editorial input, but Michal Hala, a first co-author on the Chapter 3 manuscript, as well as Lukas Syndek, Viktor Zarsky, and John Fowler contributed significantly to its writing, estimated at 50 percent of the Introduction and Discussion, as well as the vast majority of all the biochemistry sections and all of the biochemistry method descriptions. Michael Nesson at the OSU Electron Microscopy Facility assisted extensively with the TEM and associated sample preparation reported in both Chapters 2 and 4. The author also thanks Zach Dunn, a high school Apprentice in Science and Engineering student, who made most of the hypocotyl elongation measurements and initial data analysis reported in Figures 4.11, 4.13, and 4.14.

TABLE OF CONTENTS

TABLE OF CONTENTS (Continued)

LIST OF FIGURES

LIST OF FIGURES (Continued)

LIST OF TABLES

AN EMERGING ROLE FOR THE EXOCYST: PLANT MORPHOGENESIS

CHAPTER 1

Introduction

Plant cells and the organs they compose are found in a dazzling array of shapes and sizes tailored to the specific functions each must serve. Each cell develops its distinctive morphology by selectively modifying its surrounding cell wall to expand in some regions and not in others. The mechanism by which this is achieved is intimately linked to cell's the endomembrane system and the process of exocytosis. Within the endomembrane system, the endoplasmic reticulum and Golgi serve as reaction vessels for the synthesis and processing of components that will be used to build and modify both the plasma membrane and cell wall. Transport between the compartments of the endomembrane system occurs via membrane bound vesicles that form from the membrane of one compartment, are released into the cytosol, and then move to and merge with their target membranes. Of particular importance to plant cell morphogenesis is the delivery of golgi-derived secretory vesicles to specific locations at the cell periphery, where fusion of the vesicles with the plasma membrane, i.e. exocytosis, adds new membrane and proteins to the plasma membrane, and secretes materials to build and modify the cell wall.

Vesicle traffic through the endomembrane system and to the plasma membrane of eukaryotic cells is facilitated by tethering factors (reviewed in Cai, 2007; Sztul, 2006). After a vesicle buds from one membrane compartment and has moved towards another by diffusion or along a cytoskeletal track, tethering factors act as "molecular bridges" that provide an initial interaction between the vesicle and its target membrane. This tethering occurs prior to the pairing of SNAREs (soluble N-ethylmaleimide-sensitive attachment protein receptors), which are on both the vesicle and target membranes, and appear to be the central facilitators of fusion of the two membranes (Chen and Scheller, 2001). In addition to assisting the positioning of the vesicle at the membrane, tethering factors in combination with Rab GTPases (small GTPases of the Ras superfamily) may help determine the specificity of vesicle targeting within the cell. Two general types of tethering factors are recognized, long putative coiled-coil proteins generally occurring as dimers, and large multi-subunit protein complexes (e.g., the exocyst, COG, GARP, HOPS, TRAPPI and TRAPPII complexes). Of these, the targeting and tethering of

Golgi-derived secretory vesicles to the plasma membrane is associated specifically with an eight-protein complex that has been named the exocyst.

The exocyst has been extensively studied in yeast and mammals (reviewed in Hsu et al., 2004) and shown to play an essential role in a broad range of cellular processes that depend upon exocytosis. The exocyst is required for the extensive growth associated with budding in *Sacharomyces cerevisea* (TerBush and Novick, 1995), the maintenance of tip growth required for hyphal morphogenesis of *Candida albicans* (Li, et al., 2007), the outgrowth of cultured neurites (Hazuka et al., 1999; Pommereit and Wouters, 2007), and is associated with the membrane trafficking to the leading edge of migrating mammalian epithelial cells (Rosse et al., 2006; Zuo et al. 2006). In fission yeast and animal cell cultures, the exocyst is required in the late stages of cytokinesis, possibly facilitating vesicle delivery to the centrosome-related abscission site (Wang et al., 2002; Chen et al. 2006; Krasinska et al., 2007). In animal cells, the exocyst facilitates the targeting and/or recycling of specific proteins to the plasma membrane, such as the transferrin receptor in murine reticulocytes (Garrick and Garrick, 2007), the Glut4 glucose transporter in adipocytes (Inoue, et al., 2003; Chen et al., 2007), AMPA-type glutamate receptors in postsynaptic neuronal membranes (Sans, et al., 2003; Gerges et al., 2006), and specific proteins to either the basolateral or apical membrane of epithelial cells (Yeaman et al., 2001; Oztan et al., 2007; Blankenship et al., 2007).

This impressive but non-exhaustive list suggests that although the exocyst may not be required for every instance of exocytosis (e.g. the exocyst is not required for secretion of neurotransmitters, Murthy et al., 2003, Gerges et al., 2006), it becomes essential in certain situations. Specifically, the exocyst appears to be required when physiological or developmental circumstances demand extensive exocytosis to support rapid polarized growth, or when secretion and membrane cycling must be tightly controlled, both spatially and temporally, to regulate the localized placement of specific plasma membrane proteins.

Comparative genomic and phylogenetic analysis across 17 eukaryote genomes suggests that the exocyst, like the other tethering complexes, is ancient, originating very

early in eukaryotic evolution (Koumandou et al., 2007). In both yeast and mammals, the exocyst complex consists of eight subunits: Sec3, Sec5, Sec6, Sec8, Sec10, Sec15, Exo70, and Exo84 (TerBush et al., 1996; Hsu et al., 1996; Guo et al., 1999b; Matern et al., 2001). Systematic *in silico* surveys have revealed that plants have homologs to all eight exocyst subunits (Cvrckova et al., 2001; Elias et al., 2003; Jurgens and Geldner, 2002). The genome of *Arabidopsis thaliana* contains single copies of genes encoding Sec6 and Sec8, two copies each for Sec3, Sec5, Sec10 and Sec15, three copies for Exo84, and a remarkable 23 copies encoding Exo70 homologs. The research reported here began shortly after homologs for exocyst components had been identified in *Arabidopsis*, and before anyone had yet identified a functional role for the exocyst or any of its components in plants.

The potential existence of a functioning plant exocyst, a previously unrecognized component in the plant secretory pathway affecting such a fundamental process as exocytosis, presented an enticing research opportunity. Clearly, the exocyst serves vital functions in non-plant eukaryotic species, but did it serve similarly important roles in plants? If it did, then understanding exocyst function might ultimately provide new insights into currently unsolved mysteries in plant growth and development. Motivated by the exciting possibilities, and buoyed by delusions of grandeur, I proceeded to explore the function of the exocyst in plants. The results of these investigations comprise the three main chapters of this thesis.

At the onset of my research, the most established role for the exocyst was in the polarized growth associated with reproductive budding in *Sacharomyces cerevisea* (Hsu et al., 2004; TerBush and Novick, 1995). There was evidence of exocyst localization to the site of budding (Finger et al., 1998), and exocyst mutants demonstrated arrested bud formation coincident with the accumulation of secretory vesicles (Guo et al., 1999). These observations shaped my initial working hypothesis, that the exocyst is required for polarized plant cell growth. The most obvious example of polarized growth in plants is the tip-growth observed in pollen tubes and root hairs, which has a well-characterized requirement for intense and focused exocytosis. Trichomes and the intercalated borders

between leaf epidermal cells provide additional examples of localized plant cell expansion. These were considered sites that might reveal a function for the exocyst in plants, and that might provide a model for testing my hypothesis that the exocyst functions in polarized plant cell growth.

An analysis of mutants with T-DNA insertions in genes encoding exocyst components ultimately led to the identification of a role for the *SEC8* gene in *A. thaliana*. As described in chapter two, *SEC8* is required for the polarized growth associated with pollen germination and pollen tube growth (Cole, et al., 2005). Almost simultaneously, other labs reported roles for other exocyst components. In maize, a transposon insertion into a *SEC3* homolog results in the *roothairless1* mutation, causing the failure of root hairs to elongate properly (Wen et al., 2005). In Arabidopsis, *exo70A1* mutants were also shown to exhibit a short root hair phenotype, as well as other defects in cell growth (e.g., hypocotyl elongation), and a reduced cell number (Synek et al., 2006). I subsequently hypothesized that the exocyst is a component of an interconnected network of signalling pathways, which I named the tip growth LENS (for Localization Enhancing Network, Self-sustaining), that functions in the focusing of polarized tip growth of both pollen tubes and root hairs (Cole and Fowler, 2006).

My next investigations sought to determine if the exocyst components identified in plants function as a complex. Through genetic analyses, phenotypic observations, and cell biological experiments I provided strong evidence in support of the exocyst as a functioning complex in plants. In this effort I was aided by collaboration with the Viktor Zarsky lab at the Institute of Experimental Botany, Academy of Sciences of the Czech Republic, who provided the essential biochemical evidence for the complex. The results of our joint effort are described in chapter three, concluding that the exocyst does indeed function as a complex in plants (submitted for publication, Hala, Cole, et al., 2008). These studies helped further define the role of the exocyst in pollen tube tip growth, indicating that the exocyst is required for maintaining efficient and focused tip growth, but is not strictly essential for establishing polarity in that growth.

In the course of my work with *sec8* mutants, it was revealed that severe mutant alleles are associated with extreme dwarfism when homozygous in the sporophyte (i.e., the vegetative plant). Two characteristics of this dwarfism were particularly intriguing because they represent two different developmental processes, neither of which resembles the tip-growth of pollen tubes or root hairs. First, the exocyst dwarfs demonstrate a severely reduced hypocotyl elongation when grown in the dark, a process that is known in wild-type plants to depend almost entirely on cell elongation. Second, the exocyst dwarfs demonstrate significantly slower primary root growth than wild-type, a process that depends both on cell division and cell elongation. A detailed phenotypic characterization of these two types of growth in exocyst mutants substantiated the role of the exocyst in multiple developmental processes, helped define potential sites for study of the exocyst at the molecular level, exposed a developmental switch in the formation of the root's elongation zone, and unexpectedly provided a promising link of the exocyst to brassinosteroid signalling. These results are the subject of chapter four.

Overall, this work has advanced our understanding of the exocyst in plants, and its function in multiple developmental pathways affecting plant morphogenesis. Furthermore, it has set the stage for additional research that may indeed echo my naïve initial vision: using the exocyst to provide new insights into currently unsolved mysteries in plant growth and development.

CHAPTER 2

SEC8, A Subunit of the Putative *Arabidopsis* Exocyst Complex, Facilitates Pollen Germination and Competitive Pollen Tube Growth

Authors: Rex A. Cole, Lukás Synek, Viktor Zarsky, John E. Fowler

Published in: *Plant Physiology*

American Society of Plant Biologists, Dartmouth Journal Services, Waterbury,VT

August 2005, Vol. 138, pp 2005-2018

2.1 ABSTRACT

The exocyst, a complex of eight proteins, contributes to the morphogenesis of polarized cells in a broad range of eukaryotes. In these organisms the exocyst appears to facilitate vesicle docking at the plasma membrane during exocytosis. Although we had identified orthologs for each of the eight exocyst components in *Arabidopsis thaliana*, no function has been demonstrated for any of them in plants. The gene encoding one exocyst component ortholog, At*SEC8*, is expressed in pollen and vegetative tissues of *A. thaliana*. Genetic studies utilizing an allelic series of six independent T-DNA mutations reveal a role for *SEC8* in male gametophyte function. Three T-DNA insertions in *SEC8* cause an absolute, male-specific transmission defect that can be complemented by expression of *SEC8* from the *LAT52* pollen promoter. Microscopic analysis shows no obvious abnormalities in the microgametogenesis of the *SEC8* mutants, and the mutant pollen grains appear to respond to the signals that initiate germination. However, *in vivo* assays indicate that these mutant pollen grains are unable to germinate a pollen tube. The other three T-DNA insertions are associated with a partial transmission defect, such that the mutant allele is transmitted through the pollen at a reduced frequency. The partial transmission defect is only evident when mutant gametophytes must compete with wild-type gametophytes, and arises in part from a reduced pollen tube growth rate. These data support the hypothesis that one function of the putative plant exocyst is to facilitate the initiation and maintenance of the polarized growth of pollen tubes.

2.2 INTRODUCTION

Asymmetrical growth and development in eukaryotic cells is established through localized cell expansion driven by polarized exocytosis/endocytosis. Golgi-generated secretory vesicles are delivered to a specific region of the plasma membrane, where their fusion with the plasma membrane results in the incorporation of new membrane lipids and proteins to that region. In many organisms, polarized exocytosis has been found to require the involvement of a protein complex known as the exocyst (reviewed in Hsu et al., 2004). The exocyst (first described by TerBush et al., 1996) is composed of eight

proteins: Sec3, Sec5, Sec6, Sec8, Sec10, Sec15, Exo70 and Exo84, most of which were initially identified as temperature-sensitive secretory mutants of the budding yeast, *Saccharomyces cerevisiae* (reviewed in Schekman and Novick, 2004). In *S. cerevisiae,* mutation of any one of the exocyst components leads to arrested formation of the polarly-growing bud, and the accumulation of secretory vesicles (TerBush et al., 1996; Guo et al., 1999). Orthologs for genes encoding all eight of the exocyst components have subsequently been identified in a growing number of eukaryotes, and implicated in a variety of cellular processes involving polarized exocytosis. For example, the exocyst is associated with neurite outgrowth in neurons from *Drosophila melanogaster* (Murthy et al., 2003), and in differentiated PC12 cells (Vega and Hsu, 2001). In cultured Swiss 3T3 fibroblasts, the exocyst mediates filopodia formation induced by the GTPase RalA and tumor necrosis factor-ϙ(Sugihara et al., 2002). In adipocytes, the exocyst is implicated in the targeted exocytosis of the glucose transporter to the plasma membrane in response to insulin (Inoue et al., 2003). In general, the exocyst appears to be involved in polarized exocytosis to regions of the plasma membrane experiencing rapid polarized growth, or requiring tightly controlled delivery of specific membrane components. On the basis of subcellular localization and molecular associations, it has been proposed that the exocyst functions as a tethering protein complex, targeting incoming secretory vesicles to specific sites on the plasma membrane prior to the docking and fusion events mediated by SNARES (Pfeffer, 1999; Whyte and Munro, 2002; Hsu et al., 2004).

Orthologs for genes encoding all components of the exocyst have been identified in *Arabidopsis thaliana* (Jurgens and Geldner, 2002; Elias et al., 2003) and *Oryza sativa* (Cole, Fowler; Synek and Zarsky, unpublished observations), suggesting the existence of a plant exocyst. The genome of *A. thaliana* contains single copies of genes for Sec6, Sec8, and Sec10, two copies each of Sec3, Sec5, and Sec15, three copies of Exo84, and a remarkable 23 copies of Exo70. However, a demonstrated functional role for the exocyst or any of its components in plants has not been reported. The most dramatic example of polarized growth in plants is the tip growth observed in root hairs and pollen tubes (reviewed in Fowler and Quatrano, 1997; Hepler et al., 2001; Feijo et al., 2004), making

these likely sites for exocyst activity. Tip growth requires the rapid delivery of secretory vesicles to the specific region on the membrane where growth of new membrane is focused. Pollen tube tip growth also involves the localization and recycling of membrane components, such as ion channels, and possibly receptors, to the tip via endocytosis and exocytosis. The precise location of growth at the tip is essential to the guidance of the pollen tube from the stigma, through the transmitting tract of the style, and ultimately to the ovule where fertilization occurs. Such directed tip growth involves a complex interplay of signaling pathways, most notably involving ROP GTPases and calcium (Li et al., 1999; Camacho and Malho, 2003; and reviewed in Yang, 2002; Feijo et al., 2004; Gu et al., 2004). The exocyst could conceivably provide a target for regulation of this directed growth. It was therefore noteworthy when we identified a T-DNA mutant of the *A. thaliana SEC8* homolog (protein alignment in Supplemental Figure 1) with a defect affecting transmission of the mutant allele through the pollen.

The study of Sec8 orthologs has played a key role in establishing functional roles for the exocyst in non-plant species. In MDCK epithelial cells, Sec8 localization studies (Yeaman et al., 2004), combined with studies in which anti-Sec8 antibodies disrupt protein targeting (Grindstaff et al., 1998), have supported a role for the exocyst in the targeting of proteins to the baso-lateral, but not the apical plasma membrane. In heterologous cells and neurons, over-expression of a mutant Sec8 resulted in decreased NMDA (N-methyl-D-aspartate) receptor mediated current and surface expression, indicating that the exocyst may be involved in the delivery of these neurotransmitter receptors to the plasma membrane (Sans et al., 2003). Finally, in cultures of embryonic hippocampal neurons, immunofluorescent labeling of Sec8 and Sec6 have implicated the exocyst in the process of neurite outgrowth (Hazuka et al., 1999), supporting the conclusion reached by the study of other exocyst components (Vega and Hsu, 2001; Murthy et al., 2003). Thus, there is a precedent for focusing on Sec8 as an experimental handle for investigating the function of the entire complex. In addition, the examples highlighting the role of Sec8 in neurons are of particular interest because of the many parallels between the targeted growth of pollen tubes to the ovule, and the directed growth of axons to neural synapses (Palanivelu and Preuss, 2000). A demonstrated

function for *SEC8* in *A. thaliana* would provide a first step in exploring the role of the exocyst in plants.

We therefore used T-DNA insertional mutations of At*SEC8* to test the hypothesis that the exocyst is involved in tip growth in plants. We focused our attention on pollen, i.e. the male gametophyte. The germination of the pollen grain to form a pollen tube, and the growth of the pollen tube are both processes that could in theory involve the exocyst. Additionally, we considered the possibility that the putative plant exocyst could be involved in cytokinesis during microgametogenesis. Ultimately, our genetic and microscopic studies revealed that At*SEC8* is required for both pollen germination and competitive pollen tube growth, supporting our hypothesis.

2.3 RESULTS

At*SEC8* is expressed in pollen and can be investigated using reverse genetics

Recent microarray expression analyses have explored the pollen transcriptome in *Arabidopsis* at various stages of pollen development (Honys and Twell, 2004). Transcripts for all components of the putative exocyst, including At*SEC8*, were found in pollen or the developing male gametophyte (Figure 2.1), a requisite condition for exocyst function in pollen. Further analyses of microarray data from additional experiments demonstrated that transcripts for all eight components were widely distributed in vegetative tissues, raising the possibility that the putative plant exocyst functions in diverse developmental contexts. Intriguingly, some of the highest expression levels for these genes were in cells in suspension culture, an actively dividing state. Exocyst components encoded by multiple genes were expressed differentially, with certain gene family members predominating in pollen (e.g., At*SEC15a*, three of the At*EXO70* genes). Notably, the At*SEC8* transcript was detectable throughout pollen development: in uninucleate microspores following meiosis, in bicellular and tricellular pollen following the subsequent two mitotic divisions, and finally in the mature pollen grain.

We focused our attention on the large, single copy At*SEC8* gene (hereafter referred to simply as *SEC8*) to begin testing the hypothesis that the plant exocyst is crucial for polarized plant cell growth, specifically the growth of the pollen tube. We

employed a reverse genetics approach, searching the Salk collection (Alonso et al., 2003) to obtain six T-DNA insertional mutant lines in the gene. The location and insertional nature of each T-DNA mutation was verified by sequencing from both T-DNA borders (Figure 2.2A). Amino acid sequences predicted from assembled EST contigs for a number of plant species show a high degree of conservation in a region likely to form a series of alpha helices, which were also predicted to be interrupted by the insertion mutations (Figures 2.2B). Conservation fell off in the short region between *-m3* and the other three insertions (Supplemental Figure 2).

Mutations in *SEC8* cause a male-specific transmission defect

A phenotype for the *SEC8* mutants was revealed when genetic studies showed that the mutant alleles were not transmitted to progeny in the expected Mendelian ratios (Table I). Genotyping for individual plants in the progeny populations was achieved by PCR (see Figure 2.3E), using sets of primers annealing to DNA within the insert (i.e., the T-DNA sequence) and on either side of the insertion site. Self-crosses of plants heterozygous for the *sec8-m1*, *-m2*, or *-m3* alleles failed to produce homozygous mutant progeny (Table 2.1). To determine if the defect was due to a problem in male and/or female gametogenesis, reciprocal outcrosses were performed between plants heterozygous for each mutant *SEC8* allele and wild-type Columbia-0 plants. When wild-type pollen was used to pollinate the stigma of a *SEC8* heterozygote, the progeny demonstrated the expected 1:1 Mendelian ratio of heterozygotes to wild-type homozygotes for all six mutant alleles (Table 2.1). Thus no detectable defect was associated with mutation of *SEC8* in the female gametophyte.

In contrast, a strong male-specific transmission defect was evident in the reciprocal outcrosses. When the pollen of a mutant heterozygote was used on a wild-type stigma, there were significantly fewer heterozygotes in the progeny than predicted by Mendelian genetics (Table 2.1). For the *-m1*, *-m2*, and *-m3* alleles, the transmission defect was absolute, and the mutant allele never appeared in the progeny (combined n = 326). Interestingly, even though we had not detected a transmission defect in the self-crossed progeny, the *-m4*, *-m5*, and *-m6* alleles all demonstrated a partial male-specific

transmission defect when outcrossed, with the mutant allele appearing at frequencies of 18%, 22%, and 31%, respectively. The transmission defect was maintained through at least three generations for each allele. These data argued strongly for an important functional role for *SEC8* in the male gametophyte.

When the six mutant alleles were compared, it was notable that the transmission defect became less severe as the site of the insertion got closer to the 3' end of the gene. The differences in phenotypic severity among the six alleles raised the possibility that the three 5'-most insertions generated null alleles, whereas the three other insertions, located in a relatively small region in the 3' end of the gene, were associated with partially-functional (hypomorphic) alleles. In this scenario, truncated transcripts from the hypomorphic alleles should be detectable in plants homozygous for the *sec8-m4*, *-m5*, and *-m6* alleles. To test this, and to confirm the microarray expression data, we initially conducted RT-PCR on RNA samples from several wild-type tissues. *SEC8* transcript was detectable in all samples tested, including RNA from pollen (Figure 2.3A). We then utilized two different primer pairs, one located at the extreme 3' end and another further 5', producing products designated B and A, respectively (Figure 2.3B), to evaluate the presence of truncated transcripts in plants homozygous for the *sec8-m4*, *-m5*, or *-m6* allele. As predicted, RT-PCR using the 5'-most primer pair on immature floral tissue samples from the mutants produced a PCR product of the same size as that obtained for wild-type plants. However, no PCR product was detected when primers located on opposite sides of the insertion sites were used on the same samples, as might be expected for truncated transcripts (Figure 2.3C, D). To confirm the presence of the truncated transcripts, PCR products were amplified from each hypomorph, using a 5' *SEC8* primer along with a T-DNA-annealing primer, and sequenced. Each allele produced a transcript comprised of truncated *SEC8* sequence fused to a portion of the T-DNA sequence at the 3' end. Using these sequences, we predicted that the *-m4*, *-m5*, and *-m6* mutations alter the C-terminus of the wild-type protein by truncating it by 70, 63, or 45 amino acids respectively, and by adding 16, 15, or 25 amino acids translated from the T-DNA sequence (Figure 2.2A, Supplemental Figure 3 online).

We could not definitively test whether *sec8-m1, -m2, -m3* produced transcripts because we could not generate homozygotes for these three putative null *SEC8* alleles. However, no PCR products were detected in attempts to isolate truncated transcripts containing T-DNA sequences from plants heterozygous for these alleles (data not shown). Additional data supporting the idea that the three 5'-most insertions were null alleles were obtained from male outcrosses of a *sec8-m3*/*sec8-m4 trans*-heterozygote. Even when in the environment of reduced pollen competition provided by the partial *-m4* allele (see below), we never saw transmission of the *-m3* allele through the pollen (n = 98 progeny).

To verify that the transmission defect was indeed due to mutation of *SEC8*, and not a tightly-linked but unrelated mutation, a complementation experiment was performed. A construct containing the wild-type *SEC8* coding sequence driven by the pollen-specific *LAT52* promoter (Twell et al., 1991), as well as a promoter-only control, was transformed into *sec8-m3* heterozygotes (associated with an absolute transmission defect – Figure 3E). Six independent transformants were obtained, and pollen from these plants was outcrossed to wild type. Five of the six *LAT52::SEC8* transformants demonstrated complete complementation, with *sec8-m3* heterozygotes appearing in the hygromycin-resistant progeny at the expected Mendelian ratio (n = 121 plants, $\chi^2 = 1.86$, $p < 0.25$) (Figure 2.3F). As an internal control, twenty-six sibling progeny lacking the construct were also genotyped, and, as expected, revealed no heterozygotes. Additionally, transformation with a promoter-only control did not complement the transmission defect in *sec8-m3* heterozygotes (two transformant lines, 37 plants). Thus, we concluded that the transmission defect associated with the *sec8-m3* allele was complemented by a pollen-expressed *SEC8*, confirming that the transmission defect was caused by loss of *SEC8* function.

Microgametogenesis appears normal in *sec8-m3* heterozygotes

Male-specific transmission defects can arise at any of several stages of male gametophytic development, including microgametogenesis, pollen germination or pollen tube growth (reviewed in McCormick, 2004). Recent electron tomographic studies have

revealed an exocyst-like structure attached to vesicles that are assembling at the *A. thaliana* cell plate during cytokinesis, including the post-meiotic plate during tetrad formation(Otegui and Staehelin, 2004; Segui-Simarro et al., 2004). In addition, *SEC8* was expressed during the microspore, bicellular, and tricellular stages, as well as in mature pollen grains (Figure 2.1). We therefore hypothesized that *SEC8*, and more generally, the putative plant exocyst, might be involved in cytokinesis during microgametogenesis.

To evaluate early male gametophyte development, the immature pollen of *sec8-m3* heterozygotes and of homozygous wild-type siblings was compared. We used aniline blue staining of callose to detect the cytokinetic cell plate in developing pollen (Park and Twell, 2001), and DAPI staining to determine whether mature pollen had successfully become trinuclear. Finally, transmission electron microscopy (TEM) was used to examine the ultrastructure of mature pollen. If the *sec8-m3* allele transmission defect were due to an abnormality in microgametogenesis, half of the pollen from the heterozygote would exhibit a phenotype distinct from wild type. As shown in Supplemental Figure 4, developing and mature pollen from *sec8-m3* heterozygotes appeared identical to pollen from wild-type siblings at all stages of development evaluated using light microscopy. In agreement with these observations, TEM micrographs showed no gross differences between mature pollen grains from heterozygotes and those from wild-type plants (n=30 for each) (e.g., Figure 2.5I). In summary, gametophytes from *sec8-m3* heterozygotes demonstrated no obvious defect in microgametogenesis.

The absolute transmission defect in plants carrying *sec8-m3* is associated with a pollen germination defect

The absence of a *sec8* mutant phenotype in mature pollen led us to evaluate the ability of mutant pollen to germinate and grow pollen tubes post-pollination. *In vitro* techniques have been widely employed to evaluate pollen germination (Johnson-Brousseau and McCormick, 2004), but we were unable to achieve consistent results in several different media. As an alternative, we utilized an *in vivo* pollen germination

assay (Lalanne et al., 2004a) employing Alexander staining (Alexander, 1969), which stains cytoplasm deep purple. Thus, ungerminated pollen grains appear dark, whereas in germinated grains, the movement of cytoplasm into the growing pollen tube leaves a vacuolated pollen grain, which appears pale blue. Pollen germination is then scored by the appearance of an empty, or partially empty, light blue pollen grain, or a purple pollen tube growing out of the grain (Figure 2.4A-G).

Stigmas were pollinated with pollen from either a *sec8-m3* heterozygote or its wild-type sibling (n=18 of each), and then stained after four hours. In this assay, 84% (S.E. 1.8%) of pollen grains from a homozygous wild-type sibling plant germinated, compared with only 46% (S.E. 2.0%) of the pollen from the *sec8-m3* heterozygote (Figure 2.4H). This implies that the ungerminated half of the pollen from the heterozygote consisted primarily of the mutant gametophytes. Similar experiments using aniline blue staining to score for germinated pollen tubes also showed a significant decrease in germination in mutant heterozygotes (data not shown).

To verify that the pollen germination defect was due to the *sec8-m3* mutation, we also scored for germination in the complemented *LAT52::SEC8* line. Due to independent assortment, only half of the *sec8-m3* pollen from the transgenic heterozygote should contain the *LAT52::SEC8* construct. Thus, complementation should increase the rate of germination to a level midway between that of the *sec8-m3* heterozygote and wild type. As predicted, 66% (S.E. 2.5%) of pollen grains from the transgenic heterozygote germinated (Figure 2.4H). These results confirmed that the absolute transmission defect observed for the *sec8-m3* mutant allele is due to a defect in pollen germination.

Pollen grain ultrastructure suggests that the *sec8-m3* pollen responds to signals to germinate

We were curious to know whether the *sec8-m3* mutant pollen was unable to germinate due to an inability to generate tip growth, or alternatively, due to an inability to perceive stigma-originating signals initiating germination. These alternatives might be distinguishable by examining the ultrastructure of mutant pollen that failed to germinate

after placement on a stigma. TEM was, therefore, employed to compare pollen from *sec8-m3* heterozygotes and wild-type siblings after germination *in vivo* (Figure 2.5).

The TEM images, combined with the Alexander staining results (Figure 4A-E), indicated a likely progression of ultrastructural changes that occur during wild-type pollen germination. Following placement of the pollen on the stigma, vacuoles within the pollen grains appeared to enlarge, to become prominent electron-transparent regions. Initially, organelles, and small membrane-bound structures were readily observable (Figure 2.5A, B), but as the vacuoles continued to enlarge, the small membrane-bound structures became much less apparent. The growing vacuoles appeared to coalesce to form a space next to the pollen cell wall, often more prominent on one side of the germinating pollen grain and coincident with the movement of the cytoplasm into the growing pollen tube (Figure 2.5D, E, G). Ultimately, a large vacuole entirely filled the pollen grain (Figure 2.5H). The enlargement of the vacuolar space, ultimately separating the cytoplasm from the pollen wall, was observed with both TEM and Alexander staining (Figure 2.4A-E), suggesting that this change was not an artifact of the chemical fixation used to prepare the pollen for TEM.

The initial TEM examination of pollen from a *sec8-m3* heterozygote following pollination revealed no obvious novel phenotypes specific to the mutant. Non-germinating pollen grains were more prevalent in the pollen from a mutant heterozygote, as expected, but they exhibited stages of vacuolar development similar to the wild-type grains. To be more quantitative, we subsequently used TEM to categorize pollen from a *sec8-m3* heterozygote (n=59) and from a wild-type sibling (n=65) into various phenotypic classes displayed at two hours after pollination (Table 2.2). Pollen grains showing an enlarged vacuolar space next to the pollen cell wall were considered to have germinated. Based upon this criterion, only 11% percent of the wild-type pollen grains failed to germinate (i.e., lacked a large, cell wall-associated vacuole), whereas 32% from the *sec8-m3* heterozygote had not germinated, a statistically-significant difference (χ^2=8.57, $p \leq 0.01$). There were no examples of putative autolysis (i.e., osmiophilic globoids or putative lysosomes - Yamamoto et al., 2003) in this set of pollen grains from the *sec8-m3* heterozygote. Only one pollen grain from each source failed to demonstrate

a response to being placed on the stigma. The remaining eighteen ungerminated pollen grains from the mutant appeared to be undergoing changes normally associated with germinating wild-type pollen. Most of these, designated Class I, showed enlarged vacuoles but no separation from the pollen cell wall (as illustrated in Figure 2.5C). In five grains, designated Class II, these changes included both extensive vacuolar development as well as a decreased prevalence of small membrane-bound structures, typical of a late stage of pollen tube germination (Figure 2.5F). The increased prevalence of Class I and II phenotypes in heterozygous pollen, compared to homozygous wild-type (Table 2.2), strongly suggests that these are the mutant gametophytes. These observations are consistent with a defect in which the mutant was responding to the signals to germinate, but was unable to extrude its cytoplasmic contents into a growing pollen tube.

The partial transmission defect in *sec8-m4* heterozygotes results from reduced competitive ability, and is associated with a reduced pollen tube growth rate

The partial transmission defect evident in the *sec8-m4*, *-m5*, and *-m6* mutants allowed the generation of plants homozygous for these mutant alleles. Based on comparisons of silique length, seed count, incidence of seed gaps, and incidence of deformed seeds (Supplemental Table I), the siliques produced by plants homozygous for each of the three hypomorphic alleles were indistinguishable from those of their wild-type siblings. Evidently, the mutant pollen from homozygous plants is fully capable of performing its functions, leading to a fully fertilized ovary. Given that the defect was only revealed in an outcross using pollen from a heterozygote, we hypothesized that pollen carrying these alleles expressed a competitive defect, i.e., one that made it less likely to accomplish fertilization in the presence of wild-type pollen.

The importance of competition in the *sec8-m4* transmission phenotype was demonstrated in two experiments. First, competition in a set of outcrosses was reduced by applying only a sparse quantity of pollen from a *sec8-m4* heterozygote to a wild-type stigma. In the standard outcross, competition is accentuated by the application of a large quantity of pollen simultaneously to the stigma. Reducing competition by applying only

a sparse quantity of pollen was therefore predicted to increase the percentage of heterozygotes in the outcross progeny. However, it is difficult to assess the exact quantity of pollen applied to the stigma in an outcross. We made the assumption that when the number of pollen grains applied is limiting (i.e. less than the number of available ovules), then the number of seeds ultimately produced is an indirect indicator of the amount of pollen applied. Figure 2.6 is a plot of the percent heterozygotes present in the outcross progeny of a set of "sparse pollen" and "excess pollen" crosses as a function of seed count in the silique. The graph indicates that the reduced competition associated with sparse pollination was associated with an increase in the transmission of the mutant allele through the pollen.

In a second experiment, competition was increased in self-crosses by manually applying a large excess of pollen to the stigma of *sec8-m4* heterozygotes. We hypothesized that a naturally occurring self-cross creates a less-competitive situation, in which there is a more gradual and lighter deposition of pollen onto the stigma. This reduced competition in a natural cross would explain the 23% frequency of mutant homozygotes from our initial self-crosses (Table 2.1), which is far greater than would be predicted (~9%) based on the outcross transmission rate. We predicted that the increased competition created by applying a large excess of pollen would favor the wild type pollen over the *sec8-m4* pollen, and thereby result in decreased transmission of the mutant allele, when compared with natural self-pollination of the same plant. The observed genotypes of progeny of natural self-pollination (n=90) were in the expected Mendelian ratio (Table 2.3). The manual self-pollination (n=156), however, showed decreased transmission of the mutant allele, and produced progeny in a genotypic ratio of approximately 2 (+/+) to 3 (+/-*m4*) to 1 (-*m4*/-*m4*), significantly different from the Mendelian ratio (χ^2=9.37, $p<0.01$). Thus, two lines of evidence support the hypothesis that the partial transmission defect of the *sec8-m4* allele is due to a decreased ability to compete with wild-type pollen.

The reduced ability of pollen caring the *sec8-m4* allele to compete with wild-type pollen could conceivably arise from defects in pollen germination, pollen tube growth, or pollen tube guidance. However, there was no defect in the pollen germination of *sec8-m4*

pollen detected in *in vivo* pollen germination assays four hours after pollination (Figure 2.4H), or using aniline blue staining two hours after pollination (data not shown). Therefore, we turned our attention to evaluating post-germination characteristics of the *sec8-m4* gametophytes. To evaluate the possibility that the pollen tube growth rate of *sec8-m4* gametophytes was slower than wild-type, we compared the growth rate of pollen tubes from wild-type and homozygous mutant siblings (Figure 2.7). A semi-*in vivo* method was employed in which pollen was germinated on a stigma, the stigma was placed on a slide coated with growth media, and pollen tubes were subsequently visualized as they grew out from the stigma onto the media. Wild type pollen (n=100 pollen tubes) demonstrated a mean growth rate of 2.0 $\mu m\ min^{-1}$ (S.E.: 0.06 $\mu m\ min^{-1}$), compared to *sec8-m4* pollen (n=81 pollen tubes), which had a mean growth rate of 1.4 $\mu m\ min^{-1}$ (S.E.: 0.04 $\mu m\ min^{-1}$). Thus the mutant pollen has a significantly lower growth rate ($p=5x10^{-11}$, t-test) compared to pollen of a wild-type sibling.

In vivo differences in pollen tube growth rates between the wild-type and mutant pollen of a heterozygote can be evidenced by a non-random distribution of mutant seeds within the resultant silique (e.g., Goubet et al., 2003). Slower growing pollen tubes from mutant gametophytes result in the mutant allele being more prevalent in seeds from the top half (stigma end) of the silique, relative to the bottom half. Therefore, to determine if *sec8-m4* mutants show a reduced pollen tube growth rate *in vivo*, a top-bottom comparison was performed on 14 siliques harvested from heterozygous outcrosses. In this population, a significantly higher proportion of mutant heterozygotes arose from seeds in the top half of the siliques (22.9%, n=306), compared to the bottom half (13.8%, n=283) ($\chi^2 = 8.064$, $p \leq 0.01$). These results support the hypothesis that the competitive disadvantage of *sec8-m4* mutants is due, at least in part, to a slower pollen tube growth rate than wild-type. SEC8 function is thereby implicated in pollen tube growth, in addition to pollen germination.

In the course of this study, we observed that plants homozygous for the *sec8-m4* allele appeared identical to their wild-type siblings with respect to such gross morphological characteristics as leaf shape and size, appearance of inflorescences, trichome structure, and root hair shape and development. The appearance of root hairs

was of particular interest because, like pollen tubes, they demonstrate tip growth, and because another exocyst component, SEC3, is associated with a mutant root hair phenotype in maize (Wen *et al*., accompanying manuscript). However, maximum root hair lengths measured in 5 day old seedlings revealed no significant difference (p=0.182, t-test) between *sec8-m4* homozygotes (mean=0.85 mm, S.E.: 0.02 mm, n=63) and their wild-type siblings (mean=0.82 mm, S.E.: 0.02 mm, n=63). We were unable to assess the effect of stronger alleles (i.e., *sec8-m1, -m2,* or *-m3*) on sporophytic characteristics, due to our inability to obtain plants homozygous for these alleles.

2.4 DISCUSSION

The polarized growth associated with the germination of the pollen tube from a specific site on the pollen grain, and the subsequent tip growth of the pollen tube, involve the rapid and localized exocytosis of secretory vesicles. In a wide range of eukaryotes, a protein complex known as the exocyst has been shown to facilitate such localized exocytosis (reviewed in Hsu et al., 2004). The *A. thaliana* SEC8 is hypothesized, on the basis of sequence homology, to be a component of the putative plant exocyst (Jurgens and Geldner, 2002; Elias et al., 2003). We have shown that the *SEC8* gene is required for pollen germination and competitive pollen tube growth. The most severe mutant alleles of *SEC8* hinder germination of the pollen grain, resulting in an absolute male-specific transmission defect. Less severe mutant alleles of *SEC8* lead to a decline in the ability of mutant gametophytes to compete with wild-type gametophytes. This decreased competitiveness is at least in part due to a reduced pollen tube growth rate, and results in a partial male-specific transmission defect. These results, along with those of Wen *et al.* (accompanying manuscript), provide the first demonstrated functional role for a putative exocyst component in plants.

Male-specific transmission defects can result from developmental abnormalities that occur at any of a number of stages during microsporogenesis or gametogenesis (Grini et al., 1999; Procissi et al., 2001; Johnson et al., 2004; Lalanne et al., 2004b). We initially suspected that mutation of *SEC8* might affect early pollen development because of the exocyst's hypothesized role in plant cytokinesis (Otegui and Staehelin, 2004;

Segui-Simarro et al., 2004), which can be envisioned as a polarization of the exocytic pathway towards the division plane (reviewed in Bednarek and Falbel, 2002). Other mutations affecting early pollen development (e.g., those in *SCP1* - Chen and McCormick, 1996; *GEM1* - Park et al., 1998; and *MAD1* - Grini et al., 1999) display aberrant cell plate formation or abnormal cell division that is readily evident under microscopic examination. In the case of *SEC8* mutants, however, microscopic examination revealed no characteristics that would distinguish mutant pollen from wild-type prior to the time of germination, arguing against participation of SEC8 in gametophytic cytokinesis. It is possible that the mitotic divisions of male gametogenesis use an alternative form of cytokinesis that does not require SEC8, or the exocyst. It is also possible that residual wild-type *SEC8* transcripts or protein from the heterozygous microsporocytes are present in functional quantities after meiosis, compensating for the mutation in the haploid microspores. Regardless of these possibilities, our evidence strongly argues against a link between cytokinetic defects and the reduced transmission of the *SEC8* mutants.

In contrast to the apparent wild-type development of the pollen grain in the mutant, *in vivo* assays and a complementation experiment definitively demonstrated that the transmission defect in *sec8-m3* gametophytes is due to a defect in pollen germination. Mutations associated with germination defects can be assigned to two broad categories: those that affect the reception of stigma-originating signals initiating germination, and those that affect the response to these signals, i.e., the generation of polar growth. Germination signals are likely to involve adhesion and hydration, mediated by molecules in the pollen coat and its interaction with the stigma (reviewed in Edlund et al., 2004). Other possible cellular components involved in signal reception include apyrases (Steinebrunner et al., 2003), receptor-like kinases and their ligands (Tang et al., 2002; Wengier et al., 2003), as well as calcium (Iwano et al., 2004), calmodulin and calmodulin-binding proteins (Golovkin and Reddy, 2003). Mutations that appear to affect response (e.g., in *SETH1* and *SETH2*, affecting GPI anchored proteins - Lalanne et al., 2004a) often have distinct phenotypes, such as short pollen tubes. Obviously-aberrant pollen tubes from the *sec8-m3* heterozygote were not evident in the *in vivo* pollen

germination assay, leaving an important question unanswered. Were the mutant pollen grains unable to sense the signals to germinate, or were they simply unable to elicit the proper response?

To explore this question we utilized TEM to evaluate the ultrastructure of pollen grains from a *sec8-m3* heterozygote after placement on a stigma. In wild-type grains, polarized accumulation of vesicles can be seen in the grain within 10 minutes after pollination (Kandasamy et al., 1994). Then, coincident with pollen tube germination, vacuoles enlarge and coalesce dynamically, eventually filling the pollen grain as the cytoplasm moves into the growing pollen tube (Hicks et al., 2004). Unfortunately, we were unable to capture any TEM images revealing the localization of secretory vesicles during germination. However, the ungerminated pollen from a *sec8-m3* heterozygote, which most likely is primarily made up of mutant gametophytes, did respond to its placement on a stigma with the development of prominent vacuoles. In some cases, the development of vacuoles was quite extensive, typical of wild-type pollen in an advanced stage of pollen tube development. This occurred without the development of a vacuolar space near the pollen cell wall, characteristic of a pollen grain emptying its cytoplasmic contents into a growing pollen tube. Our TEM investigation was admittedly limited in several respects. First, the chemical fixation used in this study is known to be less optimal for preserving fine ultrastructure than the cryo-fixation/freeze substitution techniques used by several other groups (e.g., Yamamoto et al., 2003). Second, any unique ultrastructural differences in the mutant pollen may be spatially and temporally limited to the site of pollen tube formation at the time of germination, and thereby missed in our collection of samples. Third, the relatively low frequency of ungerminated pollen found from the heterozygote, compared to the Alexander staining results, suggests that some grains may have been lost during sample preparation. In spite of these limitations, the TEM study identified clear differences between pollen from mutant heterozygotes and pollen from wild-types, strongly suggesting that *sec8-m3* mutant pollen grains do respond to the signals initiating germination, but are simply not able to generate a pollen tube. The observations are consistent with the hypothesis that SEC8, as part of the plant

exocyst, is required for localized exocytosis at the initial site of polarized growth, leading to germination and the emergence of a pollen tube.

Further insight into the role of *SEC8* in the male gametophyte was gained from an evaluation of the three alleles demonstrating a partial transmission defect, *sec8-m4*, *-m5* and *-m6*. We hypothesized that this transmission defect was due to a competitive disadvantage for the mutant gametophyte compared to wild-type, similar to previously isolated mutations in *A. thaliana* (*seth8*, *seth9* and *seth10* - Lalanne et al., 2004b) and maize (*rop2* - Arthur et al., 2003). To test this hypothesis we reduced the competition in outcrosses by applying only sparse *sec8-m4*/+ pollen to the stigma, and observed a resultant increase in transmission of the mutant allele. In a second, converse test of the competition hypothesis, we increased pollen competition in a self-cross of heterozygous plants by manually applying an excess of pollen. We found that the transmission of the mutant allele was significantly reduced in the manual self-cross, compared to the natural self-cross, as was predicted. These results not only support our hypothesis, they also have implications for self-pollination in *A. thaliana*. Apparently, a more gradual deposition of pollen onto the stigma during natural self-crosses can allow gametophytes with certain competitive defects to successfully fertilize ovules at a frequency on par with the wild-type. These results suggest that mutant screens relying on segregation distortion to identify gametophytically-important genes (e.g., those of Grini et al., 1999; Johnson et al., 2004; Lalanne et al., 2004b) will miss mutant alleles with subtle, but reproducible, effects on pollen competitive ability.

The competitive disadvantage of the *SEC8* partial mutants could arise from defects in pollen germination, pollen tube growth, or pollen tube guidance from the stigma to the ovule. However, we found that *sec8-m4* pollen was able to germinate at the same frequency as that of wild-type siblings when evaluated at 2 hours (aniline blue staining) or 4 hours (Alexander staining) after pollination. The data did not rule out the possibility that the mutant pollen has a delayed germination of 2 hours or less, but they did point us toward later stages of gametophytic development. The role of SEC8 in post-germination pollen tube growth was explored by monitoring the growth rates of individual pollen tubes over several hours. We discovered that the growth rate of *sec8-*

m4 pollen tubes (1.4 μm min^{-1}) is significantly less than that of wild-type pollen tubes (2.0 μm min^{-1}). The slightly reduced growth rate of the mutant pollen tubes does not prevent a self-crossed *sec8-m4* homozygote from producing full-length siliques filled with viable seed, but apparently becomes a detriment when the mutant pollen must compete with wild-type pollen. In an outcross using pollen from a heterozygote, this growth rate competition results in a non-uniform distribution of seeds with the mutant allele in the resultant silique, i.e. the mutant allele is less prevalent at end of the silique farthest from the stigma. These results clearly demonstrate that SEC8 plays a role not only in pollen germination, but also in the subsequent growth of the pollen tube *in vivo*.

We were interested to calculate whether the growth rate defect was sufficient to explain the severity of the *sec8-m4* transmission disadvantage. In a typical outcross, we observed that approximately 300 pollen grains are applied to the stigma. Those with the fastest growing pollen tubes can be hypothesized to result in fertilization, and the formation of the typical 45 seeds in a silique. The growth rate distributions (Figure 2.7) predict that the 45 fastest pollen tubes in a heterozygote outcross will be comprised of approximately 18% mutant gametophytes. This proportion is the same as the observed outcross results for the *sec8-m4* allele (i.e., 18% of the outcross progeny were heterozygotes), suggesting that the growth rate defect is sufficient to account for the partial transmission defect. Caution must be taken, however, as *in vitro* measurements of pollen tube growth rates are notoriously much lower than those measured *in vivo* (4 to 16 μm min^{-1}, Kandasamy et al., 1994; Iwano et al., 2004), and our result may not represent the growth rate distribution *in vivo*. In addition, we have not ruled out the possibility that *sec8-m4* causes additional defects (e.g., in guidance) that also contribute to the mutant's competitive disadvantage *in vivo*. Nevertheless, this analysis argues that a growth rate defect is the predominant cause of the competitive disadvantage observed in the *sec8-m4* mutant gametophytes.

The existence of six different alleles of *SEC8* has potential for illuminating particular functional domains of the SEC8 protein. The three alleles with inserts closest to the 5' end of the gene demonstrate an absolute transmission defect, while those closest to the 3' end of the gene result in only a partial transmission defect. Two hundred fifty

amino acid residues span the region at the carboxyl end of the protein that is predicted to be affected by the *-m3*, *-m4*, *-m5*, and *-m6* mutations. Available EST sequence data show that this region of the protein is well conserved in homologs across a broad range of plant species, which include angiosperms (both monocots and dicots), gymnosperms, and a moss, attesting to its potential significance. In addition, the partial male transmission defects associated with all three of the C-terminal mutant alleles suggests functional importance for the C-terminus of AtSEC8. Intriguingly, mammalian homologs of SEC8 contain at their carboxyl-termini a PDZ-binding motif (the amino acids TTV) that is essential for the exocyst complex to direct PDZ-containing proteins to the correct membrane locations (Riefler et al., 2003; Sans et al., 2003). This particular motif is absent in non-mammalian homologs of SEC8, including those we identified (Figure 2.2B). Nevertheless, the mammalian results raise the possibility that the function of the plant SEC8 C-terminus is to interact with particular exocyst-directed molecules. No other hints relating structure to function could be gleaned from a search for functional domains within the primary structure of the protein. It should again be noted that we have not yet ruled out the possibility that the three hypomorphic *SEC8* mutations lead to the observed phenotypes by causing a decrease in transcript levels, rather than altered protein structure. Generating a set of transgenic lines expressing mutant derivatives of *SEC8* will be important to further address these possibilities.

2.5 CONCLUSION

This report, along with the report of Wen *et al.* (accompanying manuscript), provides the first functional data to test the hypothesis that the exocyst is involved in tip growth in plants. Orthologs of two different exocyst components in two widely divergent plant species, SEC8 in *A. thaliana* (this report) and SEC3 in maize (Wen *et al*.), have been shown to be important for the proper development of the polarly-growing pollen tube and root hair, respectively. These observations provide strong circumstantial evidence that a function for the exocyst in polarized exocytosis is conserved across plant, fungal, and mammalian species. In addition, preliminary evidence suggests that other exocyst subunits are active in pollen tube growth as a part of a high molecular weight

complex (Synek *et al.*, in prep.) Due to our inability to obtain a homozygous plant carrying a strong *SEC8* mutation, we were unable to assess whether SEC8 is important for root hair growth. The lack of an obvious pollen-associated phenotype in the maize *rth1* mutant can be explained by the relatively low expression level for *rth1* in pollen, and the possible presence of genetic redundancy for SEC3 in the maize genome. Regardless, our hypothesis would predict that mutations in additional plant exocyst genes would also affect root hair and/or pollen tube development. Intriguingly, one other class of protein shown to be important for the polarized growth of both root hair and pollen tube is the Rop GTPase, a key regulator of plant cell polarity (reviewed in Yang, 2002). Indeed, the exocyst has been mentioned as a possible target for Rop regulation (Fu and Yang, 2001), and, in mammalian and yeast cells, has been shown to be regulated by a number of related GTPases (reviewed in Novick and Guo, 2002). As new mutants and molecular tools (e.g., antibodies) become available, additional genetic, cellular and molecular experiments should be pursued to verify the existence of a plant exocyst complex, to determine its localization in both gametophytic and sporophytic cells, and to explore its regulation and functional role in plant cell morphological development

2.6 MATERIALS AND METHODS

Sequence and Expression Database Analysis

Plant sequences orthologous to At*SEC8* were identified by web-based BLAST(Altschul et al., 1997), and downloaded from Genbank for further analysis. All sequencing of PCR products (see below) used standard automated protocols, and was done at the OSU Center for Gene Research and Biotechnology (CGRB) Central Services Lab. Sequences were analyzed using either the Wisconsin Package Version 10.3 (Accelrys Inc., San Diego, CA), or web-based tools available at the OSU CGRB bioinformatics website.

Expression data for haploid male gametophyte development was extracted from the work of Honys and Twell (Honys and Twell, 2004). Additional microarray data for sporophytic tissues and cell suspensions from the NASC Affymetrix website was also

available in the Honys and Twell database, which has been subject to normalization and statistical analysis.

Growth and Assessment of Plants, and Genetic Methods

Arabidopsis lines with T-DNA insertions in the SEC8 gene in a Columbia-0 background were obtained from the SALK Institute: *SEC8-m1* (SALK 057409), *SEC8-m2* (SALK 016128), *SEC8-m3* (SALK 026204), *SEC8-m4* (SALK 118129), *SEC8-m5* (SALK 039659), and *SEC8-m6* (SALK 091118). *SEC8*-specific primers were used with either left or right border T-DNA primers to obtain PCR products on both sides of each insertion, which were sequenced to confirm the insertion site. Seeds were sterilized (1 minute in 95% ethanol, 10 minutes in 20% bleach, and 5 rinses in sterile water) and cold-treated in water for five days prior to planting on growth medium [Murashige and Skoog medium supplemented with 0.0001% (w/v) nicotinic acid, 0.0001% (w/v) thiamine-HCl, 0.0001% (w/v) pyroxidine-HCl, 0.01% (w/v) myo-inositol, 0.0004% (w/v) glycine] or potting soil (SB40, Sun Gro Horticulture). Plants were grown in a growth chamber at 24° C, 16 hours light per day. Plants used for root hair assessment were grown on growth medium in Petri dishes oriented vertically, and the three longest root hairs of each seedling were measured.

To determine plant genotypes, leaf DNA was extracted using a rapid prep method (http://www.agron.missouri.edu/mnl/77/57vejlupkova.html). PCR genotyping was performed using three primers: a primer to the left border of the T-DNA insert (LBb1), and a pair of primers designed to amplify the section of DNA containing the insert site. Primer sequences are listed in Supplemental Table II. Outcrosses were performed by applying pollen from newly dehiscing flowers onto the stigmas of flowers that had been surgically emasculated just prior to dehiscence. Columbia-0 was used as a wild-type tester in outcrosses. Silique evaluations were performed by harvesting mature intact siliques, teasing them open without disturbing the seeds, and examining them under a dissecting microscope.

For complementation, a construct was created by inserting the coding sequence from a full-length cDNA for *SEC8* (GB# AY059763, clone RAFL07-11-G22, Yamada et

al., 2003) into a pCAMBIA1300-derived plasmid containing the *LAT52* pollen promoter (a gift from the lab of Z. Yang). This binary vector was used to transform *Agrobacterium tumefaciens*, and the transformants were identified by screening for resistance to rifampicin. The transformed *Agrobacterium* was in turn used to transform *A. thaliana* plants carrying the *sec8-m3* allele using the floral dip method (Clough and Bent, 1998). Transformed plants were identified by screening for hygromycin resistance (Nakazawa and Matsui, 2003), and *sec8-m3* mutants were identified among this population of transgenics.

Expression Analysis by RT-PCR

Root and immature leaf samples from 10 day old seedlings, and mature leaf and immature floral tissue samples from 21 day old plants were harvested. Pollen was harvested from about 300 Columbia-0 plants, by collecting flowers into 300 ml ice cold 0.3M mannitol, vigorously shaking for 1 minute, filtering through a 75 mm nylon mesh, and concentrating by centrifugation (adapted from Honys and Twell, 2003). For analysis of *sec8-m4*, *-m5*, and *-m6* expression, immature floral tissue was harvested from homozygous mutant plants. All tissues were immediately frozen in liquid nitrogen and stored at –80° C. Total RNA was extracted using the RNeasy Plant Minikit (Qiagen) according to the manufacturer's instructions. The RNA yield and purity were determined spectrophotometrically. RNA derived from homozygous mutants was treated with RQ1 DNase prior to reverse transcription to eliminate any possibility of genomic contamination. Reverse transcription was performed on 1.5 □g total RNA from each source using the Superscript First-Strand Synthesis System for RT-PCR (Invitrogen) according to the manufacturer's instructions. The cDNA generated was used as the template for PCR amplification using appropriate primers (Supplemental Table II).

Electron Microscopy

Hand-pollinated stigmas were excised from Columbia-0 plants 1 to 4 hours after pollination, allowing germination of most wild-type pollen grains, while increasing the probability that the ungerminated pollen grains from the *sec8-m3* heterozygote contained

the mutant allele. For the quantitative analysis (Table IV), all samples were prepared from stigmas at 2 hours after pollination. The excised samples were embedded in 2% LMP agarose and immediately fixed and prepared for ultra-thin sectioning as described by (Park and Twell, 2001). Briefly, samples were chemically fixed in glutaraldehyde, dehydrated, sectioned, stained with uranyl acetate and lead citrate, and viewed with a transmission electron microscope (Philips CM 12, 60kV).

Light microscopy and assessment of pollen tube germination and growth rate

Premature male gametophytes were visualized by surgically removing immature anthers from early stages of flower development, and applying aniline blue [0.1% (w/v) prepared in 0.1M phosphate buffer (pH 8.5)] (adapted from Li et al., 1999) for at least 30 minutes prior to microscopic examination. Gentle pressure on the cover slip spread the gametophytes for optimal viewing. Mature pollen grains were stained with DAPI stain [1 □g/ml DAPI (4',6 diamidino-2phenylindole), 5% (v/v) DMSO, 1% (v/v) Triton X-100] for 1 to 2 hours in the dark prior to microscopic examination. Light microscopy was performed on a Zeiss Axiovert microscope with differential interference contrast optics, and a UV filter set for observing the DAPI and aniline blue fluorescent stains. Digital images were acquired using a SPOT CCD camera and software (Diagnostic Instruments).

Both *in vivo* pollen germination studies and *in vitro* pollen tube growth rate assessments were performed by a researcher blind to the pollen source. *In vivo* pollen germination was assessed as described (Lalanne et al., 2004a). Briefly, four hours after applying only a sparse quantity of pollen to the stigma, the stigmas were excised, placed on a microscope slide, stained with Alexander stain (Alexander, 1969), and examined. A similar procedure was followed using aniline blue (as described above) to stain pollen grains on stigmas two hours after pollination.

In the growth rate experiments, a moderate quantity of pollen was applied to a stigma, which was then immediately excised, placed on a microscope slide that had been coated with germination media [18% (w/v) sucrose, 0.01% (w/v) boric acid, 2mM $CaCl_2$, 1 mM $Ca(NO_3)_2$, 1mM $MgSO_4$, 0.5% (w/v) Noble agar (Difco)], and incubated in a moist chamber. Beginning one hour after pollination, the slides were photographed

microscopically at 15 to 30 minute intervals over a period of several hours. The measured lengths of individual pollen tubes as they grew onto the surface of the medium allowed the calculation of pollen tube growth rates over this series of intervals. The maximal growth rate for each pollen tube over this period was used in the comparative analysis.

Acknowledgements

The authors would like to thank M. Foss and Z. Vejlupkova for useful critiques of the manuscript, K. Carroll for consultations on procedures, M. Johnson for advice regarding competition experiments, Z. Yang for the *LAT52* construct, and P. Schnable for communicating results prior to publication. We would like to acknowledge M. Nesson and the OSU Electron Microscopy Facility for assistance with the TEM, the OSU CGRB Central Services Lab for sequencing, and the T. Wolpert Lab for assistance with the growth and transformation of *Arabidopsis*. Finally we also thank J. McElravy, J. Hines, P. Staiger, and M. Frederick for their cheerful contributions to the work of the laboratory. Upon request, all novel materials described in this publication will be made available in a timely manner for non-commercial research purposes, subject to the requisite permission from any third-party owners of all or parts of the material.

2.7 LITERATURE CITED

Alexander M (1969) Differential staining of aborted and nonaborted pollen. Stain Technol 44: 117-122

Alonso JM, Stepanova AN, Leisse TJ, Kim CJ, Chen H, Shinn P, Stevenson DK, Zimmerman J, Barajas P, Cheuk R, Gadrinab C, Heller C, Jeske A, Koesema E, Meyers CC, Parker H, Prednis L, Ansari Y, Choy N, Deen H, Geralt M, Hazari N, Hom E, Karnes M, Mulholland C, Ndubaku R, Schmidt I, Guzman P, Aguilar-Henonin L, Schmid M, Weigel D, Carter DE, Marchand T, Risseeuw E, Brogden D, Zeko A, Crosby WL, Berry CC, Ecker JR (2003) Genome-wide insertional mutagenesis of Arabidopsis thaliana. Science 301: 653-657

Altschul SF, Madden TL, Schaffer AA, Zhang J, Zhang Z, Miller W, Lipman DJ (1997) Gapped BLAST and PSI-BLAST: a new generation of protein database search programs. Nucleic Acids Res 25: 3389-3402

Arthur KM, Vejlupkova Z, Meeley RB, Fowler JE (2003) Maize ROP2 GTPase provides a competitive advantage to the male gametophyte. Genetics 165: 2137-2151

Bednarek SY, Falbel TG (2002) Membrane trafficking during plant cytokinesis. Traffic 3: 621-629

Camacho L, Malhó R (2003) Endo/exocytosis in the pollen tube apex is differentially regulated by Ca2+ and GTPases. J Exp Bot 54: 83-92

Chen YC, McCormick S (1996) sidecar pollen, an Arabidopsis thaliana male gametophytic mutant with aberrant cell divisions during pollen development. Development 122: 3243-3253.

Clough SJ, Bent AF (1998) Floral dip: a simplified method for Agrobacterium-mediated transformation of Arabidopsis thaliana. Plant J 16: 735-743

Edlund AF, Swanson R, Preuss D (2004) Pollen and stigma structure and function: the role of diversity in pollination. Plant Cell 16 Suppl: S84-97

Elias M, Drdova E, Ziak D, Bavlnka B, Hala M, Cvrckova F, Soukupova H, Zarsky V (2003) The exocyst complex in plants. Cell Biol Int 27: 199-201

Feijó JA, Costa SS, Prado AM, Becker JD, Certal AC (2004) Signalling by tips. Curr Opin Plant Biol 7: 589-598

Fowler JE, Quatrano RS (1997) Plant cell morphogenesis: plasma membrane interactions with the cytoskeleton and cell wall. Annu Rev Cell Dev Biol 13: 697-743

Fu Y, Yang Z (2001) Rop GTPase: a master switch of cell polarity development in plants. Trends Plant Sci 6: 545-547

Golovkin M, Reddy AS (2003) A calmodulin-binding protein from Arabidopsis has an essential role in pollen germination. Proc Natl Acad Sci U S A 100: 10558-10563

Goubet F, Misrahi A, Park SK, Zhang Z, Twell D, Dupree P (2003) AtCSLA7, a cellulose synthase-like putative glycosyltransferase, is important for pollen tube growth and embryogenesis in Arabidopsis. Plant Physiol 131: 547-557.

Grindstaff KK, Yeaman C, Anandasabapathy N, Hsu SC, Rodriguez-Boulan E, Scheller RH, Nelson WJ (1998) Sec6/8 complex is recruited to cell-cell contacts and specifies transport vesicle delivery to the basal-lateral membrane in epithelial cells. Cell 93: 731-740

Grini PE, Schnittger A, Schwarz H, Zimmermann I, Schwab B, Jurgens G, Hulskamp M (1999) Isolation of ethyl methanesulfonate-induced gametophytic mutants in Arabidopsis thaliana by a segregation distortion assay using the multimarker chromosome 1. Genetics 151: 849-863

Gu Y, Wang Z, Yang Z (2004) ROP/RAC GTPase: an old new master regulator for plant signaling. Curr Opin Plant Biol 7: 527-536

Guo W, Grant A, Novick P (1999) Exo84p is an exocyst protein essential for secretion. J Biol Chem 274: 23558-23564

Hazuka CD, Foletti DL, Hsu SC, Kee Y, Hopf FW, Scheller RH (1999) The sec6/8 complex is located at neurite outgrowth and axonal synapse-assembly domains. J Neurosci 19: 1324-1334

Hepler PK, Vidali L, Cheung AY (2001) Polarized cell growth in higher plants. Annu Rev Cell Dev Biol 17: 159-187

Hicks GR, Rojo E, Hong S, Carter DG, Raikhel NV (2004) Geminating pollen has tubular vacuoles, displays highly dynamic vacuole biogenesis, and requires VACUOLESS1 for proper function. Plant Physiol 134: 1227-1239

Honys D, Twell D (2003) Comparative analysis of the Arabidopsis pollen transcriptome. Plant Physiol 132: 640-652

Honys D, Twell D (2004) Transcriptome analysis of haploid male gametophyte development in Arabidopsis. Genome Biol 5: R85

Hsu SC, TerBush D, Abraham M, Guo W (2004) The exocyst complex in polarized exocytosis. Int Rev Cytol 233: 243-265
Inoue M, Chang L, Hwang J, Chiang SH, Saltiel AR (2003) The exocyst complex is required for targeting of Glut4 to the plasma membrane by insulin. Nature 422: 629-633

Iwano M, Shiba H, Miwa T, Che FS, Takayama S, Nagai T, Miyawaki A, Isogai A (2004) Ca2+ dynamics in a pollen grain and papilla cell during pollination of Arabidopsis. Plant Physiol 136: 3562-3571

Johnson MA, von Besser K, Zhou Q, Smith E, Aux G, Patton D, Levin JZ, Preuss D (2004) Arabidopsis hapless mutations define essential gametophytic functions. Genetics 168: 971-982

Johnson-Brousseau SA, McCormick S (2004) A compendium of methods useful for characterizing Arabidopsis pollen mutants and gametophytically-expressed genes. Plant J 39: 761-775

Jurgens G, Geldner N (2002) Protein secretion in plants: from the trans-Golgi network to the outer space. Traffic 3: 605-613

Kandasamy MK, Nasrallah JB, Nasrallah ME (1994) Pollon-pistil interactions and developmental regulation of pollon tube growth in Arabidopsis. Development 120: 3405-3418

Lalanne E, Honys D, Johnson A, Borner GH, Lilley KS, Dupree P, Grossniklaus U, Twell D (2004a) SETH1 and SETH2, Two Components of the Glycosylphosphatidylinositol Anchor Biosynthetic Pathway, Are Required for Pollen Germination and Tube Growth in Arabidopsis. Plant Cell 16: 229-240

Lalanne E, Michaelidis C, Moore JM, Gagliano W, Johnson A, Patel R, Howden R, Vielle-Calzada JP, Grossniklaus U, Twell D (2004b) Analysis of transposon insertion mutants highlights the diversity of mechanisms underlying male progamic development in Arabidopsis. Genetics 167: 1975-1986

Li H, Lin Y, Heath RM, Zhu MX, Yang Z (1999) Control of pollen tube tip growth by a Rop GTPase-dependent pathway that leads to tip-localized calcium influx. Plant Cell 11: 1731-1742

McCormick S (2004) Control of male gametophyte development. Plant Cell 16 Suppl: S142-153

Murthy M, Garza D, Scheller RH, Schwarz TL (2003) Mutations in the exocyst component Sec5 disrupt neuronal membrane traffic, but neurotransmitter release persists. Neuron 37: 433-447

Nakazawa M, Matsui M (2003) Selection of hygromycin-resistant Arabidopsis seedlings. Biotechniques 34: 28-30
Novick P, Guo W (2002) Ras family therapy: Rab, Rho and Ral talk to the exocyst. Trends Cell Biol 12: 247-249

Otegui MS, Staehelin LA (2004) Electron tomographic analysis of post-meiotic cytokinesis during pollen development in Arabidopsis thaliana. Planta 218: 501-515

Palanivelu R, Preuss D (2000) Pollen tube targeting and axon guidance: parallels in tip growth mechanisms. Trends Cell Biol 10: 517-524

Park SK, Howden R, Twell D (1998) The Arabidopsis thaliana gametophytic mutation gemini pollen1 disrupts microspore polarity, division asymmetry and pollen cell fate. Development 125: 3789-3799

Park SK, Twell D (2001) Novel patterns of ectopic cell plate growth and lipid body distribution in the Arabidopsis gemini pollen1 mutant. Plant Physiol 126: 899-909.

Pfeffer SR (1999) Transport-vesicle targeting: tethers before SNAREs. Nat Cell Biol 1: E17-22

Procissi A, de Laissardiere S, Ferault M, Vezon D, Pelletier G, Bonhomme S (2001) Five gametophytic mutations affecting pollen development and pollen tube growth in Arabidopsis thaliana. Genetics 158: 1773-1783

Riefler GM, Balasingam G, Lucas KG, Wang S, Hsu SC, Firestein BL (2003) Exocyst complex subunit sec8 binds to postsynaptic density protein-95 (PSD-95): a novel interaction regulated by cypin (cytosolic PSD-95 interactor). Biochem J 373: 49-55

Sans N, Prybylowski K, Petralia RS, Chang K, Wang YX, Racca C, Vicini S, Wenthold RJ (2003) NMDA receptor trafficking through an interaction between PDZ proteins and the exocyst complex. Nat Cell Biol 5: 520-530

Schekman R, Novick P (2004) 23 genes, 23 years later. Cell S116: S13-15

Segui-Simarro JM, Austin JR, 2nd, White EA, Staehelin LA (2004) Electron tomographic analysis of somatic cell plate formation in meristematic cells of Arabidopsis preserved by high-pressure freezing. Plant Cell 16: 836-856

Steinebrunner I, Wu J, Sun Y, Corbett A, Roux SJ (2003) Disruption of apyrases inhibits pollen germination in Arabidopsis. Plant Physiol 131: 1638-1647

Sugihara K, Asano S, Tanaka K, Iwamatsu A, Okawa K, Ohta Y (2002) The exocyst complex binds the small GTPase RalA to mediate filopodia formation. Nat Cell Biol 4: 73-78

Tang W, Ezcurra I, Muschietti J, McCormick S (2002) A cysteine-rich extracellular protein, LAT52, interacts with the extracellular domain of the pollen receptor kinase LePRK2. Plant Cell 14: 2277-2287

TerBush DR, Maurice T, Roth D, Novick P (1996) The Exocyst is a multiprotein complex required for exocytosis in Saccharomyces cerevisiae. EMBO J. 15: 6483-6494

Twell D, Yamaguchi J, Wing RA, Ushiba J, McCormick S (1991) Promoter analysis of genes that are coordinately expressed during pollen development reveals pollen-specific enhancer sequences and shared regulatory elements. Genes Dev 5: 496-507

Vega IE, Hsu SC (2001) The exocyst complex associates with microtubules to mediate vesicle targeting and neurite outgrowth. J Neurosci 21: 3839-3848

Wengier D, Valsecchi I, Cabanas ML, Tang WH, McCormick S, Muschietti J (2003) The receptor kinases LePRK1 and LePRK2 associate in pollen and when expressed in yeast, but dissociate in the presence of style extract. Proc Natl Acad Sci U S A 100: 6860-6865

Whyte JR, Munro S (2002) Vesicle tethering complexes in membrane traffic. J Cell Sci 115: 2627-2637

Yamada K, Lim J, Dale JM, Chen H, Shinn P, Palm CJ, Southwick AM, Wu HC, Kim C, Nguyen M, Pham P, Cheuk R, Karlin-Newmann G, Liu SX, Lam B, Sakano H, Wu T, Yu G, Miranda M, Quach HL, Tripp M, Chang CH, Lee JM, Toriumi M, Chan MM, Tang CC, Onodera CS, Deng JM, Akiyama K, Ansari Y, Arakawa T, Banh J, Banno F, Bowser L, Brooks S, Carninci P, Chao Q, Choy N, Enju A, Goldsmith AD, Gurjal M, Hansen NF, Hayashizaki Y, Johnson-Hopson C, Hsuan VW, Iida K, Karnes M, Khan S, Koesema E, Ishida J, Jiang PX, Jones T, Kawai J, Kamiya A, Meyers C, Nakajima M, Narusaka M, Seki M, Sakurai T, Satou M, Tamse R, Vaysberg M, Wallender EK, Wong C, Yamamura Y, Yuan S, Shinozaki K, Davis RW, Theologis A, Ecker JR (2003) Empirical analysis of transcriptional activity in the Arabidopsis genome. Science 302: 842-846

Yamamoto Y, Nishimura M, Hara-Nishimura I, Noguchi T (2003) Behavior of vacuoles during microspore and pollen development in Arabidopsis thaliana. Plant Cell Physiol 44: 1192-1201

Yang Z (2002) Small GTPases: versatile signaling switches in plants. Plant Cell 14 Suppl: S375-388

Yeaman C, Grindstaff KK, Nelson WJ (2004) Mechanism of recruiting Sec6/8 (exocyst) complex to the apical junctional complex during polarization of epithelial cells. J Cell Sci 117: 559-570

2.8 FIGURES

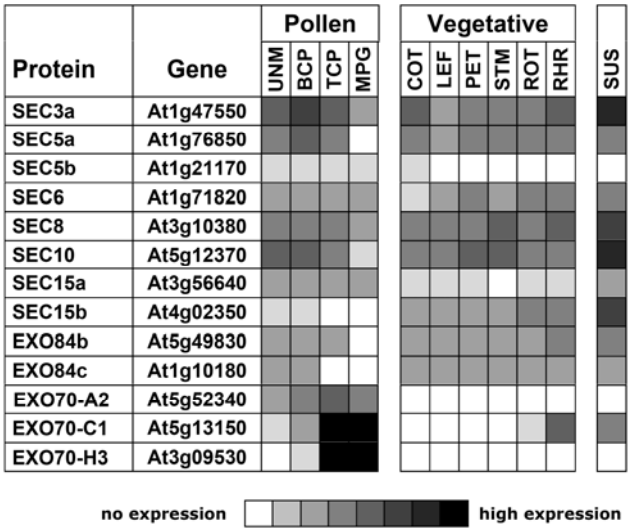

Figure 2.1 Microarray data for putative exocyst components in *A. thaliana* indicate that transcripts for all eight subunits are expressed widely. In particular, the experiments of Honys and Twell (2004) show that At*SEC8*, as well as other putative exocyst components, are expressed in developing pollen. Pollen sources of RNA for the expression analysis included uninucleate microspores (UNM), bicellular pollen (BCP), immature tricellular pollen (TCP), and mature pollen grains (MPG). Additional sources of RNA for the analysis included cotyledons (COT), leaves (LEF), petioles (PET), stems (STM), roots (ROT), root hairs (RHR), and cell suspensions (SUS). White (no expression) indicates that expression was not consistently detected among replicates. For brevity, the data shown for At*EXO70* represent only three of the 23 homologs of this exocyst component in *A. thaliana*; these are the homologs highly expressed in the pollen. Nomenclature is based upon that of Elias *et al.* (2003).

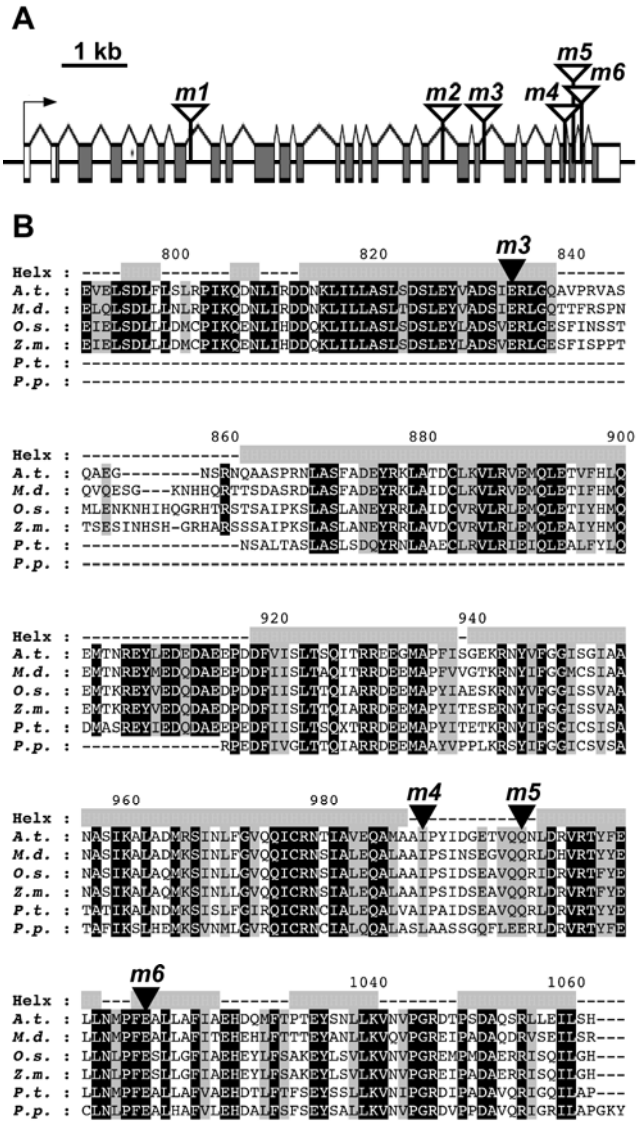

Figure 2.2. T-DNA insertional mutations interrupt the coding region of *SEC8* (At3g10380) at multiple sites. A, Six independent insertions (designated *m1* through *m6*) interrupt the ~8.5 kb gene. Based on the sequence of a full-length 3.7 kb cDNA (Genbank # AY059763), the gene contains 27 exons (boxed) and is predicted to encode a 1053 residue protein. B, Stretches of primary sequence at the C-terminal end of plant SEC8 orthologs are conserved in widely divergent species, as shown by alignment of predicted proteins sequences. Identical residues are shaded black; similar residues, gray. Insertion sites for four of the mutant alleles are designated by a black triangle. *A. thaliana* (*A.t.*) and rice (*O.s.*) sequences are based on genomic data; all others are based on a consensus of assembled ESTs. Other species: *M.d.*, *Malus domestica* (apple); *Z.m.*, *Zea mays* (maize); *P.t.*, *Pinus taeda* (loblolly pine); *P.p.*, *Physcomitrella patens* (moss). Helx shows regions of predicted α-helical structure (gray boxes).

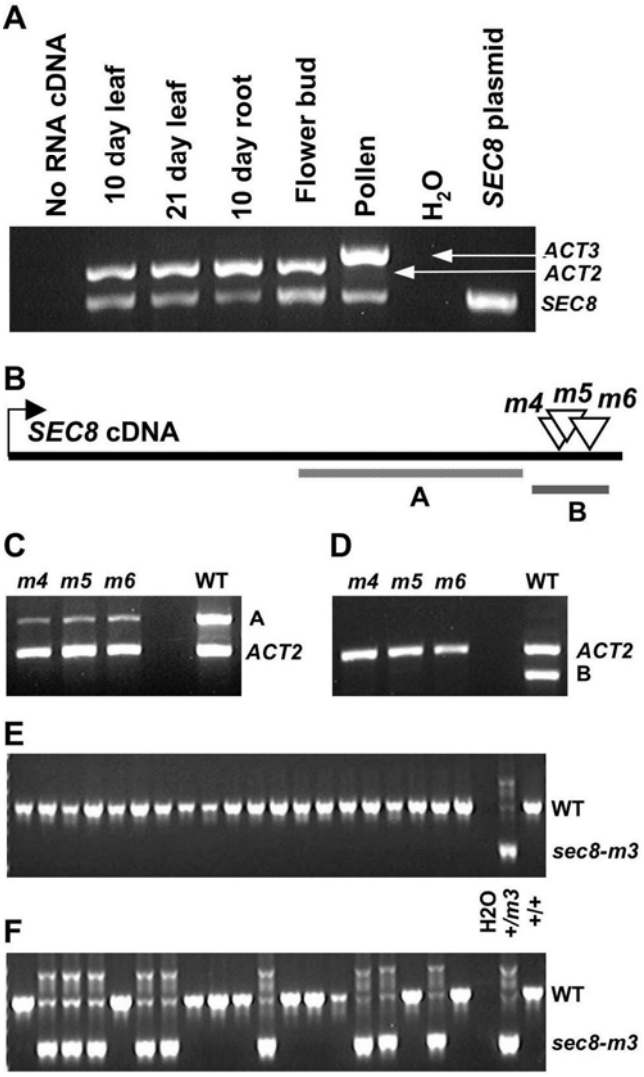

Figure 2.3. Insertional mutations affect the *SEC8* transcript and transmission through the male gametophyte. A, The *SEC8* transcript is detectable in several wild-type tissues, including mature pollen, by RT-PCR. Primers against *ACTIN2* (sporophyte) and *ACTIN3* (gametophyte) were included as internal controls. B, Schematic of the *SEC8* transcript, and the strategy to test for aberrant transcripts generated by the *-m4*, *-m5* and *-m6* alleles. RT-PCR product A is located 5' to the insertion sites, whereas product B spans all three insertion sites. C and D, In RNA made from immature floral tissue, product A is detectable in the wild type and all three mutant homozygotes (C), whereas product B is only detectable in the wild type (D). E and F, 20 outcross progeny were genotyped by PCR using a set of three primers (see methods) to produce distinct wild-type (WT) and *sec8-m3* heterozygote banding patterns. In E, no heterozygous progeny were produced in an outcross to a wild-type homozygote using pollen from a *sec8-m3* heterozygote. In F, heterozygous progeny were produced in an outcross using pollen from a *sec8-m3* heterozygote also carrying a *LAT52::SEC8* construct, demonstrating male transmission of the mutant allele, and complementation.

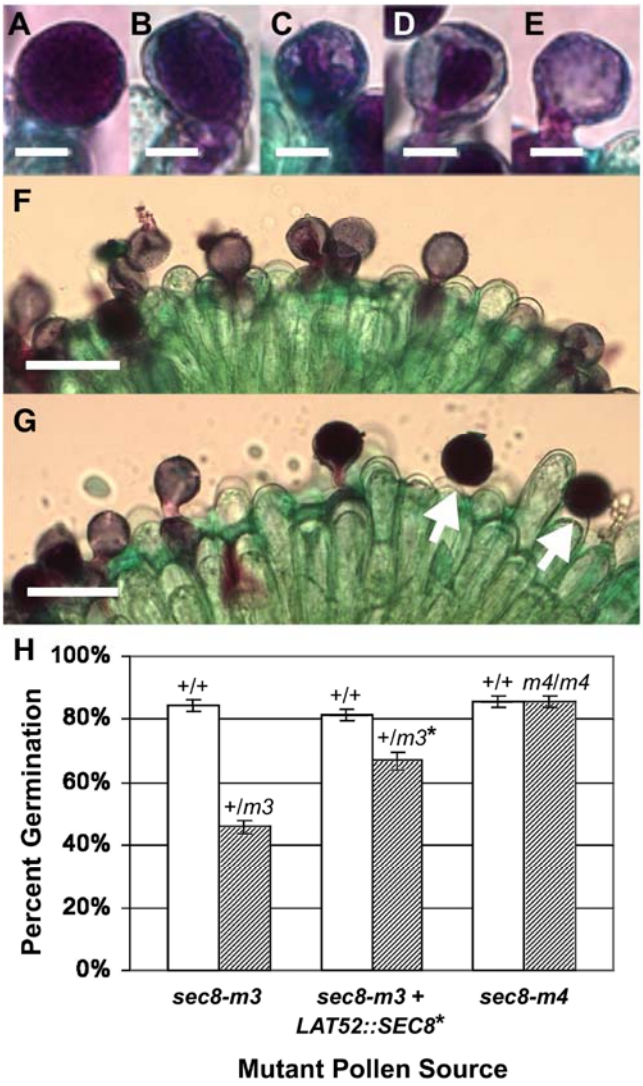

Figure 2.4. Alexander staining reveals that a *SEC8* allele with an absolute transmission defect is associated with a pollen germination defect. A - E, Staining phenotypes of wild-type pollen grains *in vivo*, illustrating (from left to right, ungerminated to empty grain) a likely progression of cytoplasm (stained purple) out of the grain and into the growing pollen tube. F and G, Representative fields of stained pollen grains from a wild-type homozygote (F) and a sibling *sec8-m3* heterozygote (G). White arrows, ungerminated grains; stigma cells stain green. H, Quantitation of *in vivo* germination rates from three different pairs of lines, assayed blindly four hours after pollination. Hatched bars, mutants; white bars, wild-type siblings.

Figure 2.5 (following page). TEM images indicate that ungerminated pollen from *sec8-m3* heterozygotes responds to signals to germinate. A, D, G, H, Wild-type pollen grains *in vivo*, illustrating (in that order) a likely progression of intracellular morphologies during germination. D and G show vacuolar space generated adjacent to the pollen cell wall (black arrow), and H shows an apparently emptied coat. Larger, apparently coalescing, vacuoles (examples marked by asterisks) are also characteristic of germinating grains, and are not present in mature pollen (I). B, Detail of (A), adjacent to the pollen cell wall. Mitochondria (white arrowhead) and small membrane-bound structures of unknown identity (black arrows) are apparent. E, Detail of a pollen grain similar to (D), showing vacuoles (asterisks) apparently fusing with the coat-associated vacuolar space, and few of the apparent small membrane-bound structures seen in (B). C, F, Representative ungerminated grains (i. e., no separation of the cytoplasm from the coat) from a *sec8-m3* heterozygote, of Class I and II, respectively (see text). Class I and II grains show certain characteristics similar to A and D, respectively. Both contain larger vacuoles (examples marked by asterisks); Class I grains (C) contain small membrane-bound structures, whereas Class II grains do not. Bar = 2 μm. White arrows, sperm cells (A, I) ; black arrowhead, vegetative nucleus (I).

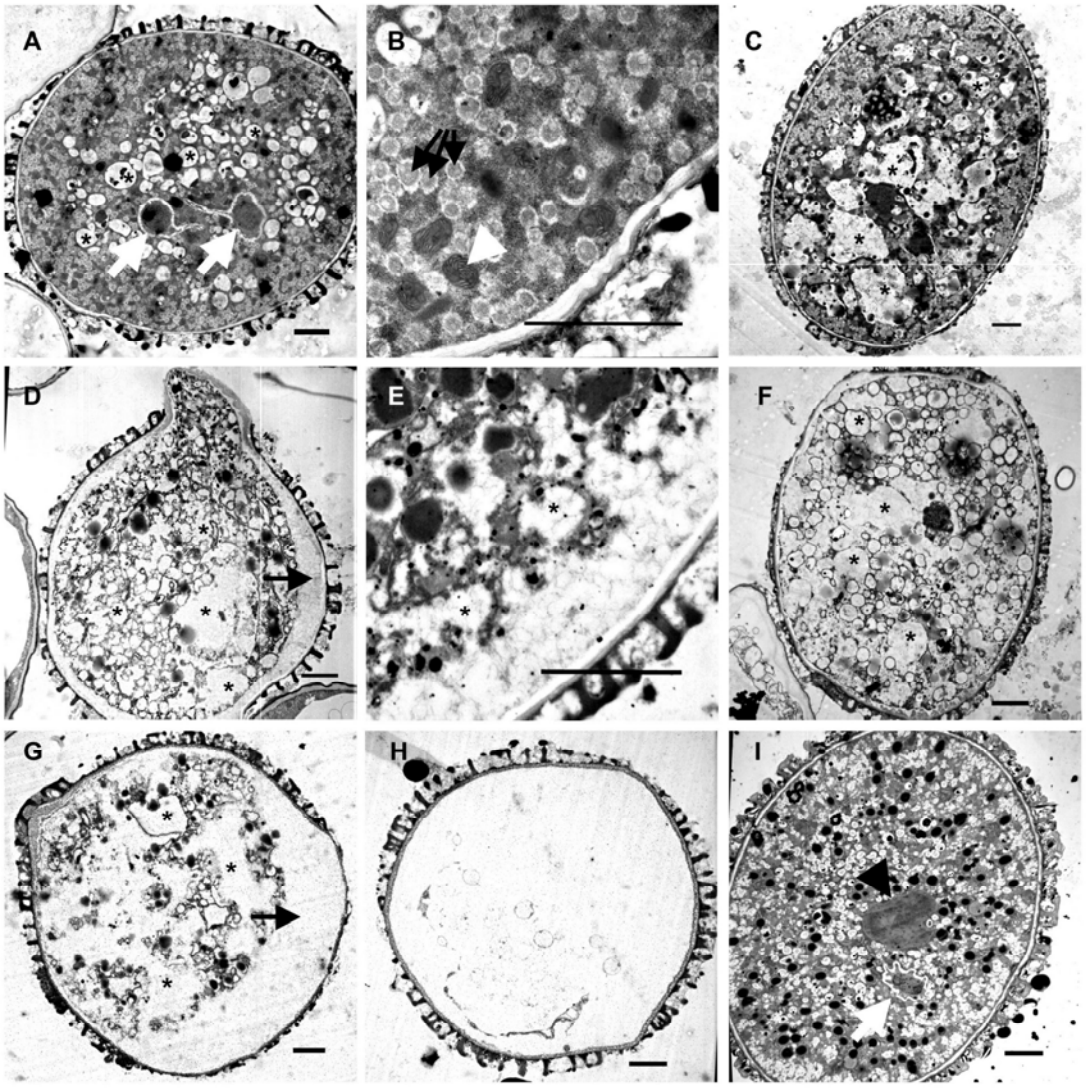

Figure 2.5. TEM images indicate that ungerminated pollen from *sec8-m3* heterozygotes responds to signals to germinate.

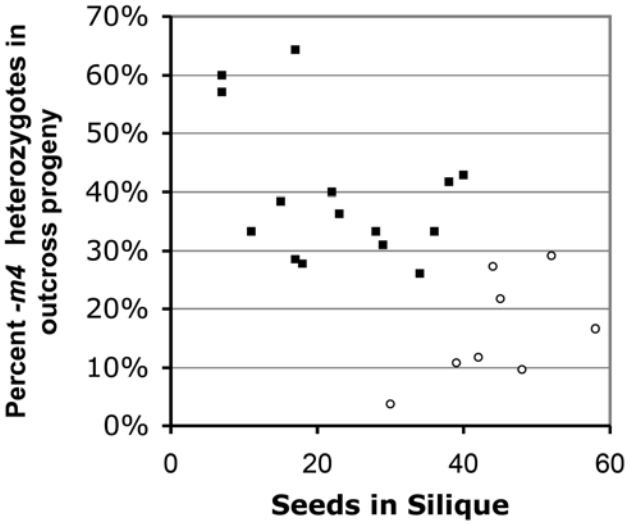

Figure 2.6. Transmission of the *sec8-m4* allele increases in incompletely-filled siliques. Pollinations (using *sec8-m4*/+ as the male) were done with either sparse (black squares) or excess (open circles) pollen placed on each wild-type stigma. Genotypes of progeny were determined by PCR.

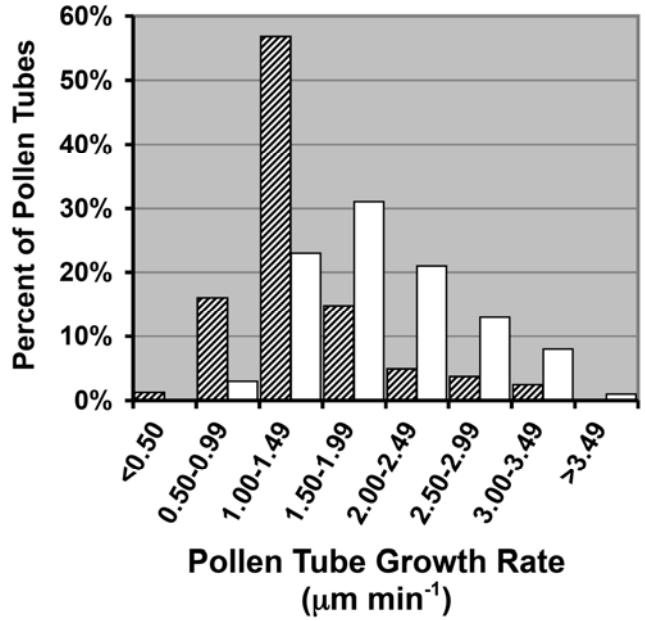

Figure 2.7. The *sec8-m4* mutation decreases pollen tube growth rate in culture. A histogram of the rates for individual pollen tubes (n = 81 mutant, 100 wild-type) from five different homozygous mutant plants (cross-hatched bars) and five different sibling wild-type plants (white bars) shows a significantly different distribution in the two genotypes. Rates were determined by imaging germinated, growing pollen tubes at 15-30 minute intervals.

2.9 TABLES

Table 2.1 Inheritance of Mutant *SEC8* alleles

Type of Cross	*SEC8* allele	Number of crosses	Number of progeny	Genotypes of progeny			χ^2	p
				+/+	+/*m*[a]	*m*/*m*		
Natural Self-cross of *SEC8* Heterozygotes				25%	50%	25%	Expected	
	m1	3	180	58%	48%	0%	127.5	≤ 0.001
	m2	4	216	50%	50%	0%	106.0	≤ 0.001
	m3	6	267	47%	53%	0%	119.8	≤ 0.001
	m4	8	260	28%	49%	23%	1.472	NS[b]
	m5	3	85	24%	47%	29%	0.832	NS
	m6	2	78	19%	58%	23%	3.178	NS
Outcross Pollen source: +/+ Pollen recipient: +/*m*				50%	50%		Expected	
	m1	4	157	47%	53%		0.516	NS
	m2	3	90	54%	46%		0.711	NS
	m3	3	101	50%	50%		0.010	NS
	m4	5	157	51%	49%		0.057	NS
	m5	4	147	52%	48%		0.333	NS
	m6	6	159	52%	48%		0.308	NS
Outcross Pollen source: +/*m* Pollen recipient: +/+				50%	50%		Expected	
	m1	4	150	100%	0%		150.0	≤ 0.001
	m2	3	71	100%	0%		71.0	≤ 0.001
	m3	3	105	100%	0%		105.0	≤ 0.001
	m4	10	577	82%	18%		238.5	≤ 0.001
	m5	6	235	78%	22%		75.27	≤ 0.001
	m6	6	157	69%	31%		22.17	≤ 0.001

[a] *m* designates a mutant *sec8* allele. [b] NS = not significantly different.

Table 2.2 Categorization of pllen grain TEM phenotypes, two hours after pollinaton.

Comparison of pollen from *sec8-m3* heterozygotes and wild-type siblings.						
Pollen Source	Germinated Pollen Grains	Non-germinated Pollen Grains[a]				TOTAL GRAINS EVALUATED
		Class I[b]	Class II[c]	No Response[d]	Putative Autolysis[e]	
+/+	58 (89.2%)	3 (4.6%)	0 (0.0%)	1 (1.5%)	3 (4.6%)	65
m3/+	40 (67.8%)	13 (22.0%)	5 (8.5%)	1 (1.7%)	0 (0.0%)	59

[a]Lacking a large vacuole separating the cytoplasm from the pollen cell wall (see Text, Figure 5). [b]Class I = larger vacuoles, small membrane-bound structures, no separation of cytoplasm from coat (example, Figure 5C). [c]Class II = larger vacuoles, no small membrane-bound structures, no separation of cytoplasm from coat (example, Figure 5F). [d]No response = no larger vacuoles, similar to mature pollen grain (Figure 5I). [e]Putative Autolysis = contains osmiophilic globoids, a characteristic of entry into a hypothesized autolysis pathway (Yamamoto et al., 2003).

Table 2.3 Natural versus Manual (excess pollen applied to stigma) self-crosses of *sec8-m4* heterozygotes

Type of Self-Cross	Number of Crosses	Number of Progeny	Genotypes of Progeny			χ^2	p
			+/+	+/*m*[a]	*m*/*m*		
Natural	3	90	23 25.6%	44 48.9%	23 25.6%	0.044	NS[b]
Manual	3	156	52 33.3%	79 50.6%	25 16.0%	9.372	$\leq$0.01
Expected Mendelian Ratio			25%	50%	25%		

[a]*m* designates a mutant *sec8* allele. [b]NS = not significantly different.

CHAPTER 3

An Exocyst Complex Functions in Plant Cell Growth

Michal Hala,[1] Rex Cole[1], Lukas Synek, Edita Drdova, Tamara Pecenkova, Alfred Nordheim, Tobias Lamkemeyer, Johannes Madlung, Frank Hochholdinger, John E. Fowler and Viktor Zarsky
[1] These authors contributed equally to this work.

The Plant Cell
American Society of Plant Biologists, Dartmouth Journal Services, Waterbury,VT
Submitted for publication on February 28, 2008

3.1 ABSTRACT

The exocyst, an octameric tethering complex and effector of Rho and Rab GTPases, is involved in polarized secretion in yeast and animals. Recent evidence implicates three plant homologs of exocyst subunits (SEC3, SEC8 and EXO70A1) in plant cell morphogenesis. However, there is no evidence yet documenting that these and other predicted subunits function together *in vivo*. We provide genetic, cell biological and biochemical evidence addressing this hypothesis. In *Arabidopsis thaliana*, double mutants in exocyst subunits (*sec5 exo70A1*, or *sec8 exo70A1*) show a synergistic defect in etiolated hypocotyl elongation. Mutants in exocyst subunits SEC5, SEC6, SEC8 and SEC15a show similarly defective pollen germination and pollen tube growth phenotypes. Antibodies against SEC6, SEC8 and EXO70A1 demonstrate co-localization of these proteins at the apex of growing tobacco pollen tubes. SEC3, SEC5, SEC6, SEC8, SEC10, SEC15a, and EXO70 subunits co-purify in a high molecular weight fraction of 900 kDa after chromatographic fractionation of Arabidopsis cell suspension extract, as shown by Western blotting and/or analysis by mass spectrometry. Blue native electrophoresis confirmed the presence of SEC3, SEC6, SEC8, and EXO70 in high molecular weight complexes. Finally, the yeast two-hybrid system revealed interaction of Arabidopsis SEC10 with SEC15b, and SEC6 with SEC8. We conclude that the exocyst functions as a complex in plant cells, where it plays important roles in morphogenesis.

3.2 INTRODUCTION

Vesicle traffic through the eukaryotic endomembrane system and to the plasma membrane is facilitated by tethering factors (reviewed in Cai et al., 2007; Sztul and Lupashin, 2006). They act as “molecular bridges” that provide an initial interaction between the vesicle and its target membrane. This tethering occurs prior to the pairing of SNAREs (soluble N-ethylmaleimide-sensitive attachment protein receptors) and the final fusion of the vesicle with the membrane. In addition to assisting the positioning of the vesicle at the membrane, tethering factors, in combination with Rab GTPases (small GTPases of the Ras superfamily), help to determine the specificity of vesicle targeting. Two general types of tethering factors are recognized: long putative coiled-coil proteins

generally occurring as dimers (e.g., Uso1p and p115), and large multi-subunit protein complexes (e.g., the exocyst, COG, GARP, HOPS, TRAPPI and TRAPPII complexes). Of these, the targeting and tethering of Golgi-derived secretory vesicles to the plasma membrane is associated specifically with the exocyst, an eight-protein complex also known as the Sec6/8 complex.

The cellular role of the exocyst has been extensively studied in yeast and animals (reviewed in Hsu et al., 2004). In these eukaryotes the exocyst is required when physiological or developmental circumstances demand extensive exocytosis to support rapid polarized growth, such as budding in *Saccharomyces cerevisiae* (TerBush and Novick, 1995), hyphal tip growth in *Candida albicans* (Li et al., 2007), the outgrowth of cultured neurites (Hazuka et al., 1999; Pommereit and Wouters, 2007), and membrane trafficking to the leading edge of migrating mammalian epithelial cells (Rosse et al., 2006; Zuo et al., 2006).

The complex of proteins that make up the exocyst was originally described in yeast (TerBush et al., 1996), and based on sequence homology the mammalian exocyst was subsequently characterized (Hsu et al., 1996; Kee et al., 1997). In both yeast and mammals, the exocyst complex consists of eight subunits: Sec3, Sec5, Sec6, Sec8, Sec10, Sec15, Exo70, and Exo84 (TerBush et al., 1996; Hsu et al., 1996; Guo et al., 1999a; Matern et al., 2001). Molecular weights of exocyst subunits range from 70 to 140 kDa, forming an 834 kDa and 743 kDa complex in yeast and mammals, respectively (TerBush et al., 1996; Hsu et al., 1996). Although overall sequence identity among different exocyst subunits is less than 10%, all subunits are predicted to contain similar helical bundles assembled into long rod-like domains (Whyte and Munro, 2001; Dong et al., 2005; Wu et al., 2005; Hamburger et al., 2006; Sivaram et al., 2006). The predicted rod-like domains have recently been verified by crystallography for four of the subunits (reviewed by Munson and Novick, 2006). Interactions between subunits of the complex in yeast and mammals have been detected by various methods, including yeast two-hybrid assays, co-immunoprecipitation and pull-down assays (Roth et al., 1998; Guo et al., 1999b; Guo et al., 1999a; Matern et al., 2001; Vega and Hsu, 2001; Moskalenko et al., 2003; Dong et al., 2005; Sivaram et al., 2005). Nevertheless, the exocyst structure and

precise mechanism of *in vivo* exocyst assembly remain unknown. Since the original discovery that the exocyst is an effector of the Rab GTPase Sec4p in yeast (Guo et al., 1999b), several exocyst subunits have been shown to interact with small GTPases of the Rab, Rho, Arf, and Ral families, which help regulate exocyst assembly and/or function in yeast and animals (Adamo et al., 1999; Guo et al., 1999a; Robinson et al., 1999; Brymora et al., 2001; Guo et al., 2001; Zhang et al., 2001; Moskalenko et al., 2002, 2003; Prigent et al., 2003; Zhang et al., 2004). Thus, the exocyst appears to have a central role in the mechanism by which small GTPases regulate vesicle trafficking.

Research investigating the exocyst in plants has only recently been reported. Systematic surveys of published plant genomes have identified *in silico* homologs to all eight exocyst subunits (Cvrckova et al., 2001; Jurgens and Geldner, 2002; Elias et al., 2003). Most of the putative plant exocyst genes are encoded by multiple copies, compared to the single copies that predominate in other eukaryotes (Elias et al., 2003; Synek et al., 2006). An important role of the exocyst in plant morphogenesis is beginning to emerge from research characterizing mutations of individual plant exocyst components. In maize, a transposon insertion into a *SEC3* homolog results in the *roothairless1* mutation, resulting in the failure of root hairs to elongate properly (Wen and Schnable, 1994; Wen et al., 2005). Arabidopsis *exo70A1* mutants exhibit a root hair phenotype that is remarkably similar to that of the *roothairless1* mutant, and also display other defects in cell growth (e.g., hypocotyl elongation), and reduced cell number (Synek et al., 2006). Arabidopsis *sec8* mutants demonstrate a defect in the germination and tip growth of pollen tubes (Cole et al., 2005). Intriguingly, electron tomographic analysis of cell plate formation during cytokinesis in Arabidopsis uncovered the existence of 24-nm-long structures that tether membrane vesicles (Otegui and Staehelin, 2004; Segui-Simarro et al., 2004), and that resemble the mammalian exocyst as observed with the electron microscope (Hsu et al., 1998). Recently, the first interaction of a putative plant exocyst subunit with a small GTPase was identified: Arabidopsis SEC3 interacts with plant-specific Rho GTPases (ROPs) via binding to the adaptor protein ICR1 *in vivo* (Lavy et al., 2007). These studies implicate plant exocyst components in polarized growth, a role

that mirrors the one demonstrated in other eukaryotes. However, the existence of the exocyst as a complex in plants has not yet been demonstrated.

Here we combine data from genetic, cell biological, and biochemical analyses, to provide evidence that the plant exocyst subunits work in concert to form a functional complex, essential in both the sporophyte and the male gametophyte for plant cell growth. In the pollen tube, our data suggest that the complex is crucial for maintaining the efficient and tightly-focused functioning of the growth machinery at the tube tip (Cole and Fowler, 2006).

3.3 RESULTS

Weak mutations in two exocyst components enhance the exo70A1 hypocotyl elongation defect in etiolated seedlings

Although strong mutant alleles of the two exocyst subunit genes tested to date cause severe sporophytic (*EXO70A1* - Synek et al., 2006) or gametophytic (*SEC8* - Cole et al., 2005) defects in Arabidopsis, exocyst subunit mutations without phenotypic effects have also been isolated. We hypothesized that if a plant exocyst complex exists *in vivo*, then combination of weak alleles could produce a phenotype that is more severe than that observed for each of the individual mutant alleles alone (i.e., a synergistic effect due to functional interaction). To test this prediction, we evaluated hypocotyl elongation in etiolated Arabidopsis seedlings harbouring mutations in *EXO70A1* and a second exocyst gene. The *exo70A1-1* and *-2* mutations are null alleles that significantly reduce the number and length of hypocotyl cells in etiolated seedlings, resulting in a shortened hypocotyl (Synek et al., 2006). An *exo70A1* mutation was combined with either the partially functional *sec8-4* allele (Cole et al., 2005; and see Table 3.1) or the *sec5a-1* allele (likely to be a null allele for one of the two genes encoding the SEC5 subunit – see below). In contrast to *exo70A1*, single mutant homozygotes for either *sec8-4* or *sec5a-1* do not display an aberrant phenotype during vegetative development. However, the combination of either of these mutations with a mutation of *exo70A1* resulted in a more severe reduction of hypocotyl elongation in etiolated seedlings than the *exo70A1* mutation alone (Figure 3.1). A similar result was obtained when the second partially

functional *SEC8* allele (*sec8-6*) was combined with *exo70A1-2* (data not shown), arguing that this phenotypic enhancement is due to properties of the gene products and not of particular alleles. Such synergism indicates a functional relationship between these putative exocyst complex components.

Exocyst subunit mutations are transmitted at a reduced rate through the pollen

Mutants in Arabidopsis *SEC8* locus have a gametophytically-expressed pollen defect, resulting in reduced transmission of the mutant alleles through the male (Cole et al., 2005). If an exocyst complex functions in the male gametophyte, mutations in other components of the complex should also have a male-specific transmission defect. To test this prediction, we focused our genetic studies on those exocyst genes that appear in the Arabidopsis genome as single copies (*SEC6* and *SEC8*) or as two-copy genes that are not tandemly arranged (*SEC5a/b* and *SEC15a/b*). Initially, *SEC10* was included in this list, but bioinformatic analysis (M. Elias, personal communication) along with analyses of several insertion alleles showed that this locus consists of two tandemly-repeated genes (data not shown). Transmission frequencies were determined for T-DNA insertion mutants of exocyst genes *SEC6*, *SEC15a*, *SEC5a*, and *SEC5b*, as well as for the *sec5a-1 sec5b-1* double mutant. Each mutant allele was reciprocally outcrossed to wild-type plants for at least three generations (Table 3.1). In each instance the mutant allele was transmitted through the female gametophyte at the expected frequency. However, in outcrosses, neither of the two independent alleles for both *SEC6* and *SEC15a* was transmitted through the pollen. Similarly, the *sec5a-1* and *sec5b-1* alleles were never transmitted through the pollen together, although neither single mutation demonstrated a transmission defect (data not shown), likely reflecting a redundant function for these genes in pollen.

The transmission defect of the *sec6-1* and *sec6-2* mutants was complemented by expression of the wild-type gene driven by the pollen-specific *LAT52* promoter (Supplemental Figure 1 and Supplemental Table 1), as had been previously demonstrated for *sec8-1* and *sec8-3* (Cole et al., 2005). RT-PCR assessment of RNA extracted from plants homozygous for the *SEC5a*, *SEC5b* or *SEC15a* mutant alleles indicates that these

do not produce full-length transcripts (Supplemental Figure 2). (The *SEC15a* homozygous mutants arose at low frequencies from unassisted self-crosses of heterozygotes, likely due to decreased pollen competition in such crosses – Cole et al., 2005). The altered *SEC5a*, *SEC5b* and *SEC15a* transcripts are predicted to encode truncated proteins that appear likely to be functionally impaired. Overall, the genetic evidence demonstrates that strong mutations in any of four putative complex components - SEC5, SEC6, SEC8, or SEC15a - result in a similar severe pollen-specific transmission defect. Furthermore, the molecular evidence suggests that this phenotype is associated with null, or near-null, alleles.

Mutations in SEC6, SEC8, SEC15a and SEC5 dramatically affect both pollen germination and pollen tube growth

We were interested to know if the transmission defect observed for components of the putative exocyst complex was associated with similar pollen developmental phenotypes. The male-specific transmission defect in *SEC8* mutants is associated with defects in pollen germination and pollen tube growth (Cole et al., 2005). However, limitations in the earlier studies (e.g., no homozygous plants were available for the most severe *SEC8* alleles) prevented determination of the null phenotype in the pollen tube. To overcome these limitations, representative alleles for each of the four exocyst components with transmission defects were crossed into the *quartet1* (*qrt1*) background. In the *qrt1* background all four products of a meiosis remain attached to each other (e.g., exactly two wild-type and two mutant pollen grains from a heterozygous plant), allowing direct observation of phenotypes in severe gametophytic mutants (Johnson-Brousseau and McCormick, 2004; Preuss et al., 1994).

Staining of mature pollen from plants homozygous for the *qrt1* mutation and heterozygous for mutations in *SEC6*, *SEC8*, or *SEC15a* with DAPI revealed two sperm cell nuclei and a vegetative nucleus in each of the pollen grains in a quartet, and none of the grains showed obvious developmental defects. This indicates that none of these mutations severely affect pollen grain development, including its mitotic divisions.

To assess for a germination defect, pollen from *qrt1* plants that were heterozygous for a mutation in *SEC6*, *SEC8*, or *SEC15a* was germinated *in vitro* and compared to the pollen of a *qrt1* sibling lacking the exocyst mutation. Due to the 2:2 distribution of wild-type versus mutant, germination of three or four pollen grains in a quartet from a heterozygote requires the germination of one or both mutant pollen grains. Thus, a pollen germination defect would reduce the relative frequency of quartets with 3 or 4 grains germinated. Indeed, we found that the *sec6-1*, *sec6-2*, *sec8-1*, *sec8-3*, *sec15a-1*, and *sec15a-2* mutant alleles were associated with a significant reduction in the percentage of germinating quartets with 3 or 4 grains germinated, compared to their wild-type siblings (mutant frequencies: 1-7%, wild-type frequencies: 10-30%; see Table 3.2). Only quartets from heterozygotes harbouring the weak *sec8-4* allele were not significantly different from wild-type.

Pollen containing mutations of both *SEC5* genes was studied by generating plants that were homozygous for *sec5a-1* and heterozygous for *sec5b-1* in the *qrt1* background. These were compared to pollen from *quartet1* siblings that had a mutation in only one of the *SEC5* genes, or in neither. The transmission data predict that a mutant pollen phenotype should only be observed in double mutant pollen grains. Indeed, the frequency of 3 and 4 pollen grain-germinating quartets was not significantly affected by either single mutant (*sec5a-1*: 18%, n=367; *sec5b-1*: 22%, n=223; wild type: 23%, n=635). In contrast, pollen from plants homozygous for *sec5a-1* and heterozygous for *sec5b-1* demonstrated a severe germination defect, with only 1.8% of quartets having 3 or 4 grains germinated (Table 3.2).

These analyses revealed that, although mutation of any of the four exocyst components dramatically reduced germination, mutant grains can occasionally produce a pollen tube. Despite the rarity of such events, the arrangement of pollen into quartets allowed us to identify a defective phenotype associated with the mutant pollen tubes, by assessing pollen tube length and width in quartets with at least 3 germinated grains. In all such cases, one or (rarely) two aberrant pollen tubes were observed (Figure 3.2B-E). The length and width of the shortest tube in quartets with 3 or 4 germinated grains from mutant heterozygotes (or *sec5a-1* homozygous; *sec5b-1* heterozygous plants) and their

corresponding wild-type siblings were determined. For all four exocyst components, the mutants were associated with significantly shorter and thicker pollen tubes than the shortest pollen tubes produced by the wild type (Figure 3.2G, H), confirming that this short/wide phenotype is caused by the exocyst mutations. The aberrant pollen tubes were only 15-25% as long as the average wild-type pollen tubes (Figure 3.2I), and occasionally irregularly shaped, with the observed range of shapes similar for all mutations evaluated. Again, only in *sec8-4* quartets were the pollen tubes morphologically indistinguishable from wild-type (Figure 3.2F). Taken together, these data show that mutation of each of four putative exocyst components – SEC6, SEC8, SEC15a, or SEC5 – results in similar developmental defects in both pollen germination and polarized pollen tube growth.

Co-localization of exocyst subunits at the tip of growing pollen tubes

Defects in pollen germination and pollen tube growth observed in Arabidopsis exocyst subunit mutants imply a common function for these proteins in pollen tube germination and tip growth. If acting as a complex, all exocyst subunits should show some overlapping localization *in vivo*. Subunit localization was investigated using indirect immunofluorescence in tobacco pollen tubes, taking advantage of their larger size and more robust *in vitro* germination. Mouse polyclonal antibodies raised against recombinant Arabidopsis proteins SEC6 and EXO70A1, and a rabbit polyclonal antibody raised against an Arabidopsis SEC8 peptide, all recognized homologs of these subunits in tobacco (data not shown). Preimmune sera for these antibodies showed a very weak homogenous background signal lacking any specific pattern (Supplemental Figure 3).

As predicted, based on a function in pollen tube tip growth, all three antibodies revealed predominant tip-focused localization of the exocyst subunits that they recognize (Figure 3). Bright tiny dots forming a granular pattern could be discerned within the apical signal. Behind the intense signal at the tip, the staining is much weaker. However, sparse small spots are also distributed in the cytoplasm and especially along the plasma membrane within the entire tube length.

We took advantage of the distinct sources for anti-SEC8 (rabbit) versus anti-EXO70A1 and anti-SEC6 (mouse), and demonstrated co-localization of SEC8 and

EXO70 proteins, and SEC8 and SEC6 proteins, respectively, by double-labeling (Figure 3G, H). We initially observed that only the SEC6 signal was visible in the tip of pollen tubes when labeled by both anti-SEC6 and anti-SEC8 simultaneously, even though either antibody stained the tip when used alone (Figure 3.3C-F). When the procedure was adjusted such that anti-SEC8 was added first, followed by the addition of anti-SEC6 one hour later, both labels were visualized at the pollen tube tip (Figure 3.3H). One possible explanation for these observations is that the SEC6 antibody spatially blocks the epitope recognized by the SEC8 antibody due to close association of these two components within the exocyst complex.

When we examined subcellular distribution of SEC6 and SEC8 in germinating tobacco pollen we observed maximum of the signal in the 100,000g pellet fraction (Figure 3.4) containing all post-nuclear membranes. In both cases, only weak signal was observed in the cytosolic fraction. Moreover, the signal increased in both cases during the first 60 min of pollen germination indicating simultaneous accumulation of exocyst subunits in the membrane fraction, and implying *de novo* synthesis of these subunits.

Overall, we conclude that the exocyst subunits SEC6, SEC8, and EXO70 have an overlapping localization pattern predominantly to the tips of growing pollen tubes, consistent with a role in the intensive exocytosis at that site.

Chromatographic fractionation reveals the plant exocyst complex exists as a biochemical entity

Shared pollen phenotypes, co-localization at the growing pollen tube tip, and the synergism of mutations in the reduction of hypocotyl elongation provide strong, but indirect, evidence that the exocyst subunits form a functional exocyst complex in plants. We adapted chromatography methods previously used to successfully characterize the exocyst complex in yeast and mammalian cells (TerBush et al., 2001; Hsu et al., 1996) to provide more direct evidence for the existence of the exocyst complex as a biochemical entity in plant cells. *Arabidopsis thaliana* suspension culture in its exponential growth phase was chosen as a source for exocyst complex purification. This cell type expresses exocyst subunit genes at high mRNA levels (Supplemental Figure 3.4), and preliminary

experiments showed co-sedimentation of the putative complex with the microsomal fraction after centrifugation at 100,000 g (Figure 3.4). Therefore, we used a crude total cell lysate depleted of heavy membranes but containing microsomes for our chromatographic analyses.

To detect the complex subunits, we used the three antibodies already described above (anti-EXO70A1, anti-SEC6, and anti-SEC8), as well as anti-SEC3, anti-SEC5, and anti-SEC15a. Multiplication of several exocyst subunits in the Arabidopsis genome raises a question about antibody specificity. Based on high sequence similarity, we expect that polyclonal antibodies against SEC3 and SEC5 recognize both isoforms of respective subunits. The polyclonal anti-SEC15a was prepared against a peptide specific for SEC15a, thus we do not expect cross-reactivity with SEC15b. On the converse, we have confirmed using an *exo70A1* mutant that the EXO70A1 antibody is specific to EXO70A1 (at least in the sporophyte), as it does not recognize any other proteins on Western blots (not shown).

We initially performed size exclusion gel chromatography (SEGC) on a HiLoad SUPERDEX 200 column. When the resultant protein fractions were subjected to SDS-PAGE and Western blotting, most of the exocyst subunits were detected in high molecular weight fractions. Figure 5A shows that signals of all polyclonal antibodies form peaks with a maximum in the same fractions, suggesting a complex size of around 900 kDa. These peaks are well behind the total protein maximum (Figure 3.5A), suggesting specific enrichment of all putative exocyst subunits detected in these fractions. Incubation of the total lysate with 0.5M phosphate in the lysis buffer led to similar results after SEGC, SDS-PAGE, and Western blots, suggesting that the presence of phosphate does not affect complex stability (data not shown).

We next employed three-step purification based on the method described by Hsu et al. (1996) to purify the mammalian exocyst. We started with high-capacity affinity chromatography on polyphosphate hydroxyapatite matrix (hydroxyapatite Bio-Gel) with discontinuous phosphate elution. All fractions were subjected to SDS-PAGE, Western blotting, and analyzed by anti-SEC6 and anti-SEC8 antibodies. Corresponding fractions containing both SEC6 and SEC8 were collected and prepared for the second purification

step by dialysis. In the second purification step, the dialyzed fractions from the affinity chromatography were loaded onto an ion exchange chromatography column (Fractogel EMD-TMAE). All expected subunits of Arabidopsis exocyst have a calculated pI under 7, with values ranging mostly between 5.2 and 5.8. Anex resin was then used to isolate the exocyst complex in the buffer with almost neutral pH. Fractions containing exocyst antibody signals were eluted with the salt concentration between 0.35 M and 0.42 M. Western analysis of these fractions demonstrated a weakened signal for the SEC5 and especially SEC15a proteins, possibly due to a partial loss of these subunits during this purification step.

The fractions obtained from ion exchange chromatography were then subjected to SEGC and Western analysis to complete the third step of the purification. Figure 3.5B shows that the distribution of the antibody signals demonstrates again co-fractionation of exocyst subunits. All signals had only one maximum, and this occurred in fractions corresponding to a molecular mass of 750 kDa. Consistent with a smaller mass for the three-step purified complex, SEC15a could not be detected, and the SEC5 signal was very weak, requiring substantially longer exposure time. This observation suggests that some subunits may form a stable core of the complex, whereas other subunits (e.g., SEC15a, SEC5) are more loosely associated, at least under these experimental conditions. Importantly, co-fractionation of five exocyst subunits (SEC3, SEC5, SEC6, SEC8 and EXO70A1) was maintained through all three steps of purification.

To complement identification of exocyst subunits by Western blot following partial purification, we used liquid chromatography electrospray ionization tandem mass spectrometry (LC-ESI MS/MS) to analyze protein bands of expected molecular weights following the three-step purification. This approach confirmed that the exocyst-positive fractions (by Western blot) contain the SEC3a, SEC6 and SEC8 subunits. In addition, SEC10 (for which we had no antibody) was also identified in these fractions (Supplemental Table 3). Taken together, using a combination of analytic methods we detected SEC3, SEC5, SEC6, SEC8, SEC10, SEC15, and EXO70A1 being components of the same protein complex.

Blue native electrophoresis and the yeast two-hybrid assay provide independent support for the Arabidopsis exocyst

To confirm data obtained from the chromatographic approach, we employed two additional methods. First, a blue native polyacrylamide gel electrophoresis (BN-PAGE) based on a mild solubilization in detergent and treatment with the dye Coomassie Blue G250 was used (Schägger and von Jagow, 1991; Berghöffer and Klösgen, 1999; Werhahn and Braun, 2002). After the solubilization with mild detergent dodecylmaltoside (DDM) in concentrations of total protein (TP) to DDM ratio of 1.33 and low NaCl concentrations (10 mM and 30 mM), a range of high molecular mass complexes was detected for four of the five exocyst complex components tested: SEC3, SEC6, SEC8 and EXO70A1 (Figure 6A). SEC5 was found only as a monomer (data not shown). Under the conditions of higher detergent concentrations (TP:DDM ratio of 0.67) and no additional salt, SEC6 and EXO70A1 were predominantly present in small, rather than in high molecular complexes (Figure 3.6B). Notably, we observed a well-defined complex detected only by anti-SEC6 that could represent SEC6 dimers. In contrast, the SEC3 subunit was still found in larger complexes under these conditions, although running at a lower mass than at lower detergent concentrations. Again, this is consistent with loss of some subunits (e.g., SEC6, EXO70) from the complex under certain conditions (see Discussion).

To further support complex formation, the interaction abilities of one of each type of the expected exocyst subunits were tested using the yeast two-hybrid assay. We used the GAL4 system, based on the split GAL4 transcription factor controlling expression of reporter genes (Figure 3.7). We found that both SEC10 and EXO84b showed high activation capacity when fused with the DNA-binding domain (DNA-BD) alone, and thus were unsuitable as bait proteins in this assay; EXO84b also showed promiscuous interactions when fused with the activation domain (AD). However, we observed two pairs of strongly interacting subunits: SEC15b/SEC10 and SEC6/SEC8 (Figure 3.7). Both pairs were confirmed by β-galactosidase assay as well as by the double auxotrophic marker.

3.4 DISCUSSION

In non-plant eukaryotic cells the octameric exocyst complex facilitates the targeting and tethering of secretory vesicles to the plasma membrane, and thereby is integral to a broad range of physiological processes requiring polarized exocytosis. Comparative genomic and phylogenetic analysis across 17 eukaryote genomes suggests that the exocyst, like the other tethering complexes, is ancient, originating very early in eukaryotic evolution (Koumandou et al., 2007). The existence of such a complex in plants has been anticipated by the discovery that genes orthologous to those encoding the eight exocyst components in yeast and mammals are present in several plant genomes, and are expressed in Arabidopsis and rice. Here we have provided biochemical evidence, supported by genetic analysis, phenotypic observations, and cell biological experiments, to conclude that the exocyst does indeed function as a complex in plants. The results of these various approaches, shown with respect to the putative complex subunits, are summarized in Table 3.3.

Composition of the plant exocyst complex

Size exclusion gel chromatography revealed co-purification in a high molecular weight fraction of all exocyst subunits for which antibodies were available, namely: SEC3, SEC5, SEC6, SEC8, SEC15a, and EXO70A1. Mass spectrometry confirmed the presence of SEC3a, SEC6, and SEC8 in the same high molecular weight fraction, and moreover identified SEC10, for which we did not have any antibody.

The maxima of all exocyst subunits signals are localized to the same fraction, corresponding to a molecular weight (MW) of approximately 900 kDa. However, the predicted size of the plant exocyst is 760 kDa, assuming that it contains one member of each subunit, consistent with the characterized exocyst complexes in yeast and mammals (TerBush et al., 1996; Hsu et al., 1996; Kee et al., 1997). A similar observation was made in yeast where the MW of soluble 19.5S particles, later identified as the exocyst complex, was reported to be between 1000-2000 kDa although the calculated MW was only 834 kDa (Bowser and Novick, 1991; Bowser et al., 1992). Also, chromatography results

indicated the mammalian exocyst to have a MW of 1000-1500 kDa, compared to the calculated 743 kDa (Yeaman et al., 2004). The difference between observed and calculated MW could be explained by association of additional interacting proteins with the complex; for example, E-cadherin co-immunoprecipitates with the mammalian exocyst (Yeaman et al., 2004). In Arabidopsis, the ICR1 adaptor protein was recently identified to interact with SEC3, providing a link to activated ROP (Rho of plants) GTPases (Lavy et al., 2007). Therefore, association of such proteins with the exocyst during purification is possible. Alternatively, the larger size indicated by SEGC may simply be a result of the predicted rod-like structure of the exocyst (Hsu et al., 1998; reviewed in Munson and Novick, 2006) inhibiting its mobility through the pores of the size exclusion matrix. Finally, the plant exocyst could have more than one member of each subunit, or additional, plant-specific subunit(s). However, the composition of the exocyst and other 'quatrefoil' tethering complexes seems to be highly conserved in evolution (Whyte and Munro, 2002; Koumandou et al., 2007).

Use of a three-step purification process (Figure 3.5B) resulted in a shift of the exocyst signal maxima toward a lower molecular mass, indicative of a reduction in the size of the complex. We hypothesize that some subunits may form a stable core of the complex that is maintained through the three-step purification, whereas other subunits are more loosely associated, at least under these conditions. Consistent with this hypothesis, higher-salt (0.35 M NaCl) conditions during ion exchange chromatography induced the loss of SEC5 and SEC15a, while leaving the remaining core complex intact. Similarly, results from Blue native electrophoresis demonstrated that increasing detergent concentration also destabilizes the complex (Figure 3.6B), with the notable loss of SEC5 in high molecular complexes. The yeast exocyst also shows a MW decrease under high salt conditions (0.5 M NaCl) at pH 8.0 (Bowser et al., 1991). However, unlike the yeast exocyst (TerBush et al., 2001), the plant exocyst did not demonstrate complex instability in phosphate buffer or at pH 8.0. A range of high molecular weight complexes (> 500 kDa) associated with exocyst subunits was detected by BN-PAGE, possibly as result of both the method used and the dynamics of the exocyst structure in plant cells. Thus, BN-

PAGE provides independent verification that subunits of the exocyst do form high molecular weight complexes.

Yeast two-hybrid analysis of plant exocyst components revealed strong interactions between SEC15b and SEC10, and between SEC6 and SEC8. These pairwise interactions are conserved in both yeast and animals, although in yeast the SEC6-SEC8 interaction was identified using immunoprecipitation or pull-down assay rather than the two-hybrid assay (Guo et al., 1999a; Mattern et al., 2001; Sivaram et al., 2005). The overall number of two-hybrid interactions identified so far among plant exocyst subunits in our experiments is similar to those reported for yeast (Guo et al., 1999a), but lower than those reported for animals (Matern et al., 2001). The notion of direct interaction between SEC6 and SEC8 subunits *in vivo* is further supported by the finding that the SEC6 antibody blocks the labeling of the pollen tube tip by the SEC8 antibody, unless anti-SEC8 is added before anti-SEC6 (Figure 3.3). Obstruction of the epitope recognized by anti-SEC8 by SEC6 antibody implies that the two proteins are located in close proximity, perhaps with the SEC8 epitope lying deeper within the exocyst structure.

A prerequisite for the exocyst to function as a complex is the co-localization of its components to regions of the cell where it is active, e.g., sites of intensive secretion. We have demonstrated by indirect immunofluorescence that SEC6, SEC8, and EXO70 all localize to such a site, the tobacco pollen tube tip, a region of vigorous polarized exocytosis. Intriguingly, our time-course evaluation of SEC6 and SEC8 accumulation in tobacco pollen shows an increase in both proteins during the first 60 minutes after germination (Figure 3.4). Although two pools of the exocyst, cytosolic and membrane-bound, have been reported in mammals and yeast (Bowser et al., 1991; Yeaman et al., 2001; Yeaman, 2003), most of the signal we observed was localized to the pellet fraction (Figure 3.4). This is consistent with the observation that upon a polarization signal in epithelial cells, the exocyst is massively recruited to plasma membrane (Yeaman et al., 2001). However, part of this signal still may represent the soluble exocyst fraction co-sedimenting with membranes at 100,000 g (Yeaman, 2003). Overall, our data clearly shows simultaneous accumulation of SEC6 and SEC8 in germinating tobacco pollen,

implying a functional link between these two subunits in polarization of the vegetative cell during pollen grain germination.

It seems that exocyst subunit interactions and complex architecture differ somewhat between animals and yeast (e.g. Guo et. al, 1999a; Matern et al., 2001; Moore et al., 2007). Our data for Arabidopsis, concerning exocyst size, more labile association of some subunits, and lack of two-hybrid interactions reported in yeast and animals support the possibility that the exocyst complex of land plants has yet another distinct architecture, perhaps one that allows functional exploitation of the multiple subunit isoforms (Synek et al., 2006) and adaptor proteins encoded by plant genomes (Lavy et al., 2007).

Genetic analyses imply an important role for the plant exocyst in cell growth

Yeast null mutants in exocyst genes are nonviable, whereas temperature-sensitive mutants block exocytosis as manifested by accumulation of secretory vesicles in the cytoplasm (Novick et al., 1980; TerBush et al., 1996; Finger and Novick, 1997; Guo et al., 1999a). The knockout of the Sec5 subunit as well as depletion of the Sec10 mRNA in *Drosophila* resulted in early post-embryonic lethality (Andrews et al., 2002; EauClaire and Guo, 2003; Murthy et al., 2003). Similarly, mice with a mutant allele for the Sec8 subunit died during an early stage of embryogenesis (Friedrich et al., 1997). Mutations in both *Drosophila* and mouse Sec15 led to developmental defects caused by affected membrane recycling (Lim et al., 2005; Jafar-Nejad et al., 2005; Garrick and Garrick, 2007).

In plants, genetic analyses of the function of exocyst subunits SEC3, SEC8 and EXO70A1 were already initiated (Cole et al., 2005; Wen et al., 2005; Synek et al., 2006). In this report we further extended this effort. SEC5, SEC6, SEC8, and SEC15a subunits were most amenable because they are encoded by one- or two-copy genes that are not tandemly duplicated (like *SEC3* and *SEC10*), and T-DNA insertional lines were available for these loci. Mutations in any of these four exocyst components result in a similar pollen-specific transmission defect. By placing the mutant lines in a *quartet1* background, it was possible to observe that each of these mutations is associated *in vitro*

with reduced pollen germination and defective polarized growth of the pollen tube as exemplified by aberrant short and wide pollen tubes. We previously proposed that the exocyst is one component of a network of signaling pathways (the Localization Enhancing Network, Self-sustaining, or LENS), that acts to focus exocytosis and growth to the tip of pollen tubes and root hairs (Cole and Fowler, 2006). The defective polarized growth of the pollen tube associated with mutations in these four exocyst components supports such a role for the complex, assuming that when any of its subunits is disrupted the entire complex becomes nonfunctional. However, it should be noted that the aberrant pollen tubes for each of the four mutated subunits retain some polarity. Among known pollen mutants, the exocyst-loss phenotype is perhaps most reminiscent of pollen tubes overexpressing a dominant-negative mutant ROP GTPase (reviewed in Yang, 2002). Although a functional connection between ROP and the exocyst has not been shown in pollen, the linkage between them in vegetative cell polarized growth (Lavy et al., 2007) makes this an attractive hypothesis.

The existence of a full octameric exocyst complex functioning in plant pollen predicts that mutations or silencing of other exocyst components will demonstrate similar defects. Indeed, our preliminary analyses have revealed equal distribution of heterozygous and wild-type plants in the progeny of self-pollinated *EXO84/exo84b* heterozygotes (WT: 48%, het: 52%, n=120). Although detailed analysis of these mutants is in progress, this phenotype seems very likely to result from a pollen-transmission defect. Segregation of mutants in the remaining two *EXO84* paralogs, *EXO84a* and *EXO84c*, is normal (data not shown).

The role of the exocyst in plants is not limited to pollen, as polarly growing root hairs are short in the *rth1* mutant, a maize *SEC3* homolog, and in Arabidopsis *exo70A1* mutants (Wen and Schnable, 1994; Wen et al., 2005; Synek et al., 2006). Mutation in *EXO70A1* also display other defects in cell growth, e.g. etiolated hypocotyl elongation, stigmatic papillae elongation, and reduced cell number (Synek et al., 2006). We utilized the *exo70A1*-related defect in hypocotyl elongation to demonstrate that mutations in two exocyst components have a synergistic effect, as would be predicted if the two components are functioning members of the same complex. The observed synergism of

the partially functional alleles, *sec8-4, sec8-6,* or *sec5a-1* with an *exo70A1* mutant supports a role for the exocyst complex in sporophytic cell growth.

We also find it noteworthy that the exocyst mutants do not show two other phenotypes that might have been predicted based on earlier evidence. Although there is evidence of exocyst-like structures at the somatic and post-meiotic cell plates in Arabidopsis (Otegui and Staehelin, 2004; Segui-Simarro et al., 2004), none of the four strong gametophytic mutants show evidence of cytokinetic defects during pollen development. In addition, none of these mutants are associated with transmission defects through the female gametophyte,suggesting that the exocyst does not play an essential role in its growth or development.

Finally, despite the fact that EXO70A1 appears to be the predominant EXO70 isoform in Arabidopsis, *EXO70A1* is poorly expressed in pollen and mutations in the gene do not cause a transmission defect (Synek et al., 2006). *EXO70* proliferated into 23 paralogous genes in Arabidopsis (Elias et al., 2003), so it is highly probable that other EXO70 isoforms function as genuine components of the exocyst complex in pollen. Based on analysis of expression data, at least six EXO70 paralogs are transcriptionally active in pollen (Synek et al., 2006). While single-copy plant exocyst genes are expressed in both sporophyte and gametophyte, the multiplied genes typically are expressed at different levels in different tissues, with some overlap in expression of paralogs, particularly of those for *EXO70* (Cole et al., 2005; Synek et al., 2006). This raises the possibility that plant cells and tissues might be endowed with different versions of the exocyst, each performing specific functions. Consequently, the plant exocyst may have evolved distinctive structures and functions, compared to the single complex of fungi and mammals.

Overall, we have demonstrated that an exocyst complex functions in plants, opening the doorway to a host of related questions. Data available so far hints that we might expect the involvement of exocyst complex not only in cell growth, but also in cell wall formation, meristem regulation, polar auxin transport and general cell defense against pathogen attack.

3.5 MATERIALS AND METHODS

Plant material and growth conditions

Lines of Columbia-0 ecotype of *Arabidopsis thaliana* L. Heynh with T-DNA insertions as well as the *quartet1* mutant (*qrt1*) were obtained from the SALK Institute (Alonso et al., 2003) and GABI-Kat (Rosso et al., 2003). See Table 4 for gene and line codes. The location of each T-DNA insertion within a gene of interest was verified by sequencing from each end of the insert. The Arabidopsis suspension culture was derived from vegetative tissue of the Columbia ecotype. For indirect immunofluorescence experiments on pollen, we exploited mature pollen of *Nicotiana tabacum* cv. Samsun.

Arabidopsis seeds were surface-sterilized, stratified at 4 °C for 3-5 days, and planted on growth media (1x MS, 2% (w/v) sucrose, and vitamins) or soil as previously described (Cole et al., 2005). Plants were grown in a climate chamber at 22 °C under long-day conditions (16 h of light per day), with the exception of dark grown seedlings used in hypocotyl elongation experiments. In the hypocotyl elongation experiments, surface sterilized, stratified, and plated seeds were placed in a lighted incubator at 22 ºC for 2-4 hours to stimulate germination, and then wrapped in foil, oriented vertically, and placed in a dark box in the incubator. After 5 days, images of the hypocotyls were captured with a Moticam 1000 camera attached to a Zeiss Stemi SV 11 dissecting microscope. Measurement of hypocotyl lengths was performed from the digital photographs using ImagePro software (MediaCybernetics, www.mediacy.com).

Pollen germination experiments

Flowers shedding pollen from Arabidopsis plants of desired genotype were placed in each well of a 96 well plate (1 flower per well) containing 50 µl liquid pollen germination medium (18% sucrose, 0.01% boric acid, 2 mM $CaCl_2$, 1 mM $Ca(NO_3)_2$, 1 mM $MgSO_4$, with pH adjusted to 6.5 with KOH). Each plate was incubated at 22 ºC overnight. A researcher blind to the genotypic source of the flowers microscopically screened the plate for wells with greater than 50 percent of the quartets showing germinated pollen grains. For these wells, the number of quartets showing 1, 2, 3, or 4

pollen grains germinated were counted, and images of quartets with three or four grains germinated were captured with a SPOT camera for subsequent measurement of pollen tube widths and lengths with ImagePro software. DAPI staining of ungerminated quartet pollen was performed as previously described (Cole et al., 2005).

Antibodies preparation

Polyclonal mouse anti-AtSEC3a, anti-AtSEC5a and anti-AtEXO70A1 were raised against full length proteins expressed in *E. coli*. The anti-AtSEC3a antibody was affinity purified on Ni-NTA agarose according to the manufacturer protocol (Qiagen). Polyclonal mouse anti-AtSEC6 antibody was prepared against truncated AtSEC6Δ protein (AtSEC6 cDNA cleaved by BamHI and religated).

Polyclonal anti-AtSEC8 was raised by synthesis of a peptide (C-LREELARIDESWAAA) corresponding to amino acids 16-30 of the predicted Arabidopsis protein, conjugation of the peptide to KLH via the N-terminal cysteine, immunization of rabbits using a standard protocol, and affinity purification of the antibody against the peptide on a column (Genemed Synthesis Inc., San Antonio, TX – www.genemedsyn.com). Polyclonal anti-AtSEC15a was raised against a peptide (CZ-TAKKKSMDMLKKRLKEFN) corresponding to amino acids 772-789 (the C-terminus) of the predicted Arabidopsis protein, which was conjugated to KLH via the N-terminal cysteine, with the aminocaproic acid ('Z') serving as a spacer between the cysteine/KLH and SEC15a sequence. Chickens were immunized using a standard protocol, and the antibody was affinity-purified against the peptide on a column (Aves Labs Inc., Tigard, OR - www.aveslab.com).

Indirect immunofluorescence on pollen tubes

Tobacco pollen was cultivated in germination medium (10% sucrose, 0.01% H_3BO_3) for 1 h, and then fixed with 3.7% formaldehyde in PEM (50 mM PIPES, 5 mM EGTA, 5 mM $MgSO_4$, pH 6.9) containing 10% sucrose for 1 h (equal volumes of double-concentrated fixation solution and pollen suspension were mixed together). After two rinses with PEM and one rinse with PEM/PBS (1:1), pollen was treated by the cell wall

degrading enzyme mix (0.3% cellulase, 0.3% pectinase, 0.05% pectolyase in PBS) for 20 min. Then Tween 20 was added to final concentration of 0.05% and it was incubated for 10 min. After incubation in 1% bovine serum albumin (BSA) in PBS for 30 min, specimens were processed as follows: 1) overnight incubation with primary antibody (mouse anti-SEC6, anti-EXO70A1 and anti-tubulin DM1 (Sigma, T-9026), or rabbit anti-SEC8, respectively) in PBS containing 1% BSA; 2) three rinses in PBS for 10 min; 3) 1-hour-incubation with FITC-conjugated sheep anti-mouse antibody (Sigma, F-6257) or TexasRed-conjugated donkey anti-rabbit antibody (Santa Cruz Biotechnology, SC-2784), both diluted 1:150; 4) three rinses in PBS for 10 min. Finally, pollen was mounted into anti-fade mounting medium (50% glycerol with 0.1% p-phenylenediamine in PBS) and observed using a fluorescence microscope Olympus BX51 and a confocal laser scanning microscope Zeiss LSM 5 Duo. The anti-tubulin antibody served as a positive control for the labeling procedure, revealing a pattern of tubulin cytoskeleton typical for tobacco pollen tubes (Supplemental Figure 3).

Chromatographic purification

Hydroxyapatite Chromatography (HC). Seven-day-old Arabidopsis suspension culture (90 g) was ground in liquid nitrogen with a pestle in a mortar. Then 1 ml of Sec6/8 buffer (20 mM HEPES, pH 6.8; 150 mM NaCl; 1 mM EDTA; 1 mM DTT; 0.5% Tween 20) supplemented with 1x PIC (Sigma) per 1 g of the fresh weight was added and grinded again. The total lysate was sequentially centrifuged at 5000 g, 10 min, and 30000 g, 30 min at 4°C. Supernatant was then supplemented with 110 mM sodium phosphate (final concentration) and applied to 25 ml hydroxyapatite column (BioRad), which was equilibrated with Sec6/8 buffer supplemented with 110 mM sodium phosphate at room temperature (flow rate 24 ml/h). The column was washed with 70 ml of wash buffer (WB; 0.15 M sodium phosphate, pH 7.4; 0.15 M NaCl, 1 mM DTT) and elution was done in ten 5 ml steps by WB with sodium phosphate concentration between 0.2-0.65 M, pH 7.4. Fractions containing exocyst subunits (Western analysis) were pooled and dialyzed twice against 1 l of 20 mM Tris, pH 6.8; 100 mM NaCl; 0.2 mM EDTA, and 0.5 mM DTT.

Ion Exchange Chromatography (IEC). Dialyzed hydroxyapatite fractions were diluted with the equal volume of 20 mM Tris, pH 6.8 and loaded on the 3 ml Fractogel EMD TMAE (S) column (Merck) equilibrated with 10 ml of 20 mM Tris, pH 6.8, 50 mM NaCl, and 1 mM DTT. The column was then washed with 20 ml of equilibration buffer and eluted with 3 ml fractions containing 150-450 mM NaCl (50 mM increment) in equilibration buffer. All was done at 4 °C using flow rate 24 ml/min.

Size Exclusion Gel Chromatography (SEGC). Pooled IEC fractions containing exocyst subunits or 80mg of total protein (in one-step analysis) were applied on equilibrated (Sec6/8 buffer) Superdex300 HiLoad 26/60 column (Pharmacia) at 4°C, flow rate 60 ml/min. Protein concentration in eluate was measured with a UV detector (254 nm). 5 ml fractions were taken and Western-analyzed.

Western Blot Analysis

Appropriate volume of the sample was acetone-precipitated and loaded on 10% SDS- PAGE. Proteins were transferred on nitrocellulose membrane and blocked overnight with 5% non-fat dry milk in TBS. Primary antibody dilutions in TBS supplemented with 0.5% Tween 20 were as follows: polyclonal mouse anti-AtSEC3a 1:500, polyclonal mouse anti-AtSEC5a 1:1500, polyclonal mouse anti-AtSEC6 1:1000, polyclonal rabbit anti-AtSEC8 1:500, polyclonal chicken anti-AtSEC15a 1:500. Appropriate secondary HRP-conjugated antibodies were applied followed by chemiluminiscent ECL detection (SuperSignal, Amersham).

nanoHPLC-ESI-MS/MS mass spectrometry analysis

Protein bands were excised from the SDS-PAGE gel in the expected area visible after Coomassie staining after the last step (i.e., SEGC fractionation) of the three-step procedure. Excised proteins were digested in-gel using trypsin (porcine, sequencing grade, modified; Promega, Mannheim, Germany) overnight at 37°C. Reversed-phase nano-LC-MS/MS was performed using an Ultimate nanoflow LC system (Dionex / LC Packings,Idstein, Germany) containing the components Famos (autosampler), Switchos (loading pump and switching valves), and Ultimate (separation pump and UV-detector).

The LC system was coupled to a QSTAR Pulsar i hybrid QqTOF masspectrometer (Applied Biosystems / MDS Sciex, Darmstadt, Germany), equipped with a nanoelectro-spray ion source (Column Adapter (ADPC-PRO) and distal coated SilicaTips (FS360-20-10-D-20) (both from New Objective, Woburn, USA)).

Briefly, the tryptic peptide mixtures were autosampled at a flow rate of 30 µl/min in 0.1% aqueous trifluoroacetic acid, and desalted on a PepMap C18 trapping cartridge (LC Packings). The trapped peptides were eluted and separated on the analytical column (PepMap C18, 75 µm i.d. *x* 15 cm; LC Packings) using a linear gradient of 7–50% solvent B (acetonitrile 84% (v/v) in 0.1% (v/v) formic acid) for 27 min at a flow rate of 220 nl/min, and ionized by an applied voltage of 2200 kV to the emitter.

The mass spectrometer was operated in data-dependent acquisition mode to automatically switch between MS and MS/MS. Survey MS spectra were acquired for 1.5 s, and the three most intense ions (doubly or triply charged) were isolated, and sequentially fragmented for 1.5 s by low-energy collision-induced dissociation. All MS and MS/MS spectra were acquired with the Q2-pulsing function switched on, and optimized for enhanced transmission of ions in the MS (m/z 400–1000) and MS/MS (m/z 75–1300) mass ranges.

Proteins were identified by correlating the ESI-MS/MS spectra with the NCBI.nr-protein sequence database *Viridiplantae* (green plants) as of 07/25/07 using the MOWSE-algorithm as implemented in the MS search engine MASCOT (Matrix Science Ltd. London, UK, Perkins (Perkins et al., 1999)). All results from 2-dimensional electrophoresis and mass spectrometry and all search results where stored in a LIMS-database (Proteinscape 1.3, Bruker Daltonics, Bremen, Germany).

Blue native electrophoresis

Five-day-old Arabidopsis cell suspension culture (100 mg) was ground in liquid nitrogen to fine powder and protein extraction was performed using 100 µl of solubilization buffer (0.5 mM EDTA, 500 mM aminohexanoic acid, 50 mM BisTris, 2 mM PMSF and protease inhibitor cocktail (Sigma) supplied with either 10 mM, 30 mM or 100 mM NaCl, and 0.5 or 1% dodecylmaltoside (DDM, Fluka). Additionally, an

extraction with no salt added and a ratio of proteins to DDM 0.67 and 1.33 was performed. The protein concentration was determined by Lowry method. Approximately 300 μg of protein samples were loaded onto 6-10% gradient BN-PAGE (6x8 cm) at 4 ^{o}C under constant current of 3.5 mA – 7 mA for 2-3 h (Eubel et al., 2005). A mixture of thyroglobulin (670 kDa, Sigma) and ferritine (440 kDa, Sigma) was used as the marker. Additionally, the plant green tissue extract was used as a marker with distinct chlorophyll-binding complexes of approximately 600 and 150 kDa. The individual lanes were cut out, incubated for 30 minutes with 2% SDS and 2% β-mercaptoethanol and placed on the top of the 12% SDS-PAGE and Western- analyzed.

Yeast two-hybrid system

The yeast two-hybrid screening employed the MATCHMAKER GAL4 Two-Hybrid System 3 (Clontech) and all procedures followed manufacturer protocols. The yeast strain AH109 (*MATa*, *trp1-109, leu2-3, 112, ura3-52, his3-200, gal4Δ, gal80Δ*, *LYS2::GAL1*$_{UAS}$*-GAL1*$_{TATA}$*-HIS3, MEL1, GAL2*$_{UAS}$*-GAL2*$_{TATA}$*-ADE2, URA3::MEL1*$_{UAS}$*-MEL1*$_{TATA}$*-lacZ*) was stepwise transformed with all possible combinations of exocyst subunits (*SEC3a, SEC5a, SEC6, SEC8, SEC10, SEC15b, EXO70A1,* and *EXO84b*), fused either with the GAL4 DNA-binding domain (pGBKT7vector) or with the GAL4 activation domain (pGADT7 vector). Yeast were grown on -LEU-TRP selective media and then transferred both to -ADE-HIS-LEU-TRP selective media and to filter paper for the β-galactosidase assay. Murine p53 (BD) and SV40 large T-antigen (AD), provided by the kit manufacturer, were used as a positive control, combination of empty pGBKT7 and pGADT7 vectors was used as a negative control. Only combinations positive in β-galactosidase assay and growing on -ADE-HIS-LEU-TRP selective media were accepted as true interactors.

Accession numbers

Sequence data from this article can be found in the EMBL/GenBank data libraries under following accession numbers (gene- AGI code):

AtSEC3a- At1g47550; *AtSEC5a*- At1g76850; *AtSEC5b*- At1g21170; *AtSEC6*- At1g71820; *AtSEC8*- At3g10380; *AtSEC10*- At5g12370; *AtSEC15a*- At3g56640; *AtSEC15b*- At4g02350; *AtEXO70A1*- At5g03540; *AtEXO84a*- At1g10385; *AtEXO84b*- At5g49830; *AtEXO84c*- At1g10180; *AtQRT1*- At5g55590.

Supplementary Material

The following material is available in the online version of this article.

Supplemental Figure 1. Complementation of *sec6* mutants.

Supplemental Table 1. Genotyping results for *sec6* mutants complementation experiments.

Supplemental Figure 2. Altered transcripts predicted to encode truncated proteins in the T-DNA insertion mutants in exocyst subunits.

Supplemental Figure 3. Negative and positive controls used for indirect immunofluorescence on tobacco pollen tubes.

Supplemental Figure 4. Expression analysis of exocyst genes in different Arabodopsis tissues.

Supplemental Table 2. List of PCR Primers used in this work.

Supplemental Table 3. ESI-MS identification of SEC3, SEC6, SEC8 and SEC10 exocyst subunits.

Acknowledgements

The authors would like to thank Z. Vejlupkova and H. Pham for assistance with Arabidopsis growth and genotyping in the lab, and the OSU Central Services Lab for sequencing. Authors also thank to F. Cvrckova, M. Elias, M. Fendrych, and D.Ziak for their practical contributions and comments to the manuscript. Last but not least, we gratefully acknowledge bioinformatic analyses performed by Claudia Fladerer (Proteom Centrum Tübingen).

The work in the lab of V.Z. was supported by the Ministry of Education, Youth and Sports (MSMT) of the Czech Republic (MSMT Kontakt ME841, MSMT LC06034 ”REMOROST”) and the Grant Agency of AS CR (IAA6038410). Part of V.Z. income is covered by MSM0021620858. The work in the lab of J.E.F. was supported by the US National Science Foundation (#IBN-0420226), which also supported this international collaboration. The Proteom Centrum Tübingen is supported by the Ministerium für Wissenschaft und Kunst, Landesregierung Baden-Württemberg.

Upon request, all novel materials described in this publication will be made available in a timely manner for non-commercial research purposes, subject to the requisite permission from any third-party owners of all or parts of the material.

3.6 LITERATURE CITED

Adamo, J.E., Rossi, G., and Brennwald, P. (1999). The Rho GTPase Rho3 has a direct role in exocytosis that is distinct from its role in actin polarity. Mol. Biol. Cell 10: 4121-4133.

Alonso, J.M., Stepanova, A.N., Leisse, T.J., Kim, C.J., Chen, H., Shinn, P., Stevenson, D.K., Zimmerman, J., Barajas, P., Cheuk, R., Gadrinab, C., Heller, C., Jeske, A., Koesema, E., Meyers, C.C., Parker, H., Prednis, L., Ansari, Y., Choy, N., Deen, H., Geralt, M., Hazari, N., Hom, E., Karnes, M., Mulholland, C., Ndubaku, R., Schmidt, I., Guzman, P., Aguilar-Henonin, L., Schmid, M., Weigel, D., Carter, D.E., Marchand, T., Risseeuw, E., Brogden, D., Zeko, A., Crosby, W.L., Berry, C.C., and Ecker, J.R. (2003). Genome-wide insertional mutagenesis of *Arabidopsis thaliana*. Science 301: 653-657.

Andrews, H.K., Zhang, Y.Q., Trotta, N., and Broadie, K. (2002). Drosophila Sec10 is required for hormone secretion but not general exocytosis or neurotransmission. Traffic 12: 906-921.

Berghöfer, J., and Klösgen, R.B. (1999). Two distinct translocation intermediates can be distinguished during protein transport by the TAT (Deltaph) pathway across the thylakoid membrane. FEBS Lett. 460: 328-332.

Bowser, R., and Novick, P. (1991). Sec15 protein, an essential component of the exocytotic apparatus, is associated with the plasma membrane and with a soluble 19.5S particle. J. Cell Biol. 6: 1117-1131.

Bowser, R., Muller, H., Govindan, B., and Novick, P. (1992). Sec8p and Sec15p are components of a plasma membrane-associated 19.5S particle that may function downstream of Sec4p to control exocytosis. J. Cell Biol. 5: 1041-1056.

Brymora, A., Valova, V.A., Larsen, M.R., Roufogalis, B.D., and Robinson, P.J. (2001). The brain exocyst complex interacts with RalA in a GFP-dependent manner: identification of a novel mammalian Sec3 gene and a second Sec15 gene. J. Biol. Chem. 276: 29792-97.

Cai, H., Reinisch, K., and Ferro-Novick, S. (2007). Coats, tethers, Rabs, and SNAREs work together to mediate the intracellular destination of a transport vesicle. Dev. Cell 12: 671-682.

Cole, R.A., Synek, L., Zarsky, V., and Fowler, J.E. (2005). SEC8, a subunit of the putative Arabidopsis exocyst complex, facilitates pollen germination and competitive pollen tube growth. Plant Physiol. 138: 2005-2018.

Cole, R.A., and Fowler, J.E. (2006). Polarized growth: maintaining focus on the tip. Curr. Opin. Plant Biol. 9: 579-588.

Cvrckova, F., Elias, M., Hala, M., Obermeyer, G., and Zarsky, V. (2001). Small GTPases and conserved signalling pathways in plant cell morphogenesis: From exocytosis to Exocyst. In A. Geitmann, M. Cresti, eds, Cell Biology of Plant and Fungal Tip Growth, IOS Press, Amsterdam, pp 105-122.

Dong, G., Hutagalung, A.H., Fu, C., Novick, P., and Reinisch, K.M. (2005). The structures of exocyst subunit Exo70p and the Exo84p C-terminal domains reveal a common motif. Nat. Struct. Mol. Biol. 12: 1094-1100.

EauClaire, S., and Guo, W. (2003). Conservation and specialization: The role of the exocyst in neuronal exocytosis. Neuron 3: 369-370.

Elias, M., Drdova, E., Ziak, D., Bavlnka, B., Hala, M., Cvrckova, F., Soukupova, H., and Zarsky, V. (2003). The exocyst complex in plants. Cell Biol. Int. 27: 199-201.

Eubel, H., Braun, H.P., and Millar, A.H. (2005). Blue-native PAGE in plants: a tool in analysis of protein-protein interactions. Plant Methods 1: 11.

Finger, F.P., and Novick, P. (1997). Sec3p is involved in secretion and morphogenesis in *Saccharomyces cerevisiae*. Mol. Biol. Cell 8: 647-662.

Friedrich, G.A., Hildebrand, J.D., and Soriano, P. (1997). The secretory protein Sec8 is required for paraxial mesoderm formation in the mouse. Dev. Biol. 2: 364-374.

Garrick, M.D., and Garrick, L.M. (2007). Loss of rapid transferrin receptor recycling due to a mutation in Sec15l1 in hbd mice. Biochim. Biophys. Acta. 1773: 105-108.

Guo, W., Grant, A., and Novick, P. (1999a). Exo84p is an exocyst protein essential for secretion. J. Biol. Chem. 33: 23558-23564.

Guo, W., Roth, D., Walch-Solimena, C., and Novick, P. (1999b). The exocyst is an effector for Sec4p, targeting secretory vesicles to sites of exocytosis. EMBO J. 4: 71-80.

Guo, W., Tamanoi, F., and Novick, P. (2001). Spatial regulation of the exocyst complex by Rho1 GTPase. Nat. Cell Biol. 3: 353-360.

Hamburger, Z.A., Hamburger, A.E., West, A.P., and Weis, W.I. (2006). Crystal structure of the *S. cerevisiae* exocyst component Exo70p. J. Mol. Biol. 356: 9-21.

Hazuka, C.D., Foletti, D.L., Hsu, S.C., Kee, Y., Hopf, F.W., and Scheller, R.H. (1999). The sec6/8 complex is located at neurite outgrowth and axonal synapse-assembly domains. J. Neurosci. 4: 324-334.

Hsu, S.C., Ting, A.E., Hazuka, C.D., Davanger, S., Kenny, J.W., Kee, Y., and Scheller, R.H. (1996). The mammalian brain rsec6/8 complex. Neuron 6: 209-219.

Hsu, S.C., Hazuka, C.D., Foletti, D.L., Heuser, J., and Scheller, R.H. (1998). Subunit composition, protein interactions and structures of the mammalian brain sec6/8 complex and septin filaments. Neuron 20: 1111-1122.

Hsu, S.C., TerBush, D., Abraham, M., and Guo, W. (2004). The exocyst complex in polarized exocytosis. Int Rev Cytol 233: 243-265.

Jafar-Nejad, H., Andrews, H.K., Acar, M., Bayat, V., Wirtz-Peitz, F., Mehta, S.Q., Knoblich, J.A., and Bellen, H.J. (2005). Sec15, a component of the exocyst, promotes notch signaling during the asymmetric division of Drosophila sensory organ precursors. Dev. Cell 9: 351-363.

Johnson-Brousseau, S., and McCormick, S. (2004). A compendium of methods useful for characterizing Arabidopsis pollen mutants and gametophytically expressed Genes. Plant J. 39: 761–775.

Jurgens, G., and Geldner, N. (2002). Protein secretion in plants: from the trans-Golgi network to the outer space. Traffic 3: 605-613.

Kee, Y., Yoo, J.S., Hazuka, C.D., Peterson, K.E., Hsu, S.C., and Scheller, R.H. (1997). Subunit structure of the mammalian exocyst complex. Proc. Natl. Acad. Sci. USA 94: 14438-14443.

Koumandou, V.L., Dacks, J.B., Coulson, R.M., and Field, M.C. (2007). Control systems for membrane fusion in the ancestral eukaryote; evolution of tethering complexes and SM proteins. BMC Evol. Biol. 7: 29.

Lavy, M., Bloch, D., Hazak, O., Gutman, I., Poraty, L., Sorek, N., Sternberg, H., and Yalovsky, S.A. (2007). Novel ROP/RAC Effector Links Cell Polarity, Root-Meristem Maintenance, and Vesicle Trafficking. Curr. Biol. 17: 947-952.

Li, C.R., Lee, R.T., Wang, Y.M., Zheng, X.D., and Wang, Y. (2007). *Candida albicans* hyphal morphogenesis occurs in Sec3p-independent and Sec3p-dependent phases separated by septin ring formation. J. Cell Sci. 120: 1898-1907.

Lim, J.E., Jin, O., Bennett, C., Morgan, K., Wang, F., Trenor, C.C. 3rd, Fleming, M.D., and Andrews, N.C. (2005). A mutation in Sec15l1 causes anemia in hemoglobin deficit (hbd) mice. Nat. Genet. 37: 1270-1273.

Matern, H.T., Yeaman, C., Nelson, W.J., and Scheller, R.H. (2001). The Sec6/8 complex in mammalian cells: characterization of mammalian Sec3, subunit interactions, and expression of subunits in polarized cells. Proc. Natl. Acad. Sci. USA 98: 9648-9653.

Moore, B.A., Robinson, H.H., and Xu, Z. (2007). The crystal structure of mouse Exo70 reveals unique features of the mammalian exocyst. J. Mol. Biol. 371: 410-421.

Moskalenko, S., Henry, D.O., Rosse, C., Mirey, G., Camonis, J.H., and White, M.A. (2002). The exocyst is a Ral effector complex. Nat. Cell Biol. 4: 66-72.

Moskalenko, S., Tong, C., Rosse, C., Mirey, G., Formstecher, E., Daviet, L., Camonis, J., and White, M.A. (2003). Ral GTPases regulate exocyst assembly through dual subunit interactions. J. Biol. Chem. 278: 51743-48.

Munson M., and Novick P. (2006). The exocyst defrocked, a framework of rods revealed. Nat. Struct. Mol. Biol. 13: 577-581.

Murthy, M., Garza, D., Scheller, R.H., and Schwarz, T.L. (2003). Mutations in the exocyst component Sec5 disrupt neuronal membrane traffic, but neurotransmitter release persists. Neuron 37: 433-447.

Murthy, M., Garza, D., Scheller, R.H., and Schwarz, T.L. (2003). Mutations in the exocyst component Sec5 disrupt neuronal membrane traffic, but neurotransmitter release persists. Neuron 37: 433-447.

Novick, P., Field, C., and Schekman, R. (1980). Identification of 23 complementation groups required for post-translational events in the yeast secretory pathway. Cell 21: 205-215.

Otegui, M.S., and Staehelin, L.A. (2004). Electron tomographic analysis of post-meiotic cytokinesis during pollen development in *Arabidopsis thaliana*. Planta 218: 501-515.

Perkins, D.N., Pappin, D.J., Creasy, D.M., and Cottrell, J.S. (1999). Probability-based protein identification by searching sequence databases using mass spectrometry data. Electrophoresis 20: 3551-3567.

Pommereit, D., and Wouters, F.S. (2007). An NGF-induced Exo70-TC10 complex locally antagonises Cdc42-mediated activation of N-WASP to modulate neurite outgrowth. J. Cell Sci. 120: 2694-2705.

Preuss, D., Rhee, S.Y., and Davis, R.W. (1994). Tetrad analysis possible in Arabidopsis with mutation of the QUARTET (QRT) genes. Science 264: 1458-1460.

Prigent, M., Dubois, T., Raposo, G., Derrien, V., Tenza, D., Rossé, C., Camonis, J., and Chavrier, P. (2003). ARF6 controls post-endocytic recycling through its downstream exocyst complex effector. J. Cell Biol. 163: 1111-1121.

Robinson, N.G., Guo, L., Imai, J., Toh-E, A., Matsui, Y., and Takanou, F. (1999). Rho3 of *Saccharomyces cerevisiae*, which regulates the actin cytoskeleton and exocytosis, is a GTPase which interacts with Myo2 and Exo70. Mol. Cell. Biol. 19: 3580-3587.

Rosse, C., Hatzoglou, A., Parrini, M.C., White, M.A., Chavrier, P., and Camonis, J. (2006). RalB mobilizes the exocyst to drive cell migration. Mol. Cell. Biol. 26: 727-734.

Rosso, M.G., Li, Y., Strizhov, N., Reiss, B., Dekker, K., and Weisshaar, B. (2003). An *Arabidopsis thaliana* T-DNA mutagenized population (GABI-Kat) for flanking sequence tag-based reverse genetics. Plant Mol. Biol. 53: 247-259.

Roth, D., Guo, W., and Novick, P. (1998). Dominant-negative alleles of SEC10 reveal distinct domains involved in secretion and morphogenesis in yeast. Mol. Biol. Cell 7: 725-739.

Schägger, H., and von Jagow, G. (1991). Blue native electrophoresis for isolation of membrane protein complexes in enzymatically active form. Anal. Biochem. 199: 223-31.

Segui-Simarro, J.M., Austin J.R 2nd, White, E.A., and Staehelin, L.A. (2004). Electron tomographic analysis of somatic cell plate formation in meristematic cells of Arabidopsis preserved by high-pressure freezing. Plant Cell 16: 836-856.

Sivaram, M.V., Saporita, J.A., Furgason, M.L., Boettcher, A.J., and Munson, M. (2005). Dimerization of the exocyst protein Sec6p and its interaction with the t-SNARE Sec9p. Biochemistry 44: 6302-6311.

Sivaram, M.V., Furgason, M.L., Brewer, D.N., and Munson, M. (2006). The structure of the exocyst subunit Sec6p defines a conserved architecture with diverse roles. Nat. Struct. Mol. Biol. 13: 555-556.

Synek, L., Schlager, N., Elias, M., Quentin, M., Hauser, M.T., and Zarsky, V. (2006). AtEXO70A1, a member of a family of putative exocyst subunits specifically expanded in land plants, is important for polar growth and plant development. Plant J. 48: 54 - 72.

Sztul, E., and Lupashin, V. (2006). Role of tethering factors in secretory membrane traffic. Am. J. Physiol. Cell Physiol. 290: C11-26.

TerBush, D.R., and Novick, P. (1995). Sec6, Sec8, and Sec15 are components of a multisubunit complex which localizes to small bud tips in *Saccharomyces cerevisiae*. J. Cell Biol. 130: 299-312.

TerBush, D.R., Maurice, T., Roth, D., and Novick, P. (1996). The Exocyst is a multiprotein complex required for exocytosis in *Saccharomyces cerevisiae*. EMBO J. 15: 6483-6494.

Terbush, D.R., Guo, W., Dunkelbarger, S., and Novick P. (2001). Purification and characterization of yeast exocyst complex.Methods Enzymol. 329:100-10.

Vega, I.E., and Hsu, S.C. (2001). The exocyst complex associates with microtubules to mediate vesicle targeting and neurite outgrowth. J. Neurosci. 21: 3839-3848.

Wen, T.J., and Schnable, P.S. (1994). Analyses of mutants of three genes that influence root hair development in *Zea mays* (Gramineae) suggest that root hairs are dispensable. Am. J. Bot. 81: 833–842.

Wen, T.J., Hochholdinger, F., Sauer, M., Bruce, W., and Schnable, P.S. (2005). The roothairless1 gene of maize encodes a homolog of sec3, which is involved in polar exocytosis. Plant Physiol. 138: 1637-1643.

Werhahn, W., and Braun, H.P. (2002). Biochemical dissection of the mitochondrial proteome from *Arabidopsis thaliana* by three-dimensional gel electrophoresis. Electrophoresis 23: 640-646.

Whyte J.R., and Munro S. (2001). The Sec34/35 Golgi transport complex is related to the exocyst, defining a family of complexes involved in multiple steps of membrane traffic. Dev. Cell 1: 527-37.

Whyte, J.R., and Munro, S. (2002). Vesicle tethering complexes in membrane traffic. J. Cell Sci. 115: 2627-2637.

Wu, S., Mehta, S.Q., Pichaud, F., Bellen, H.J., and Quiocho, F.A. (2005). Sec15 interacts with Rab11 via a novel domain and affects Rab11 localization in vivo. Nat. Struct. Mol. Biol. 12: 879-885.

Yang, Z. (2002). Small GTPases: versatile signaling switches in plants. Plant Cell 14: S375-S388.

Yeaman C., Grindstaff, K.K., Wright, J.R., and Nelson, W.J. (2001). Sec6/8 complexes on trans-Golgi network and plasma membrane regulate late stages of exocytosis in mammalian cells. J. Cell Biol. 155: 593-604.

Yeaman, C. (2003). Ultracentrifugation-based approaches to study regulation of Sec6/8 (exocyst) complex function during development of epithelial cell polarity. Methods 30: 198-206.

Yeaman, C., Grindstaff, K.K., and Nelson, W.J. (2004). Mechanism of recruiting Sec6/8 (exocyst) complex to the apical junctional complex during polarization of epithelial cells. J. Cell Sci. 117: 559-570.

Zhang, X., Bi, E., Novick, P., Du, L., Kozminski, K.G., Lipschutz, J.H., and Guo, W. (2001). Cdc42 interacts with the exocyst and regulates polarized secretion. J. Biol. Chem. 276: 46745-50.

Zhang, X.M., Ellis, S., Sriratana, A., Mitchell, C.A., and Rowe, T. (2004). Sec15 is an effector for the Rab11 GTPase in mammalian cells. J. Biol. Chem. 279: 43027-34.

Zimmermann, P., Hirsch-Hoffmann, M., Hennig, L., and Gruissem, W. (2004). GENEVESTIGATOR. Arabidopsis microarray database and analysis toolbox. Plant Physiol. 136: 2621–2632.

Zuo, X., Zhang, J., Zhang, Y., Hsu, S.C., Zhou, D., and Guo, W. (2006). Exo70 interacts with the Arp2/3 complex and regulates cell migration. Nat. Cell Biol. 8: 1383-1388.

3.7 FIGURES

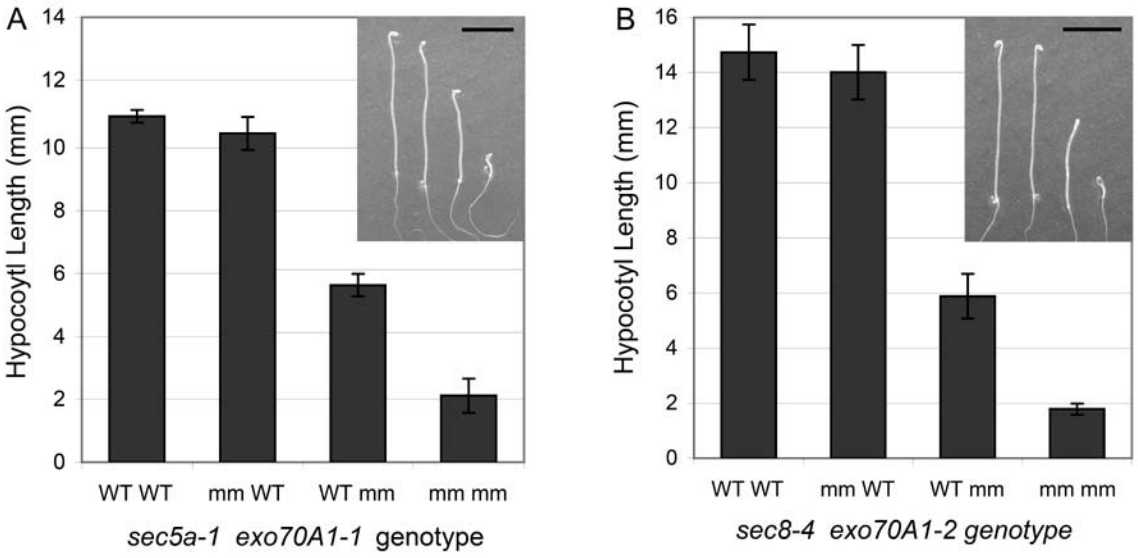

Figure 3.1. Mutations in two different exocyst components show a synergistic effect on hypocotyl elongation in 5 day old etiolated seedlings.
(A) Comparison of hypocotyl lengths of siblings that differ with respect to *SEC5a* and *EXO70A1* genotypes. WT denotes plants that are homozygous wild-type or heterozygous for the gene of interest; mm denotes plants that are homozygous mutants. Plants homozygous for the *sec5a-1* mutation alone (mm WT, n=25) resemble wild-type (WT WT, n=76). Plants homozygous for the *exo70A1-1* mutation alone (WT mm, n=53) have a moderately reduced hypocotyl length compared to wild-type ($p<0.001$). In contrast, plants homozygous for both the *sec5a-1* and *exo70A1-1* mutations (mm mm, n=8) demonstrate severely reduced hypocotyl elongation, significantly less than that observed for the *exo70A1-1* mutation alone ($p<0.001$). (B) Analogous results for *sec8-4* and *exo70A1-2* mutations (WT WT, n=22; mm WT, n=16; WT mm, n=33; mm mm, n=10). Error bars = standard error. Inset are photos of representative dark-grown hypocotyls arranged in the same order of genotypes as in the graphs; bar = 5 mm.

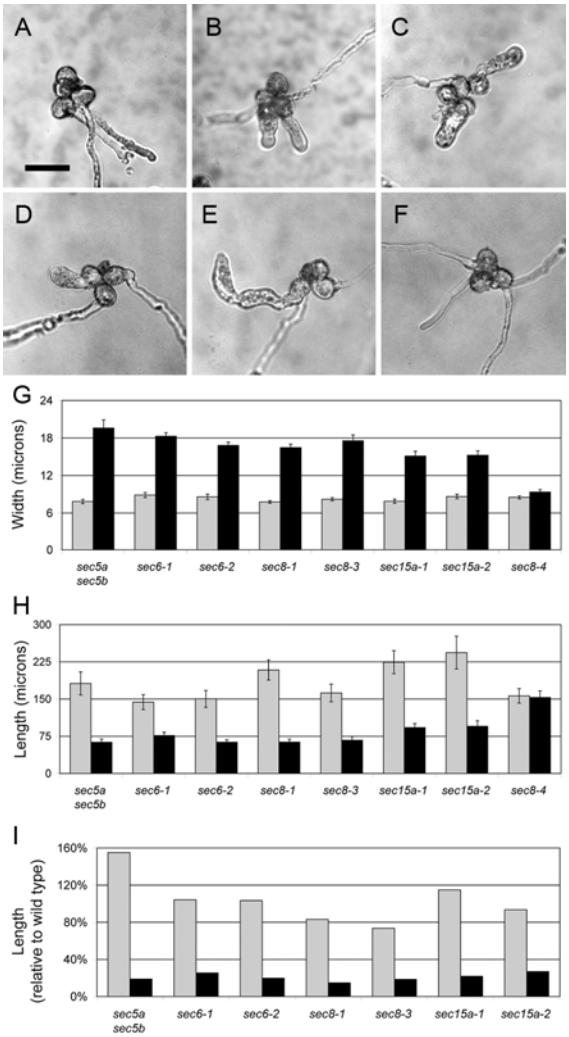

Figure 3.2. Exocyst mutants share a similar aberrant pollen tube phenotype. Germinated pollen from plants that carried the *qrt1* mutation and that were homozygous wild-type with respect to exocyst genes (A) was compared to the pollen from sibling plants that were heterozygous for a mutation in one of the putative exocyst component genes: *sec6-1* (C), *sec8-3* (D), *sec15a-1* (E), *sec8-4* (F), or in the case of the duplicate *SEC5* genes, homozygous *sec5a-1* and heterozygous *sec5b-1* (B) (bar=50 μm). For each of the mutants (in black), when three or four of the pollen tubes in a quartet germinated, one or two of the pollen grains were significantly ($p<0.001$) wider (G) and shorter (H) than the shortest pollen tubes in the quartet pollen from wild-type siblings (in grey) (n=22-44 for each genotype). The aberrant pollen tubes (in black) were only about 15-25% as long as the average length of all pollen tubes generated in wild-type siblings, whereas the length of the longer tubes in these same quartets (in grey) closely resembled wild-type (I) (n=76-199 long pollen tubes). Pollen from plants heterozygous for *sec8-4*, a weak allele which does not demonstrate a pollen transmission defect in naturally occurring self-crosses, correspondingly did not demonstrate the mutant pollen tube phenotype (F, G, and H).

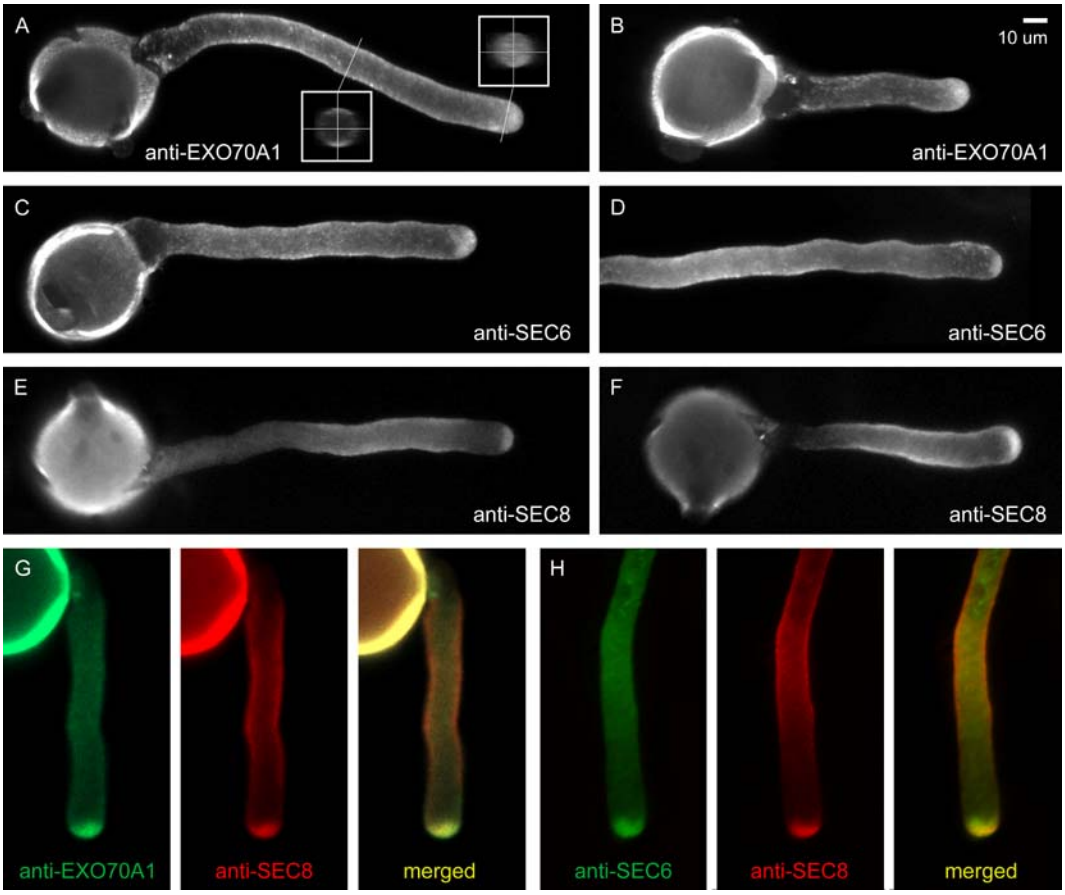

Figure 3.3. Localization of EXO70, SEC6, and SEC8 to the tip in tobacco pollen tubes by indirect immunofluorescence.

Projections of confocal sections labeled by the EXO70A1 antibody (A, B), SEC6 antibody (C, D), and SEC8 antibody (E, F). Transverse sections through the pollen tube made by 3D reconstruction are displayed for anti-EXO70A1 in A. Double labeling by mouse EXO70A1 antibody and rabbit SEC8 antibody, or by mouse SEC6 antibody and rabbit SEC8 antibody, respectively, shows co-localization of these subunits at the tip of pollen tubes.

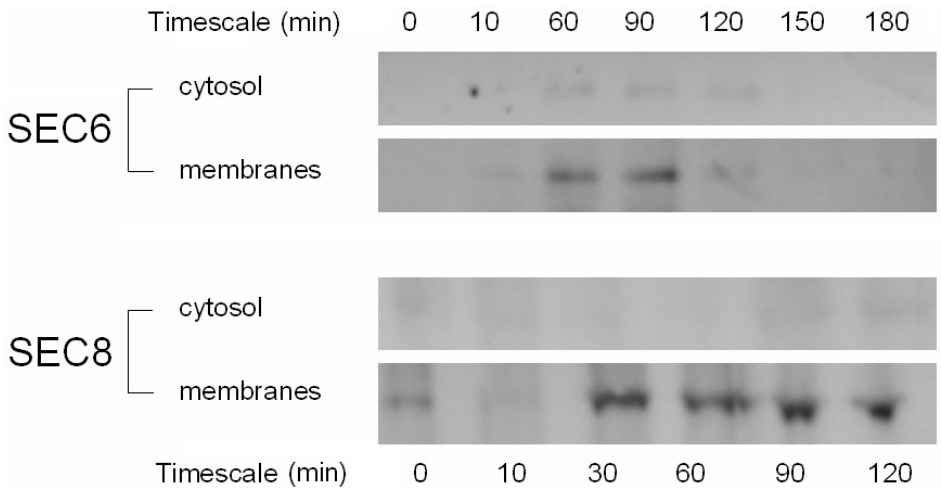

Figure 3.4. Accumulation of SEC6 and SEC8 in germinating pollen.
N. tabacum (cv. Samsun) pollen was incubated in 10% sucrose and 0.01% boric acid for time periods described. Cytosolic and membrane fractions (100,000 g pellet) were loaded on 10% SDS-PAGE, 50 μg of total protein per lane and Western analyzed.

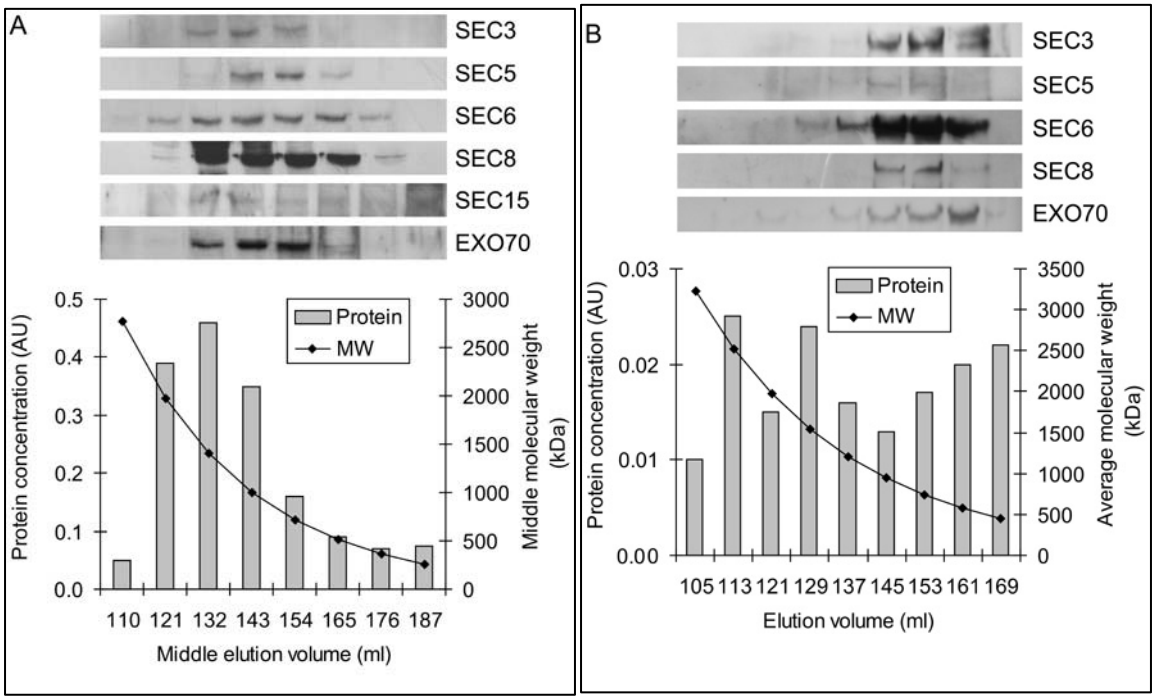

Figure 3.5. Co-fractionation of exocyst subunits in column chromatography.

(A) Size exclusion gel chromatography (SEGC) of total protein extract from Arabidopsis suspension culture.
(B) SEGC as the third purification step of the same extract, following hydroxyapatite affinity chromatography and ion exchange chromatography.
Both panels show co-fractionation of exocyst subunits in high molecular fractions as detected with exocyst-specific antibodies. Columns show relative total protein concentration measured at UV detector at 254 nm. MW indicates approximate middle molecular weight calculated for each fraction.

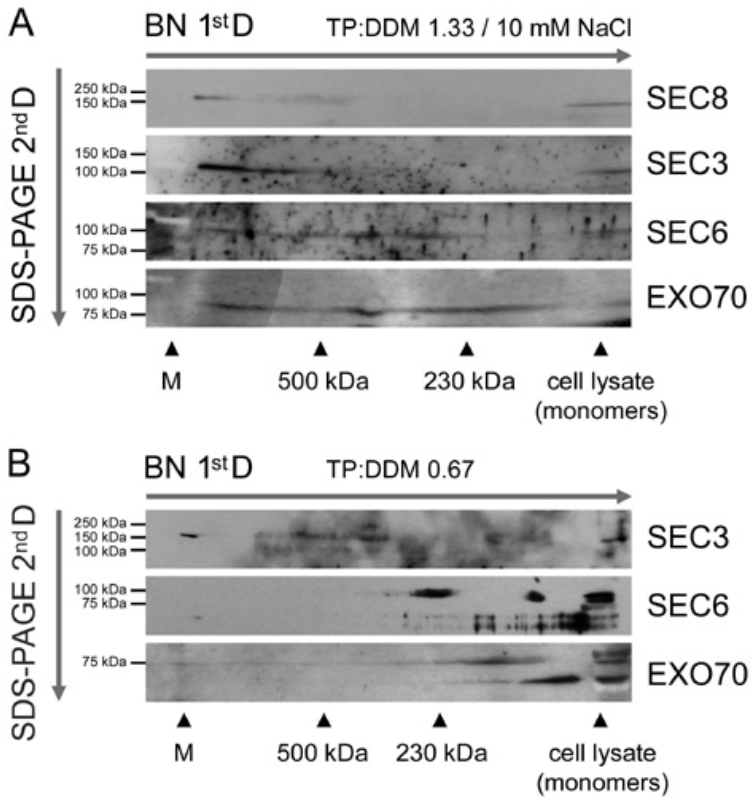

Figure 3.6. Blue native electrophoresis of the exocyst complex from Arabidopsis suspension culture.
Immunoblots of second-dimension SDS-PAGE were probed for exocyst subunits. Molecular weights of complexes are shown below the blot images.
(A) The first dimension was 6-10% gradient BN-PAGE after the solubilization with mild detergent concentrations (TP:DDM ratio of 1.33) and low NaCl concentrations (10 mM). The same membrane was probed, antibodies stripped off and reprobed, subsequently for four antibodies: anti-SEC8, anti-SEC3, anti-SEC6, anti-EXO70A1.
(B) The first dimension was 6-10% gradient BN-PAGE after the solubilization under TP:DDM ratio 0.67. The same membrane was reprobed subsequently with three different antibodies: anti-SEC3, anti-SEC6, anti-EXO70A1.
BN – blue native electrophoresis; TP – total protein concentration; DDM – dodecylmaltoside; M – protein weight marker.

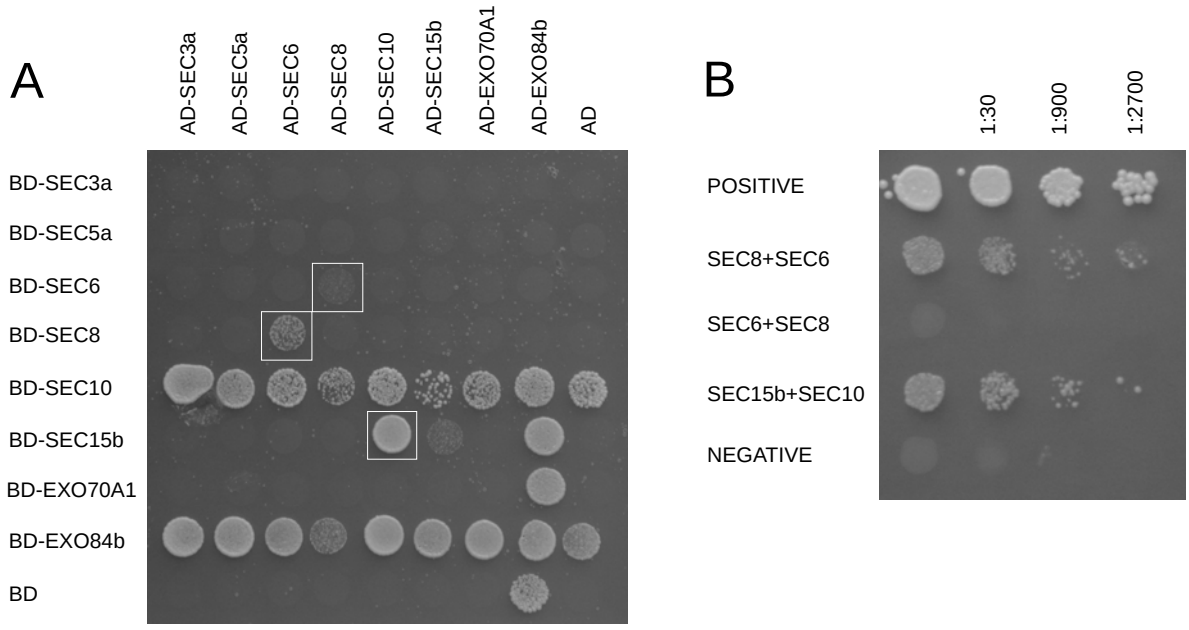

Figure 3.7. Yeast two-hybrid analysis of pairwise interactions of exocyst subunits.
(A) Pairwise interaction of all exocyst subunits. Lines and columns describe fusion forms of exocyst subunits used for transformation (BD- the DNA-binding domain; AD- the activation domain). Single colonies were resuspended in 150 µl of sterile water and dropped on selective plates, each drop 10 µl. Yeast strain AH109 was grown on -ADE-HIS-LEU-TRP plates at 28 °C. Combinations boxed by white squares also showed positive β-galactosidase activity.
(B) Strength of interaction compared to a positive control (see Methods). Single colonies were resuspended in 150 µl of sterile water. Serial dilution 1:100 and 1:10,000 in sterile water were prepared and dropped on –ADE-HIS-LEU-TRP plates at 28 °C, each drop 10 µl.

3.8 TABLES

Table 3.1. Outcross data indicate that mutations in any of the four putative exocyst genes evaluated result in a pollen-specific transmission defect.

Allele	Pollen donor: +/m Pollen recipient: +/+					Pollen donor: +/+ Pollen recipient: +/m				
	n	+/+	+/m	χ^2	p	n	+/+	+/m	χ^2	p
(Expected)		50%	50%				50%	50%		
sec6-1	79	100%	0%	79	<0.0001	82	50%	50%	0.000	NS
sec6-2	88	100%	0%	88	<0.0001	80	48%	53%	0.200	NS
[a]*sec8-1*	150	100%	0%	150	<0.0001	157	47%	53%	0.516	NS
[a]*sec8-3*	105	100%	0%	105	<0.0001	101	50%	50%	0.010	NS
[a]*sec8-4*	577	82%	18%	235.9	<0.0001	157	51%	49%	0.057	NS
[a]*sec8-6*	157	69%	31%	22.1	<0.0001	159	52%	48%	0.308	NS
sec15a-1	99	100%	0%	99	<0.0001	100	56%	44%	1.440	NS
sec15a-2	62	100%	0%	62	<0.0001	62	44%	56%	1.032	NS

	Pollen donor: +/m;+/m Pollen recipient: +/+; +/+					Pollen donor: +/+; +/+ Pollen recipient: +/m;+/m				
	n	(+/+;+/m), (+/m;+/+), or (+/+;+/+)	+/m;+/m	χ^2	p	n	(+/+;+/m), (+/m;+/+), or (+/+;+/+)	+/m;+/m	χ^2	p
(Expected)		75%	25%				75%	25%		
sec5a-1 *sec5b-1*	185	99.5%	0.5%	58.6	<0.0001	190	72.6%	27.4%	0.568	NS

[a] Previously published data for *sec8* mutant alleles (Cole et al., 2005) is included for comparison. NS = not significantly different from expected

Table 3.2. Percent of germinating quartets with 3 or 4 grains germinated.

Allele	Genotype of pollen source				χ^2	p
	Wild-type		Heterozygous			
	n[a]	% 3 or 4	n[a]	% 3 or 4		
sec5a sec5b[b]	635	23.1	227	1.8	54.51	<0.001
sec6-1	809	12.0	607	4.0	28.66	<0.001
sec6-2	944	20.3	1086	7.4	70.35	<0.001
sec8-1	518	29.7	652	3.1	162.09	<0.001
sec8-3	760	21.7	655	1.2	137.63	<0.001
sec15a-1	606	12.4	972	3.7	42.93	<0.001
sec15a-2	301	10.3	175	1.7	11.72	<0.001
sec8-4	576	13.4	741	11.2	1.43	NS

[a] number of germinating quartets evaluated
[b] the pollen source for *sec5a sec5b* was heterozygous for *sec5b* and homozygous for *sec5a*. NS = not significantly different from expected

Table 3.3. Summary of evidence for inclusion of various subunits in a plant exocyst complex.

Subunit	Genetic interaction in sporophyte	Male-specific transmission defect	Pollen germination and tube growth defect	Immuno-localization at pollen tube tip	SEGC on crude extract	Three-step purification; western blot	Three step purification; protein sequencing	BN-PAGE	Interaction in yeast two-hybrid system
SEC3					+	+	+[a]	+	
SEC5a/b	+[b]	+[c]	+[c]		+	+			
SEC6		+	+	+	+	+	+	+	+
SEC8	+	+	+	+	+	+	+	+	+
SEC10							+		+
SEC15a/b		+	+		+[d]				+[e]
EXO70A1	+			+	+	+		+	

[a] SEC3a identified by mass spectrometry.
[b] Interaction only tested with *sec5a* mutant.
[c] Double mutants (*sec5a sec5b*) produce a phenotype; single mutants in either gene are unaffected.
[d] Polyclonal SEC15a antibody likely recognizes only SEC15a isoform.
[e] SEC15b was used in the two-hybrid assay

Table 3.4. List of Arabidopsis mutants used in this work.

Mutant	MISP code	Line	Published in
exo70A1-1	At5g03540	SALK_014826	Synek et al., 2006
exo70A1-2	At5g03540	SALK_135462	Synek et al., 2006
sec5a-1	At1g76850	SALK 010127	this work
sec5b-1	At1g21170	SALK 001525	this work
sec6-1	At1g71820	SALK_078235	this work
sec6-2	At1g71820	SALK_072337	this work
sec8-1	At3g10380	SALK 057409	*Cole et al., 2005*
sec8-3	At3g10380	SALK 026204	Cole et al., 2005
sec8-4	At3g10380	SALK 118129	Cole et al., 2005
sec8-6	At3g10380	SALK 091118	Cole et al., 2005
sec15a-1	At3g56640	SALK 006302	this work
sec15a-2	At3g56640	SALK 067498	this work
exo84a	At1g10385	*SAIL_504_B10*	this work
exo84b	At5g49830	*GABI_459C01*	this work
exo84c-1	At1g10180	SALK_017883	this work
exo84c-2	At1g10180	SALK_011569	this work
qrt1 (quartet)	At5g55590	CS8050	Preuss et al., 1994

CHAPTER 4

The exocyst participates in brassinosteroid signalling to regulate cell division and elongation in different developmental contexts

4.1 INTRODUCTION

The plant exocyst complex functions in cell and plant organ morphogenesis. It is required for pollen germination and tip growth of pollen tube (Cole, et al., 2005, Hala, et al., 2008), and is implicated in the development of root hairs, the hypocotyl elongation observed in etiolated seedlings, and primary root growth (Hala, et al., 2008, Synek et al., 2006, Wen et al., 2005). However, how the exocyst functions at cellular level to affect these processes of morphogenesis is unknown.

We know from comparative genomic and phylogenetic analysis that the exocyst, like the other vesicle tethering complexes, is likely to be ancient, originating very early in eukaryotic evolution (Koumandou, et al. 2007), and that it is currently present throughout the spectrum of known eukaryotic genomes. Consequently, our exploration of how the exocyst functions in plants can initially be guided by what is known about the exocyst in non-plant organisms. The exocyst has been most extensively studied in yeast and mammals, where it is believed to be required for the targeting and tethering of secretory vesicles to the plasma membrane. In this capacity it is vital to a wide range of physiological and developmental processes including budding in *Sacharomyces cerevisea* (TerBush, et al., 1996), the outgrowth of cultured neurites (Hazuka et al., 1999; Pommereit and Wouters, 2007), the recycling of the transferrin receptor in the plasma membrane of reticulocytes (Garrick and Garrick, 2007), and the targeting of the glucose transporter, Glut4, to the plasma membrane of adipocytes (Inoue, et al., 2003; Chen et al., 2007). Surprisingly, although the exocyst is involved in the targeting and insertion of AMPA-type glutamate receptors in postsynaptic membranes (Gerges et al., 2006), it does not appear to be involved in the tethering of synaptic vesicles involved in the secretion of neurotransmitters. Three conclusions can be drawn from this impressive, but non-exhaustive list. First, the exocyst may not be required in every instance of exocytosis. Second, the exocyst becomes essential in specific situations when physiological or developmental circumstances demand extensive exocytosis to support rapid polarized growth. And third, the exocyst is often required when secretion and membrane cycling must be tightly controlled, both spatially and temporally, to regulate the localized

placement of specific plasma membrane proteins. These general observations provide a preliminary guide to investigating exocyst activity in plants.

The demonstrated requirement for the exocyst in pollen tube tip growth would seem to provide the obvious model to study the function of the exocyst at the cellular level. Tip growth in pollen tubes requires both extensive exocytosis to support the rapid polarized growth, and the tip localization of specific plasma membrane components that serve to maintain that focus of growth (Cole and Fowler, 2006). However, the phenotypic work to date on the plant exocyst has relied on T-DNA insertional mutants in Arabidopsis. This presents a difficulty, because Arabidopsis pollen does not germinate robustly *in vitro*. Additionally, the severe exocyst alleles that might most clearly reveal exocyst function at the cellular level also cause a severe pollen germination defect. The result is that Arabidopsis pollen that both germinates *in vitro* and harbors the strongest exocyst mutations is prohibitively rare for the convenient study of exocyst function.

The pollen defect associated with severe exocyst mutations also prevents the generation of mutant homozyogotes useful for the study of the exocyst in sporophytic cells (e.g., root hairs). I was able to overcome this technical hurdle using two methods: first, a pollen-specific expression construct that complemented the exocyst pollen defect, and second, a combination of weak exocyst mutants. This chapter uses observations of and experiments with the resultant exocyst mutants to characterize the role of the exocyst in two distinct developmental contexts, primary root growth and hypocotyl elongation in etiolated seedlings. In wild-type plants primary root growth occurs by a process of cell division and cell elongation, whereas hypocotyl elongation in dark-grown seedlings occurs almost entirely by cell elongation. Both developmental processes require alterations in the cell walls that require secretion of cell wall components or cell wall modifying enzymes. Both processes are regulated by a complex interplay of signaling pathways involving many phytohormones, some dependent on plasma membrane-localized hormone receptors. In short, both developmental processes possess numerous potential sites for involvement of the exocyst.

The goal of this research described in this chapter was to first, determine more specifically the role of the exocyst in primary root growth and etiolated hypocotyl

elongation by characterizing the developmental defects in the mutants, and second, to formulate more specific hypotheses about the molecular and cellular role of the exocyst in these processes. In contrast to its role in pollen, where it appears to be solely associated with cell growth, my work demonstrates that the exocyst is important in the sporophyte not only for cell elongation, but also for maintaining wild-type cell division patterns in the root meristem. Surprisingly, in both cases, the action of exocyst is demonstrated to be most closely linked to brassinosteroid signaling.

4.2 RESULTS

Exocyst mutations in the sporophyte lead to extreme dwarfism

Mutations of single exocyst components severe enough to fully disrupt exocyst function often result in a severe defect in pollen transmission (Cole et al., 2005). The pollen defect consequently prevents the generation of the mutant homozyogotes useful for the study of the exocyst in the sporophyte. This difficulty was circumvented using a construct harboring the wild-type *SEC8* driven by the pollen-specific *LAT52* promoter, which was used to complement the severe *sec8-3* allele. The construct corrected the pollen germination and pollen tube growth defects (Cole et al., 2005), allowing the mutant allele to transmit through the pollen to generate mutant homozyotes. Because the pollen-specific *LAT52* promoter results in minimal or no expression of the wild-type *SEC8* in the sporophyte, the sporophytic mutant phenotype was revealed in these homozygotes. The resultant *sec8-3* mutant homozygotes were extreme dwarfs (Figure 4.1), a phenotype similar to, but more severe than, that seen for the sporophytically-expressed exocyst component *EXO70A1* (Synek et al., 2006). The dwarfism includes smaller flowers and leaves, shorter stems, shorter hypocotyls, and shorter primary roots. To verify that this phenotype was not specific to the *sec8-3* allele, the construct was also crossed into plants with the *sec8-1* allele (Cole et al., 2005). The homozygous *sec8-1* plants ultimately produced showed an identical dwarf phenotype. In both cases, the dwarf phenotype co-segregated with the homozygous *sec8* condition (data not shown).

As an alternative approach, avoiding some of the inherent uncertainties associated with transformed plants, we took advantage of synergistic combinations of less severe exocyst mutant alleles (as previously described in Chapter 2 and Hala, et al., 2008). In this case, combining any of three weak alleles in two different exocyst genes (*sec8-4, sec8-6*, or *sec5a-1*) with knockout alleles of *EXO70A1* produced an extreme dwarfism that was comparable to that seen in the severe *sec8* mutants (data not shown). I conclude that the exocyst provides an essential function (or functions) required for optimal sporophytic growth.

The Exocyst and primary root growth

Establishment of a the cell elongation zone is aberrant in exocyst mutants

Prior to seed germination, the embryonic root (i.e. the radical) in both wild-type and *sec8-1 Arabidopsis* embryos is composed of ovoid shaped cells. In wild-type plants following seed germination, the radical begins to elongate, developing into the three distinct zones of the seedling root: the root apical meristem at the root tip, the elongation zone, and the differentiation zone (Figure 4.2). Because cells within the root do not move with respect to each other, and because all cells in the root are derived from the growing meristem at the root tip, a root exhibits a developmental time-course along its length, with cells generated earlier in development located nearer the root base. In wild-type, the cell elongation zone first appears close to the hypocotyl-root junction, known as the collet, and is apparent within hours following germination (Figure 4.3C). At seven days after germination, the boundary between the ovoid cells of the collett, which have expanded isotropically, and the elongated cells of the root epidermis and cortex, which have expanded anisotropically, occupies a span of only a few cells just below the collett (Figure 4.3A). Thus, the generation and differentiation of these elongated cells and the establishment of the elongation zone occurs very early in wild-type roots.

In contrast, seven days after germination roots of the severe exocyst mutants do not show elongated cells near the base of the collett. In *sec8-1* and *sec8-3* mutants the region of isotropic cell expansion, with only minimal elongation, is continuous from the collet far into the length of the growing seedling root (Figure 4.3B). Occasionally, the

epidermal cells in this region appear to balloon out from their cell file (Figure 4.3F). Equally remarkable is the observation that the length of root in which this isotropic cell growth occurs is highly variable. In most *sec8* roots, cells which have adopted a prominent elongated morphology appear within 2 mm of the collett (Figure 4.3B). Notably, when the roots are examined from the collet to the root tip, once a region of elongated cells are encountered, there are no subsequent regions of isotropically-expanded cells observed between that point and the meristematic region near the root tip. In addition, lateral roots growing out of regions of isotropic root cell growth commonly, but not always, demonstrate wild-type cell elongation. It is thus evident, that the mutant plants possess the appropriate cellular machinery to accomplish root cell elongation. Yet in the mutants, it appears that early in root development (i.e., nearer the collett), the mutant root cells do not express the developmental program that generates an elongated morphology. However, at some later stage of root growth, root cells in the mutant nearer the meristem appear to have switched to expressing a more wild-type morphology, evident by the presence of an elongation zone. This switch is not reversed as the meristem generates additional cells that enter the cell elongation zone. One interpretation is that the defect is a delay in the developmental transition that initially allows the formation of an elongation zone behind the meristem.

Although most mutants show an eventual transition from anisotropic cell expansion to elongated root cells, in some cases there is no root elongation zone in the *sec8-1* and *sec8-3* mutants, i.e. isotropic cell expansion occurs throughout the root from the collet to the root apical meristem, even after seven days of growth. Significantly, this complete failure to establish a wild-type elongation zone is consistently observed in the *exo70A1-2 sec8-4* double mutant, which has a more severe root growth phenotype. This lack of a proper elongation zone certainly contributes to the short root length phenotype in exocyst mutants, but it does not explain the reduced root growth rate observed seven days after germination, when all but a few of the *sec8* homozygotes have clearly established zones of elongation.

A decreased root growth rate in exocyst mutants is primarily associated with a smaller meristem and an associated reduction in cell division

The short roots in exocyst mutants are the result of a reduced growth rate, and not premature termination of growth (Figure 4.4). The growth rate of plant roots depends upon the rate of cell division in the meristem, and the extent of anisotropic cell expansion in the root's elongation zone. To explore the exocyst's potential involvement in these two processes, *sec8-3* mutant roots were compared to wild-type using confocal microscopy and staining with propridium iodide (Figure 4.5). Cell lengths were measured along a cell file of cortex cells, beginning at the initials. Cells within the root meristem do not increase in size to greater than double their length before dividing transversely to add a new cell to the cell file. Consequently, the point along the cell file at which the cell lengths demonstrate greater than a two-fold increase marks the boundary between the root apical meristem and the elongation zone. In *sec8-3* mutant roots there were fewer cortical cells in the cell file between the root tip and this boundary, compared to wild-type (Figure 4.5), resulting in root meristems that were only half the length of wild-type.

To determine directly whether exocyst mutations affect cell division patterns in the root meristem, the activity and distribution of a *CycB1::GUS* reporter was analyzed. Fusion of the *CycB1* promoter with GUS and a mitotic degradation signal allows this reporter to mark only actively dividing cells (Colon-Carmona, et al., 1999). The fixed and stained roots of seven day old *sec8-3* seedlings were compared to those of their wild-type siblings (n=23). Homozygous *sec8-3* roots were analyzed in two groups: those with an elongation zone adjoining the meristem (Group A, n=19), and those without – i.e., isotropically-expanded cells from collet to meristem (Group B, n=8). GUS staining verified that *sec8-3* mutants have shorter meristems, indicated by a shorter zone of dividing cells compared to their wild-type siblings (Figure 4.6A, B). The length of the zone of active cell division was the same in both Group A and Group B roots, and approximately half the length of the cell division zone in wild-type siblings. The number of dividing cells per meristem was reduced from 45.7 in wild type to 13.2 and 14.5 in Group A and Group B mutants respectively (Figure 4.6). When analyzed as the number

of dividing cells per meristem volume, the difference between wild-type and *sec8-3* mutants was less significant; suggesting that the reduced number of dividing cells in the mutants is primarily a problem of reduced meristem size. However, a reduced rate of cell division within the meristem is also evident. To assess whether the root growth defect in the mutants was solely a problem with the meristem, the potential for elongation was estimated by measuring the maximum cortical cell lengths observed throughout each entire root (3 cells per root). Group B *sec8-3* mutants had a dramatically reduced maximum cell length, as expected, but the maximum cell lengths for Group A were also significantly reduced compared to wild type. Compared to wild type, *sec8-3* Group A mutants had a 24 percent reduction in maximal cell elongation, but demonstrated a 70 percent reduction in cell division within the meristem. This indicates that the *sec8* mutation's effect on root growth rate is most prominently a defect in meristematic cell division.

The effect of exocyst mutations on cell division in the root meristem and in cortical cell elongation was verified by the examination of *exo70A1-2* mutants, and *exo70A1-2 sec8-6* double mutants that possessed the *CycB::GUS* reporter (Figure 4.7). Root growth in *EXO70A1* mutants is only slightly reduced compared to wild-type, whereas the root growth defect in *exo70A1-2 sec8-6* double mutants is severe, resembling that of the *sec8-3* Group B mutants. In the *exo70A1-2* mutant the number of dividing cells per meristem or per meristem volume was not statistically different from wild-type, nor was the average maximum cortical cell length. The double mutant with a severly shortened root had meristem parameters similar to the *sec8-3* mutant. Thus, the presence of a short root phenotype correlates with the presence of the documented cell division and cell elongation defects.

Exocyst mutations have minimal effects on auxin signaling during root growth

The size and cell division activity of the root meristem, as well as the size of the elongation zone and ultimate length of the root cells, is thought to be determined by the interplay of phytohormones, including brassinosteroids, auxin, cytokinins, ethylene, and gibberellins (Ioio et al., 2007; Kim et al., 2007; Li et al., 2005; Mitchum et al., 2006;

Mussig et al., 2003; Ruzicka et al., 2007; Werner et al., 2003). To test whether the exocyst participates in the regulation of root growth via a role in one or more of these pathways, the dose-response of the exocyst mutants to the exogenous application of phytohormones was therefore investigated. The EC50 (effective concentration at which the response was 50 percent of control) was determined from the dose-response curves for the purposes of comparison to wild-type siblings.

Auxin signaling was considered a probable target for exocyst involvement for a number of reasons. The formation of an auxin gradient at the root tip helps regulate the size of the root meristem and elongation zones (Blilou, et al., 2005). Influx (e.g. AUX protein) and efflux (e.g. PIN proteins) auxin transport facilitators are asymmetrically localized in the plasma membrane of root cells in a precisely-regulated pattern to create this gradient. The placement and repositioning of these transport facilitators in the plasma membrane is known to involve vesicle trafficking machinery, and thus could conceivably require the exocyst. As an initial test of this hypothesis, the response of *SEC8* and *EXO70A1* mutants to exogenous auxin was investigated. Seedlings germinated on media without auxin were transferred on day 3 to vertically oriented plates containing various concentrations of the auxin, indole acetic acid (IAA), and allowed to grow until the growth rate on day 7 could be determined. Although the baseline growth rate for *sec8-1* was significantly slower than that for *exo70A1* or *Columbia-0* ($p<0.001$, n=24-30, one-tailed t-test), the shape of the dose-response curves for all three genotypes to exogenous IAA was nearly identical (EC50s: *sec8-1* (75.6 nM), *exo70A1* (76.1 nM), and *Col-0* (77.0 nM)) (Figure 4.8). Similar results were obtained for the synthetic auxin 1-naphthaleneacetic acid (NAA), which can enter the cells without an influx transport facilitator (data not shown).

To determine if the distribution of endogenous auxin might be altered in exocyst mutants, *DR5::GUS*, a reporter of auxin response, was crossed into lines containing *sec8-1*, *exo70A1-2*, or the double mutant *sec8-6 exo70A1-2*. GUS staining from this reporter construct spreads laterally across the entire root at a level surrounding the quiescent center in *pin1 pin4 pin7* triple mutants (Blilou et al., 2005). It has also been observed that GUS expressed from this construct accumulates in the provascular tissue (i.e. in the

root's center, next to the quiescent center) when the lateral distribution of auxin through the columella is blocked by toxin-mediated ablation of root cap cells (Blilou et al. 2005). Therefore, if mutations in the exocyst cause mislocalization of auxin transport facilitators and altered auxin distribution, such a defect might be revealed as a differential pattern of staining using the *DR5::GUS* construct in the mutant lines. Seedlings harboring *DR5::GUS* were fixed and stained after 7 days of growth on vertical plates. In most cases the mutant roots had staining patterns that were nearly identical to those observed in wild-type siblings (Figure 4.8B and C). The concentration of the staining at the root tip demonstrates that polarized auxin transport is occurring, and suggests that the exocyst mutations do not result in a major defect in the localization of auxin transport facilitators at the plasma membrane. Taken together, these experiments indicate that the profound root growth defects observed in exocyst mutants are unlikely to be primarily a result of altered auxin signaling.

The root growth rate of exocyst mutants is distinctively altered by treatment with exogenous epi-brassinosteroid

Brassinosteroid hormones are also known to affect root growth (Clouse et al., 1996; Mouchel et al., 2006; Mussig, et al., 2003; Noguchi et al., 1999), although their specific roles in the root meristem and elongation zone are not as well-characterized as those of auxin. In addition, the BRI1 hormone receptor is localized to the plasma membrane (Friedrichsen, et al., 2000; Geldner et al., 2007), and its transport could be affected by disruption of the exocyst. To test involvement of this hormone, root growth rate was measured after 7 days of growth on vertical plates containing various concentrations of the brassinosteroid, 24-epibrassinolide (EBR). Intriguingly, the *sec8-1* mutant was found to have a dramatically different dose-related response compared to wild-type (Figure 4.9). Consistent with an earlier report (Mussig, et al., 2003), in wild-type plants low concentrations of EBR resulted in a mild, but significant, increase in growth rate (from 5.2 to 6.1 mm/day, $p=0.005$, $n=17, 31$, t-test), whereas at concentrations above 0.13 nM the growth rate declined ($EC50 = 4.0$ nM). The roots of *exo70A1* mutants, which grow similarly to wild-type, demonstrated an EBR dose

response that was also similar to wild-type, with a mild stimulation of growth at low concentrations (5.6 to 6.2 mm/day, p=0.012, n=17, 31, t-test) and inhibition of growth at higher concentrations (EC50 = 1.6 nM). In contrast, the dose response curve for *sec8-1* roots showed a dramatic 82 percent increase in growth rate in response to exogenous EBR, approaching the growth rate observed in non-treated wild-type plants. Importantly, this peak stimulatory response was observed at an EBR concentration (1 nM) which inhibited growth in both wild-type and *exo70A1* roots. Ultimately, higher EBR concentrations had an inhibitory effect on *sec8-1* root growth (EC50 = 9.8 nM) as well, and resulted in a similar loss of gravitropism in both wild type and exocyst mutants. Thus, brassinosteroid response is less sensitive to exogenous hormone in the severe *sec8* exocyst mutant, correlating with its effect on root growth (as opposed to the *exo70A1* mutant). Furthermore, the exogenous EBR can partially correct this mutant phenotype.

The existence of an interwoven network of multiple signaling pathways that regulate root growth raises the possibility that the exocyst does not affect brassinosteroid signaling directly, but indirectly through an effect on another part of the network that is more directly linked to brassinosteroids. To explore this possibility, the EBR dose-response of a selection of other root growth mutants was evaluated. Of specific interest was *rsw1-1*, a mutant of a cellulose synthase (CESA1) in root cells; *eto1-1*, an ethylene overproducer; and *ga3ox1-3*, a mutation in a gene involved in the production of bioactive gibberellic acid. Figure 9B shows the results of this analysis. None of these mutants demonstrated a dose-response similar to that of the *sec8-1* mutants, consistent with the hypothesis that the exocyst is having a direct effect on EBR signaling.

Root growth response to doses of cytokinin, an ethylene precursor, or a cellulose synthase inhibitor are not significantly altered by exocyst mutations

Cytokinins play a role in determining the size of the root apical meristem (Ioio, et al., 2007). Significantly, the effect of cytokinins on meristem size does not appear to involve the stem cells, or cell division within the meristem. Instead, cytokinins appear to help regulate the transition from the meristem into the elongation zone. To reveal if the exocyst might be involved in cytokinin signaling, the root growth response to application

of an exogenous cytokinin (N6 benzyladenine (BA)) was studied. The resultant dose-response observed for *Col-0, exo70A1-2*, and *sec8-1* seedlings were not remarkably different.

Ethylene is known to inhibit seedling root growth, primarily by affecting cell elongation, not the meristem and cell division (Ruzicka, et al., 2007). To investigate if the exocyst mutants showed altered sensitivity to ethylene, the growth response of mutant roots to elevated ethylene was investigated by growing plants on media containing the etylene precursor, 1-aminocyclopropane-1-carboxylate (ACC). The results indicated a similar dose response for *sec8-1*, *exo70A-1*, and *Col-0* (EC50's of 0.20 nM, 0.16 nM, and 0.18 nM respectively). This experiment does not rule out the possibility that the mutant root growth defect arises in part from ethylene over-production. Arguing against such a possibility is the observation that excessive ethylene is known to induce profuse root hair formation, which is not seen in exocyst mutants. Furthermore, ethylene is not recognized as having an effect on meristem activity, although altered meristem activity seems integral to the exocyst mutant phenotype. The similar ACC dose-response of mutants and wild-type is consistent with these observations, implying a limited role for ethylene in the mutant root growth defect.

The exocyst could also conceivably be involved in the placement of cellulose synthase subunits in the plasma membrane, as required for building new cell wall. The herbicide isoxaben is a specific inhibitor of cellulose biosynthesis, and some cellulose synthase mutants demonstrate resistance to isoxaben (Desprez, et al., 2002; Scheible, et al., 2001). Therefore, a hypothesized link between the exocyst and placement of cellulose synthases in the plasma membrane might be revealed if exocyst mutants showed an altered response to isoxaben. To evaluate this possibility the effect of isoxaben on root growth in *sec8-1* seedlings was evaluated, and only minimal differences between mutant and wild-type were observed. Thus, I found no evidence in roots to link the exocyst to transport of cellulose synthase to the plasma membrane.

The exocyst and etiolated hypocotyl elongation

The hypocotyl cells of dark grown exocyst mutants demonstrate reduced elongation that occurs at a slower rate, and is less spatially defined, compared to wild-type

Hypocotyl elongation in dark-grown exocyst mutants is severely reduced (up to 10-fold) compared to wild-type (Figure 4.10). This difference could potentially arise from a difference in cell number and/or cell length. A count of the number of cells in a hypocotyl cell file (from the collet to the base of the cotyledons) after five days of growth in the dark revealed significantly fewer cells in *sec8-1* versus wild-type siblings (20.2 $\pm$ 1.6 versus 21.8 $\pm$ 2.5; n = 20 for each; $p<0.01$ t-test), but this difference is not enough to explain the large effect on hypocotyl length. Conversely, when cell lengths for cells at two different positions from the collet were measured, both *sec8-1* and *exo70A1* mutants demonstrate significantly shorter cells compared to wild-type (up to 10-fold) (Figure 4.11). Thus, the reduced length of the mutant hypocotyls is almost entirely the result of reduced cell elongation. My observations of the *exo70A1* mutant are similar to those already published (Synek et al., 2006).

To determine whether the elongation defect was due to altered developmental patterning of the hypocotyl tissue, or alternatively, to a cellular defect in otherwise anatomically normal structure, mid-hypocotyl cross sections were made of dark-grown mutant and wild-type seedlings (Figure 4.12 A-C). The hypocotyls of *sec8-1*, *exo70A1-2*, and *Columbia-0* seedlings possessed approximately the same number of cells in each of the concentric layers of epidermis, cortex, and endodermis surrounding the vascular bundle. The epidermal cells in the mutants appear to have a slightly larger radius compared to wild-type, and their endodermal cells appear to be collapsed. The collapsed endodermal cells could be an artifact of the fixing and staining process, but it was consistently observed in mutants, and not in wild-type, in three different preparations. Nevertheless, the overall anatomy in the mutant hypocotyl is similar to wild-type.

To gain further insight, transmission electron microscopy was performed on hypocotyl cross sections (Figure 4.12 D-F). Mutants demonstrated thicker outer walls in the cells of the epidermis. Also notable was the dark staining cuticle, which was generally less prominent in the wild-type cross sections. Cell walls thin concomitant with

elongation in wild-type plants (Refregier et al., 2004), so the thicker walls in the *sec8-1* mutants could be the result and not the cause of reduced elongation. The cytoplasm next to the cell membranes was examined to determine if there were any evidence of a secretory defect (e.g., an accumulation of secretory vesicles) in the exocyst mutants, compared to wild-type. In general, there was more cytoplasm between the vacuole and the cell membrane in the mutants, making it easier to find organelles, but evidence of an obvious secretory defect was not observed.

Dark-grown *prc1* (celluose synthase) mutants show dramatically shorter hypocotyls, as they fail to develop the rapid exponential growth of the hypocotyl seen in wild-type plants, but instead maintain a slower constant rate of elongation (Desnos et al., 1996). Thus, this phenotype is superficially very similar to that of the exocyst mutants. To explore the possibility that an alteration in cellulose synthase activity might be involved in the mutant phenotype, cell elongation rates and isoxaben sensitivity were evaluated. Cell elongation as a function of time for exocyst mutants and Columbia 0 seedlings is shown in Figure 4.13. Wild-type plants showed the characteristic exponential elongation, until growth eventually slowed as a maximum length was approached. The *sec8-1* mutants demonstrated a slower, more constant rate of growth. Elongation in *exo70A1-2* mutants as a function of time was more erratic, but in general appeared to fall between that of *sec8-1* and wild-type plants. Although these results are similar to those seen for *prc1*, the isoxaben dose-response curve for dark-grown *exo70A1* hypocotyls, like that for *sec8* root growth, was similar to wild-type. Thus, no specific linkage between the exocyst and cellulose synthase was established.

To further characterize the altered hypocotyl elongation in exocyst mutants, the spatial distribution of cell elongation along the length of the hypocotyl was evaluated. In dark-grown wild-type seedlings, cell elongation begins after seed germination in the basal cells of the hypocotyl, and with time this region of elongation shifts up the hypocotyl towards the cotyledons (Gendreau, 1997). To evaluate the pattern of elongation in exocyst mutants, hypocotyls cells from seedlings grown in the dark for 84 hours were measured. In contrast to the expected pattern of differential elongation seen in Columbia-0, *sec8-1* mutants had a uniform distribution of cell lengths along the length of the

hypocotyls (Figure 4.14). The *exo70A1* mutants also demonstrated a relatively flat distribution of cell length compared with wild-type, but with slightly enhanced elongation at the base. The magnitude of hypocotyl cell elongation in *sec8-1* was comparable to the less elongated cells at the apical end of wild-type hypocotyls. Thus, one possible explanation for the exocyst mutant phenotype is a defect in a hypothesized signaling process that triggers cell elongation as it travels from base to apex of the hypocotyl (see discussion).

A link between brassinosteroid signaling and the exocyst is also implicated in dark-grown hypocotyl elongation

Exocyst mutants demonstrate not only a short hypocotyl, but other aspects of a partially de-etiolated phenotype (i.e., light-dependent characteristics when grown in the dark) as well. This includes relaxed hypocotyl hooks, and cotyledons that sometimes appear to have separated, although they remain diminuative rather than expanded in the exocyst mutants (Figure 4.15). Apical hook development is under the control of auxins, ethylene, gibberellins, and brassinosteroids (DeGrauwe, et al., 2005; Knee et al., 2000). The partially de-etiolated phenotype observed in the exocyst mutants, therefore, is likely to involve more than an effect on cellulose synthase, or altered secretion of a wall-modifying enzyme, which then restricts cell wall expansion and thus cell elongation. One possibility suggested by the partially de-etiolated phenotype is that the exocyst is involved in the phytohormone-mediated switch controlling the transition between skotomorphogenesis and photomorphogenesis (dark-grown vs. light-grown development) (Alabadi et al., 2008; de Lucas et al., 2008).

Brassinosteroid signaling seemed a likely candidate for involvement with the exocyst in the hypocotyl, because of the connection revealed between brassinosteroids and the exocyst in primary root growth. To begin exploring this possibility, *sec8-1*, *exo70A1-2*, and *Columbia-0* seeds were grown in the dark for 5 days on plates containing a range of 24-epibrassinolide (EBR) concentrations. Both *Columbia-0* and *exo70A1* demonstrated a decreased hypocotyl elongation with increasing concentration of exogenous EBR (Figure 4.16A). The *sec8-1* mutants, however, showed a slight

stimulation of hypocotyl elongation with increasing concentration that appeared to peak at an EBR concentration of 500 nM, which caused severe inhibition of hypocotyl elongation in wild-type and *exo70A1* seedlings. Similar results were seen across a broader range of lower EBR concentrations in a second experiment (Figure 4.16B). The result appears to parallel that obtained for primary root growth: the *sec8-1* exocyst mutant has a decreased sensitivity to exogenous EBR, showing both hormone-mediated growth stimulation and growth inhibition at a higher concentration than is seen in wild-type. In contrast to the root, however, a strong rescue of the shortened hypocotyl phenotype was not achieved by exogenous EBR treatment.

Hypocotl elongation in etiolated seedlings is regulated by a number of phytohormones (Collett et al., 2000; DeGrauwe et al., 2005) The response of mutants in other pathways with defects in hypocotyl elongation to doses of EBR was determined to test whether the response of *sec8* mutants to EBR was specific. The *ga3ox1*, *eto1-1*, and *prc1-1* mutations are all associated with shortened hypocotyls, yet none of these mutants responded to exogenous EBR with an increase in hypocotyl elongation (Figure 4.16C). Additional hormone pathways that have been linked to hypocotyl elongation were again tested for interaction with the exocyst mutants in this developmental context. Growing the mutants on plates with exogenous auxin (IAA) or gibberelin (GA3) did not rescue the exocyst mutant phenotypes (data not shown). The responsivity of exocyst mutants to additional ethylene was also evaluated by growing the dark-grown seedlings on media containing ACC. Both *Columbia 0*, and *exo70A1-2* demonstrated similarly decreasing hypocotyl elongation with increasing ACC, while the *sec8-1* mutant showed no response to exogenous ACC, likely because its hypocotyl growth was already severely inhibited. Overall, the only potential role for the exocyst revealed by this array of phytohormone experiments was in brassinosteroid signaling.

4.3 DISCUSSION

The exocyst and primary root growth

Microscopic characterization of the root of exocyst mutants has revealed that the observed short root phenotype is the result of a reduced number of cell divisions

(primarily associated with a shortened meristem), a slight reduction in root cell elongation, and a delayed development of a root elongation zone following seed germination. These root growth processes are regulated by a host of hormones, whose signaling pathways interact at multiple levels. My observations suggest that the exocyst may play a specific role in brassinosteroid signaling. I propose two hypotheses. First, I hypothesize that the exocyst facilitates the transport of brassinosteroids to the exterior of the cell. Second, I hypothesize that the exocyst is required for the exocytosis that places the BRI1 brassinosteroid receptor in the plasma membrane of root cells.

The exocyst's effect on root growth involves brassinosteroid signaling

Although the brassinosteroid signaling pathway is incompletely understood, many of its essential components have recently been identified (see recent reviews, Gendron and Wang, 2007; Mussig et al., 2006; Symons et al., 2008). Enzymes for brassinosteroid (BR) synthesis are localized to the endoplasmic reticulum. However, BR perception is believed to occur at the cell surface by BRI1, a plasma membrane- and endosome-localized receptor kinase (Geldner, et al. 2007). The mechanism by which BR is transported from its presumed site of synthesis, the endoplasmic reticulum, to the exterior of the cell is currently unknown (Symons et al., 2008). The BR receptor, BRI1, is expressed ubiquitously and is localized to the plasma membrane of both the hypocotyl and root, and especially in the root meristem (Friedrichsen, et al., 2000; Geldner et al., 2007). Activation of the BRI1 receptor stimulates a signaling pathway that ultimately leads to the activation of BRZ transcription factors and the modulation of gene expression (Wang, et al., 2002).

This current understanding of brassinosteroid signaling suggests two sites for potential exocyst involvement. First, it can be hypothesized that the exocysst facilitates the transport of BR to the plasma membrane, presumably acting to target and tether BR containing vesicles to sites of exocystosis. BR's are relatively nonpolar, and may not be secreted in the usual sense. Instead their non-polarity may allow them to be carried within vesicle membranes to the plasma membrane, and ultimately to cross the plasma membrane to enter the extracellular environment. A second hypothesis is that the exocyst

affects root growth by facilitating the placement of BRI1 in the plasma membrane and assisting its cycling through the endomembrane system.

Initial supportive evidence for a role of the exocyst in brassinosteroid signaling comes from the dose-response data for exogenously applied BRs. Data resulting from the application of exogenous hormones must be interpreted with caution, because the applied hormone can circumvent or overwhelm endogenous signaling pathways or disrupt the balance between pathways (Mussig, 2005). In the case of brassinosteroids, it is essential to evaluate the response to low concentrations (e.g. EBR: 0.1-1.0 nM). As confirmed in Figure 4.9, high BR concentrations inhibit root growth in wild-type plants, but low concentrations of exogenous brassinosteroids promote root elongation (Clouse, et al., 1996; Mussig et al., 2003), a phenomenon known as hormesis. Others have demonstrated that brassinosteroid biosynthesis mutants require a higher BR concentration before the threshold is reached for inhibition of growth, and mutations in the BRI1 receptor can make the plant completely resistant to exogenous BRs (Clouse et al., 1996; Noguchi et al., 1999). The dose-response curve to 24-epibrassinolide (EBR) of the *sec8-1* mutant was informatively different from wild-type. The root growth rate increased much more gradually with increasing EBR concentration, reaching a maximum growth rate at an EBR concentration that inhibits growth in both wild-type and *exo70A-1* plants. At this maximum growth rate, the growth rate of the *sec8-1* mutant was nearly restored to that of untreated wild-type plants, a 2-fold increase in growth rate. Wild-type root growth can also be increased by EBR treatment, but demonstrates only a 0.2 fold increase to this treatment.

In the scenario envisioned by the first proposed hypothesis, exocyst mutants transport less BR to the exterior of the cell, reducing BR signaling and root growth. The addition of exogenous hormone partially compensates for this defect. According to this hypothesis, the baseline extracellular BR in the mutant is lower than in wild-type plants, so that more exogenous BR must be applied to the mutant to achieve the maximum stimulatory effect, or to result in the ultimate inhibition of growth. This was the observed result. In the scenario envisioned by the second proposed hypothesis, the short root phenotype would be explained by the exocyst mutant's decreased ability to place an

adequate number of BRI1 receptors in the plasma membrane. A reduced number of BRI1 receptors in the membrane might lead to decreased sensitivity to the stimulating effects of EBR. However, wild-type growth is restored when the reduction in the number of receptors is compensated for by increasing the EBR concentration, and consequently increasing the probability that the available receptors are activated. Additional research is needed to determine which, if either, of these hypotheses is correct.

Additional evidence supporting a role of the exocyst in brassinosteroid signaling comes from a comparison of the root growth phenotype of the *SEC8* mutants with that observed in mutants affecting BR signaling. Like *sec8-1*, both BR deficient (*dwf1-6* and *cbb3*) (Mussig, et al., 2003) and BR signaling (*bri1*) (Clouse et al., 1996; Mouchel et al., 2006) mutants have roots that are significantly shorter than wild-type; however, the cellular nature of this defect has not been described. In *Allium cepa* root tips, low doses of exogenous EBR results in doubling of root length associated with a doubling of the number of cells undergoing mitosis (Howell et al. 2007). This suggests that the root growth defect in brassinosteroid signaling mutants may reflect a fundamental problem affecting cell division and the meristem, just as it does in the *SEC8* mutants.

The most thorough description available for a root growth defect associated with a brassinosteroid-related mutant comes from work on *BREVIS RADIX (BRX),* a gene identified by quantitative trait locus analysis as accounting for ~80% of the observed difference in root lengths observed among 44 Arabidopsis accessions (Mouchel et al., 2004). Mutation of BRX results in a root-specific deficiency of brassinosteroid, due to a reduced BRX-dependent expression of the rate limiting enzyme in brassinosteroid biosynthesis (Mouchel et al., 2006). Comparing the root phenotype of brx^{s} with that of *sec8-1* (mutant type A) reveals striking similarities. In both cases total root length was reduced to about 33 percent of the associated wild-type plants. In both cases, the reduced growth was partially the result of reduced root cell length, with mature cortical cell lengths about 75 percent of wild-type in each. In both cases there was evidence of a shortened meristem. In brx^{s}, the meristem length was 25 percent of wild type when measured by number of cortical cells, whereas in *sec8-1* mutants meristem lengths were 50 percent of wild type when measured by *CYCB:GUS* staining. Both had remarkably

fewer dividing cells when compared to wild-type. Finally, both *brx*^{s} and *sec8-1* mutants had shorter elongation zones, noted to be about 40 percent of wild-type in the *brx*^{s} mutants. This comparison indicates that a defect in brassinosteroid signaling could account for most of the specific characteristics associated with the root growth phenotype in the severe exocyst mutants.

Intriguingly, the *brx*^{s} root growth phenotype could be rescued by application of brassinolide early in embryogenesis (Mouchel et al., 2006). Siliques dipped once into brassinolide one day after fertilization produced progeny in which meristem size, root growth rate, and cell elongation were fully rescued until eight days after germination, after which growth was reduced compared to wild-type. This result suggests brassinosteroids are required early in the embryo to establish meristem size, and post-embryonically for optimal root growth. Hence, if the exocyst is required for optimal brassinosteroid signaling, that requirement may be particularly acute in early embryonic development. An interesting possibility is that the exocyst's failure during this developmental window leads not only to the shortened root apical meristem, but also to inhibition of expression of the elongated cell phenotype in the earliest cells derived from that root meristem. No published reports indicate whether other brassinosteroid-related mutants also exhibit the larger region of isotropically-expanding cells, which I hypothesize is caused by a delayed establishment of the elongation zone in mutant roots.

No evidence supported linkage of the exocyst to other root growth-related hormone signalling

Plasma membrane associated auxin efflux facilitators (i.e. PIN proteins), are continuously undergoing endocytosis and recycling to the plasma membrane, where their polarized localization provides the mechanism for directional auxin transport and the development of auxin gradients (Geldner et al. , 2001; Bouette et al., 2005; Bouette et al. 2007; Wisniewska et al., 2006). The incorporation of PIN proteins into the plasma membrane via secretory vesicles or recycling endosomes could potentially depend upon the exocyst. Combined mutations in multiple PIN genes disrupts the auxin transport network in Arabidopsis roots and results in a reduction in root length, meristem size,

elongation zone size, and final root cell length (Biliou, 2005). These defects echo those seen in the exocyst mutants. It was therefore anticipated that the observed root growth defects in exocyst mutants would be discovered to involve altered auxin transport caused by the alterations in the placement of auxin transport facilitators in the plasma membrane. Surprisingly, the root growth response to exogenous auxin and the *DR5:GUS* staining experiments did not support this conclusion.

Additional experiments did not provide evidence to support a connection between the exocyst and cytokinin or ethylene signaling, or with cellulose synthase. Subtle effects of the exocyst on non-brassinosteroid signaling pathways may not have been detected by these experiments, and thus such connections may exist. However, it would be surprising if such a subtle effect were responsible for the extreme root growth defect seen in the severe exocyst mutants.

The exocyst and hypocotyl elongation in dark grown seedlings

Hypocotyl elongation in dark-grown exocyst mutants occurs not by cell division, but by cell elongation, just as it does in wild-type plants. However, the exponential phase of elongation that begins in wild-type plants about two days after germination apparently does not occur in severe exocyst mutants, such as *sec8-1*. The lack of an exponential growth phase is reminiscent of hypocotyl growth observed in dark grown *procuste1* mutants, which have a defective cellulose synthase (Desnos et al., 1996). This suggested that the exocyst might be required for effective cellulose synthase placement in the plasma membrane. Such a hypothesis predicts that an exocyst mutation might display an altered response to the herbicide, isoxaben; however, no such difference was observed.

A partially de-etiolated phenotype, which included effects on the apical hook as well on hypocotyl elongation, was observed in the exocyst mutants, and suggests a defect in adopting the full skotomorphogenetic (dark-grown) developmental program. Conceivably, such a defect could affect photoreceptors, generating dark-grown plants that in effect have not perceived that they are in the dark. However, phenotypic evidence does not support such a conclusion: *sec8-1*, *sec8-3*, *exo70A1-1*, *exo70A1-2*, and *sec8-4 exo70A1-2* double mutants all develop hypocotyls when grown in the dark that are longer

(n=16-96, $p<0.001$, t-test) than when grown in the light (Figure 10). In addition, dark-grown mutant cotyledons remain diminutive, folded together, and unexpanded, all characteristics of wild-type cotyledons grown in the dark. Finally, both *sec8-1* mutants and wild-type seedlings showed similar dark-dependent reductions in auxin production, as revealed by *DR5:GUS* staining (data not shown). Together, these observations indicate that the hypocotyl elongation defect is not due to an inability of the mutant seedlings to detect that they are in the dark. However, in exocyst mutants the apical hook is not developed or maintained, a characteristic of light-grown seedlings (Figure 4.15). One possibility is that this reflects a defect downstream of light perception, e.g., an inability to differentially regulate cell elongation on opposite sides of the apical hook. Analysis of transcripts associated with either skotomorphogenesis or photomorphogenesis would be useful for determining whether particular branches of the skotomorphogenic developmental program (e.g., those that are brassinosteroid-dependent) are affected by loss of exocyst function.

The exocyst may have a role in brassinosteroid signaling in hypocotyl elongation

The partial rescue of hypocotyl elongation in *sec8-1* mutants by treatment with exogenous EBR, as well as its altered dose-response curve, indicates that the exocyst may have a role in brassinosteroid signaling in the hypocotyl as well as the root. Dark-grown brassinosteroid synthesis mutants have long been associated with similar de-etiolated phenotypes: hypocotyls that fail to elongate, and diminished apical hooks with diminutive cotyledons (Kauschman, 1996; Li, 1996; Nakamoto 2006;, Szekeres, 1996). Significantly, brassinosteroid synthesis mutants can be fully rescued by application of exogenous brassinosteroids, whereas hypocotyl elongation in the exocyst mutants is not. This places the exocyst downstream of brassinosteroid synthesis. The hypotheses proposed for exocyst function in the root can also be applied to the hypocotyl: the exocyst facilitates transport of brassinosteroids or the brassinosteroid receptor, BRI1, to the plasma membrane, where BR initiates the signaling to generate a subset of the changes associated with skotomorphogenesis (e.g., the apical hook). The BRI1 receptor is highly expressed on the cell surface of the hypocotyl in wild-type seedlings

(Friedrichsen, et al., 2000). In light-grown *bri1* null mutants (which are extreme dwarfs), epidermal-specific expression of BRI1 can restore hypocotyl length to wild-type stature (Salvaldi-Goldstein et al., 2007). Unfortunately, the specific role of BRI1 in the hypocotyl elongation of etiolated seedlings has not been reported.

Evidence does not reveal a role for the exocyst in auxin, gibberellin, or ethylene signaling to affect hypocotyl elongation

Only a limited investigation of the effect of other phytohormones, auxin, gibberellin, and ethylene on hypocotyl elongation in exocyst mutants was performed. The role of auxin in etiolated hypocotyl growth has been primarily associated with the formation of the apical hook (deGrauwe, et al., 2005). High concentrations of exogenous auxin resulted in only a mild inhibition on overall hypocotyl elongation in the exocyst mutants or *Columbia-0*, suggesting it has a limited role in this growth process.

Exogenous gibberellin also had little effect on hypocotyl elongation of dark-grown seedlings and did not rescue the exocyst mutant phenotype. Others have observed similar lack of response for dark-grown wild-type plants, which they have related to saturation of GA signaling (Cowling and Harberd, 1999). The *ga3ox1-3* gibberellin biosynthesis mutant did not phenocopy the *sec8-1* mutant with respect to its response to exogenous BR (Figure 16C), although this mutant may not have a complete gibberellin deficiency, due to the redundancy of enzyme (Mitchum et al., 2006).

Ethylene overproduction has also been tied to reduced hypocotyl elongation, as part of the seedling "triple response" to ethylene. However, the increased curvature of the apical hook expected in the presence of high ethylene was not observed in the exocyst mutants, suggesting this was not a likely mechanism to explain the phenotype. The *exo70A1-2* mutant responded to increased endogenous ethylene (produced by growth on the ethylene precursor, ACC), with the same dose-response as wild-type controls. Additionally, the ethylene overproducer, *eto1-1*, did not phenocopy the *sec8-1* mutants response to exogenous BR. In summary, neither auxin, gibberellin, nor ethylene signaling pathways were revealed by these experiments to be strong candidates for direct involvement with the exocyst during hypocotyl elongation in etiolated seedlings.

4.4 CONCLUSION

A detailed developmental and phenotypic characterization has provided the basis for exploring the role of the exocyst in two developmentally distinct types of plant morphogenesis, primary root growth and etiolated hypocotyl elongation. This analysis has led to the hypotheses that the exocyst is involved in brassinosteroid signaling via a role in the trafficking of brassinosteroids or the BRI1 receptor to the plasma membrane. Specifically, it has been hypothesized that the root growth defect in exocyst mutants is primarily related to an associated defect in brassinosteroid signaling. Furthermore, the defect in hypocotyl elongation observed in dark-grown exocyst mutants is also hypothesized to be associated, at least in part, with a defect in brassinosteroid signaling. A connection between the exocyst and brassinosteroid signaling was unexpected, but it may be a fortuitous discovery. Roots are accessible to live imaging without dissection, and GFP-tagged BRI1 has already been successfully employed to investigate receptor trafficking in this tissue (Geldner, et al. 2007). Consequently, roots and hypocotyls may prove to be ideal models for studying the function of the exocyst at the cellular and molecular levels, at least with respect to trafficking of a specific protein. While determining if the exocyst is involved in brassinosteroid signaling, it may be possible to answer more fundamental questions, such as, does the exocyst play a role in the secretory pathway of plants, and what are the molecular mechanisms that underpin exocyst function?

Future research to explore the exocyst's potential role in BRI1 trafficking may provide important insights about brassinosteroid signaling as well. Recent evidence suggests that brassinosteroid signaling is dependent upon the subcellular partitioning of the BRI1 receptor between endosomes and the plasma membrane (Geldner, et al. 2007). Surprisingly, BRI1 appears to localize to endosomes independent of its activation by brassinosteroids, and appears to be constitutively recycled. The exocyst's hypothesized role in brassinosteroid signaling would likely alter the cycling of BRI1. Consequently, the use of exocyst mutants may provide valuable insights that will further advance our understanding of how endosomes are used as signaling compartments in plants. Alternatively, if the exocyst is involved in the movement of brassinosteroids to the cell

exterior, demonstration of that role may solve a current mystery in brassinosteroid signaling: how braassinosteroids are transported from their presumed site of synthesis within the endoplasmic reticulum to the plasma membrane.

Finally, the developmental analysis presented here uncovered a previously undescribed phenotype. In newly germinated seedlings with severe exocyst mutations, root growth is initially driven entirely by cell division in the meristem without the formation of an elongation zone and without significant cell elongation. Then at a seemingly random point in root growth, a developmental switch apparently occurs in the mutant root, such that an elongation zone with wild-type activity forms, generating cells with a more typical elongated morphology. This appears to be a novel developmental phenotype, and it may provide a new avenue for exploration of factors that define the elongation zone, as well as meristem-elongation zone interactions.

4.5 MATERIALS AND METHODS

Plant material and growth conditions

Lines of Columbia-0 ecotype of *Arabidopsis thaliana* with T-DNA insertions and other mutants were obtained from the SALK Institute (Alonso et al., 2003): *exo70A1-1* (At5g03540) SALK_014826; *exo70A1-2* (At5g03540) SALK_135462; *sec5a-1* (At1g76850) SALK 010127; *sec8-1* (At3g10380) SALK 057409; *sec8-3* (At3g10380) SALK 026204; *sec8-4* (At3g10380) SALK 118129; *sec8-6* (At3g10380) SALK 091118; *bri-* (At4g39400) SALK 003371; *eto1-1* (At3g51770); *ga3ox1-3* (At1g15550) CS6943; *prc1-1* (At5g64740) CS297; *rsw1-1* (At4g32410) CS6554. Exocyst T-DNA insertion sites for exocyst related SALK lines were verified by sequencing. Arabidopsis seeds were surface-sterilized, stratified at 4 °C for 3-5 days, and planted on growth media (1x MS, 2% (w/v) sucrose, and vitamins) or soil as previously described (Cole et al., 2005). Serial dilutions of hormones were prepared and added to media cooled to 50°C prior to pouring plates. Phytohormones: 3-Indoleacetic acid (IAA), Naphalene acetic acid (NAA), gibberellic acid (GA3), N6 benzyladenine, kinetin, 24-epibrassinolide, and 1-aminocyclopropane-1-carboxylate (ACC) were all obtained from Sigma-Aldrich. Light grown plants were grown in a climate chamber at 22 °C under long-day conditions (16 h

of light per day). In dark grown hypocotyl elongation experiments, surface sterilized, stratified, and plated seeds were placed in a lighted incubator at 22 ºC for 2-4 hours to stimulate germination, and then wrapped in foil, oriented vertically, and placed in a dark box in the incubator for 5 days unless otherwise specified.

Whole Root and Hypocotyl elongation measurements

Images of roots and whole hypocotyls were captured with a Moticam 1000 camera attached to a Zeiss Stemi SV 11 dissecting microscope, or with a Canon Power Shot A710IS digital camera. Root growth rates at 7 days of growth were calculated from plants growing on vertical plates, by marking the location of the root tip on the plates at precisely the same time on days 6, 7 and 8, and then photographing the plates on day 8. Measurement of hypocotyl and root lengths was performed from the digital photographs using ImagePro software (MediaCybernetics, www.mediacy.com). EC_{50} (the exogenous hormone concentration that provokes a response halfway between the baseline and maximum responses) was determined graphically, or by curve-fitting data to a sigmoidal model using DataFit version 8.2.79 software by Oakdale Engineering.

Hypocotyl cell measurements

In hypocotyl cell length experiments, seeds plated on foil wrapped plates, were removed from the dark box in the incubator at specified times. At early times, prior to seed germination, seed coats were surgically removed to expose the embryo, prior to fixation and staining. The embryo or whole seedling was immediately fixed in 3:1 ethanol:acetic acid solution for at least one hour at room temperature, rinsed with H_2O, cleared in 8N NaOH for 1 hour, rinsed with H_2O, and stained with 0.05% w/v Toluidine Blue in citrate buffer pH 4.6 only briefly (typically 5 seconds), before viewing. Light microscopy was performed on a Zeiss Axiovert microscope with differential interference contrast optics.

Preparation of cross sections for light and electron microscopy

Excised root, hypocotyl, or whole seedling samples were embedded in 2% LMP agarose and immediately fixed and prepared for ultra-thin sectioning as described by (Park and

Twell, 2001). Briefly, samples were chemically fixed in glutaraldehyde, dehydrated, and sectioned. For electron microscopy the sections were stained with uranyl acetate and lead citrate, and viewed with a transmission electron microscope (Philips CM 12, 60kV). For light microscopy the sections were stained with Toluidine blue and Azure II.

Preparation of samples for GUS staining

Seedlings were fixed in 0.3% formaldehyde in 0.33 M phosphate buffer pH 7.2 for 30 min at room temperature, then rinsed three times in 50 mM phosphate buffer pH 7.2. GUS activity was analyzed after staining the fixed seedlings overnight at 37°C and then cleared as described by Melamy and Benfey (1999) and modified by Ivanchenko et al., (2006).

Analysis of root tips stained for *CYCB:GUS* activity

Procedure was essentially that of Werner, et al. (2003). Root Length corresponds to length of entire primary root; Max Cell Length corresponds to the average cell length of the three longest cortical cells identified throughout the entire root, and is provided as an indication of elongation potential; Meristem Length corresponds the length of the region identified by GUS staining to contain dividing cells; Number of Dividing Cells per Meristem is based on counting GUS-positive stained cells; Dividing Cells per Meristem Volume is based on the following calculation to estimate meristem volume. The tip of the meristem was modeled as a hemisphere with a volume determined after measuring its diameter. The remainder of the meristem volume was modeled as the frustrum of a cone, extending from the hemisphere to the base of the meristem, with a volume calculated using the measured diameter at the hemisphere end, the measured merstem diameter at the base and the measured meristem length. Empirically, this provided a closer fit to the shape of the meristem than a more simple elliptical cone model, over the range of meristem shapes and sizes encountered.

4.6 LITERATURE CITED

Alabadi, D., Gallego-Bartolome, J., Orlando, L., Garcia-Carcel, L., Rubio, V., Martinez, C., Frigerio, M., Iglesias-Pedraz, J., Espinosa, A., Deng, X., Blazquez, M. (2008). Gibberellins modulate light signaling pathways to prevent Arabidopsis seedling de-etiolation in darkness. Plant Journal 53: 324-335.

Alonso, J.M., Stepanova, A.N., Leisse, T.J., Kim, C.J., Chen, H., Shinn, P., Stevenson, D.K., Zimmerman, J., Barajas, P., Cheuk, R., Gadrinab, C., Heller, C., Jeske, A., Koesema, E., Meyers, C.C., Parker, H., Prednis, L., Ansari, Y., Choy, N., Deen, H., Geralt, M., Hazari, N., Hom, E., Karnes, M., Mulholland, C., Ndubaku, R., Schmidt, I., Guzman, P., Aguilar-Henonin, L., Schmid, M., Weigel, D., Carter, D.E., Marchand, T., Risseeuw, E., Brogden, D., Zeko, A., Crosby, W.L., Berry, C.C., and Ecker, J.R. (2003). Genome-wide insertional mutagenesis of Arabidopsis thaliana. Science 301: 653-657.

Blilou, I., Xu, J., Wildwater, M., Willemsen,V., Paponov, I., Frimi, J., Heidstra, R., Aida, M., Palme, K., Scheres, B. (2005) The PIN auxin efflux facilitator network controls growth and patterning in Arabidopsis roots. Nature 433: 39-44.

Boutte,Y., Crosnier, M., Carraro, N., Traas, J, Satiat-Jeunemaitre, B. (2006). The plasma membrane recycling pathway and cell polarity in plants: studies on PIN proteins. Journal of Cell Science 119:1255-1265.

Boutte, Y., Ikeda, Y., Grebe, M. (2007). Mechanisms of auxin-dependent cell and tissue polarity. Current Opinion in Plant Biology 10: 616-623.

Chen, X.W., Leto, D., Chiang, S.H., Wang, Q. and Saltiel, A.R. (2007). Activation of RalA is required for insulin-stimulated Glut4 trafficking to the plasma membrane via the exocyst and the motor protein Myo1c. Dev. Cell 13(3):391-404.

Clouse, S., Langford, M., McMorris, T. (1996). A brassinosteroid-insensitive mutant in *Arabidopsis thaliana* exhibits multiple defects in growth and development. Plant Physiology 111:671-678.

Cole, R.A., and Fowler, J.E. (2006). Polarized growth: maintaining focus on the tip. Curr. Opin. Plant Biol. 9: 579-588.

Cole, R.A., Synek, L., Žárský, V., and Fowler, J.E. (2005). SEC8, a subunit of the putative Arabidopsis exocyst complex, facilitates pollen germination and competitive pollen tube growth. Plant Physiology 138: 2005-2018.

Collett, C., Harberd, N., Leyser, O. (2000). Hormonal interactions in the control of Arabidopsis hypocotyl elongation. Plant Physiology 124: 553-561.

Colon-Carmona, A., You, R., Haimovitdh-Gal, T., and Doerner, P. (1999). Spatio-temporal analysis of mitotic activity with a labile cyclin-GUS fusion. Plant J. 20: 503-508.

Cowling, R.,Harberd, N. (1999). Gibberellins control Arabidopsis hypocotyl growth via regulation of cellular elongation. J. of Experimental Botany 50 (337): 1351-1357.

De Grauwe, L., Vandenbusssch, F., Tietz, O., Palme, L.,Van Der Straeten, D. (2005). Auxin, ethylene and brassinosteroids: triparitite control of growth in the Arabidopsis hypocotyl. Plant Cell Physiol. 46(6):827-836.

de Lucas, M., Daviere, J., Rogriguez-Falcon, M., Pontin, M., Iglesias-Pedraz, J., Lorrain, S., Fankhauser, C., Blazquez, M., Titarenke, E., Prat, S. (2008) A molecular framework for light and gibberellin control of cell elongation. Nature 451: 480-484.

Desnos, T., Orbovic, V., Bellini, C., Kronenberger, J., Caboche, M., Traas, J., Hofte, H. (1996). Procuste1 mutants identify two distinct genetic pathways controlling hypocotyl cell elongation, respectively in dare-and light-grown Arabidopsis seedlings. Development 122: 683-693.

Desprez, T., Vernhettes, S., Fagard, M., Refregier, G., Desnos, T., Aletti, E., Py, N., Pelletier, S., Hofte, H. (2002). Resistance against herbicide isoxaben and cellulose deficiency mutations in same cellulose synthase isoform CEXA6. Plant Physiology 128: 482-490.

Ferreira, F., Kieber, J. (2005). Cytokinin signalling. Current Opinion in Plant Biology 8: 518-525.

Friedrichsen,D., Joazeiro, C., Li, J., Hunter,T., Chory, J. (2000). Brassinosteroid-insensitive-1 is a ubiquitously expressed leucine-rich repeat receptor serine/threonine kinase. (2000). Plant Physiology 123: 1247-1255.
Garrick, M.D., and Garrick, L.M. (2007). Loss of rapid transferrin receptor recycling due to a mutation in Sec15l1 in hbd mice. Biochim. Biophys. Acta. 1773: 105-108.

Garrick, M.D., and Garrick, L.M. (2007). Loss of rapid transferrin receptor recycling due to a mutation in Sec15l1 in hbd mice. Biochim. Biophys. Acta. 1773: 105-108.

Geldner, N., Frimi, J., Stierhof, Y., Jurgens, G., Palme, K. (2001). Auxin transport inhibitors block PIN1 cycling and vescicle trafficking. Nature 413: 425-428.

Geldner, N., Hyman, D., Wang, X., Schumacher, K., Chory, J. (2007). Endosomal signaling of plant steroid redeptor kinase BR11. Genes & Development 21: 1598-1602.

Gendreau, E., Traas, J., Desnos, T., Grandjean, O., Caboche, M., Hofte, H. (1997). Cellular basis of hypocotyl growth in *Arabadopsis thaliana.* Plant Physiol. 114: 295-305.

Gengron, J., Wang, Z. (2007). Multiple mechanisms modulate brassinosteroid signaling. Current Opinion in Plant Biology 10:436-441.

Gerges, N.Z., Backos, D.S., Rupasinghe, C.N., Spaller, M.R., and Esteban, J.A. (2006). Dual role of the exocyst in AMPA receptor targeting and insertion into the postsynaptic membrane. EMBO J. 25: 1623-1634.

Gomi, K., Matsuoka, M. (2003). Gibberellin signalling pathway. Current Opinion in Plant Biology 6: 489-493.

Hala, M., Cole, R., Synek, L., Drodova, E., Pecenkova, T., Nordheim, A., Lamkemeyer, T., Madlung, J., Hochholdinger, F., Fowler, J., and Zarsky, V. (2008) An exocyst complex functions in plant cell growth. Submitted to Plant Cell. February 28, 2008.

Hazuka CD, Foletti DL, Hsu SC, Kee Y, Hopf FW, Scheller RH (1999) The sec6/8 complex is located at neurite outgrowth and axonal synapse-assembly domains. J Neurosci 19 (4): 1324-1334.

Howell, W., Keller III, G., Kirkpatrick, J., Jenkins, R., Hunsinger, R., McLaughlin, E. (2007). Effects of the plant steroidal hormone, 24-epibrassinolide, on the mitotic index and growth of onion (*Allium cepa)* root tips. Genet. Mol. Res. 6 (1):50-58.
Hsu, S.C., TerBush, D., Abraham, M., and Guo, W. (2004). The exocyst complex in polarized exocytosis. Int Rev Cytol 233: 243-265.

Inoue, M., Chang, L., Hwang, J., Chiang, S.H., and Saltiel, A.R. (2003). The exocyst complex is required for targeting of Glut4 to the plasma membrane by insulin. Nature 422: 629-633.

Ioio, R., Linhares, F., Scacchi, E., Casamitjana-Martinez, E., Heidstra, R., Costantino, P., Sabatini, S. (2007). Cytokinins determine Arabidopsis root-meristem size by controlling cell differentiation. Current Biology 17: 678-682.

Ivanchenko, M., Coffeen, W., Lomax, T., and Dubrovsky, J. (2006) Mutations in the Digeotropica (Dgt) gene uncouple patterned cell division during lateral root initiation form proliferative cell division in the pericycle. Plant J. 46: 436-447.

Kauschmann, A., Jessop, A., Koncz, C., Szekeres, M., Willmitzer, L., Altmann, T. (1996). Genetic evidence for an essential role of brassinosteroids in plant development. Plant Journal 9 (5) 701-713.

Kim, T., Lee, S., Joo, S., Yun, H., Lee, Y., Kaufman, P., Kirakosyan, A., Kim S., Nam, K., Lee, J., Chang, S., Kim., S. (2007). Elongation and gravitropic responses of Arabidopsis roots are regulated by brassinolide and IAA. Plant, Cell, and Environment 30: 679-689.

Knee, E., Hangarter, R., Knee, M. (2000). Interactions of light and ethylene in hypocotyl hook maintenance in *Arabidopsis thaliana* seedlings. Physiologia Plantarum 108:208-215.

Koumandou, V.L., Dacks, J.B., Coulson, R.M., and Field, M.C. (2007). Control systems for membrane fusion in the ancestral eukaryote; evolution of tethering complexes and SM proteins. BMC Evol. Biol. 7: 29.

Li, J., Johnson, P., Stepanova, A., Alonso, J., Echer, J. (2004). Convergence of signaling pathways in the control of differential cell growth in Arabadopsis. Developmental Cell 7: 193-204.

Li, J., Nagpal, P., Vitart, V., McMorris, T., Chory, J. (1996). A role for brassinosteroids in light-dependent development of Arabidposis. Science 272: 398-401.

Li, L., Xu, J., Xu, Z., Xue, H. (2005). Brassinosteroids stimulate plant tropism through modulation of polar auxin transport in brassica and Arabidopsis. Plant Cell17: 2783-2753.

Mitchum, M., Yamaguchi, S., Hanada, A., Kuwahara, A., Yoshioka, Y., Kato, T., Tobata, S., Kamiya, Y., Sun, T. (2006). Distinct and overlapping roles of two gibberellin 3-oxidases in Arabidopsis development. Plant Journal 445: 804-818.

Malamy, J. and Benfey, P. (1997) Orcanization and cell differentiation in lateral roots of Arabidopsis thaliana. Development 124: 33-44.

Mouchel, C., Briggs, G., Hardtke, C. (2004). Natural genetic variation in Arabidopsis identifies *Brevis radix,* a novel regulator of cell proliferation and elongation in the root. Genes & Development 18: 700-714.

Mouchel, C., Osmont, K., Hardtke, C. (2006). *BRX* mediates feedback between brassinosteroid levels and auxin signalling in root growth. Nature 443:458-461.

Mussig, C., Lisso, J., Coll-Garcia, D., Altmann, T. (2006). Molecular analysis of brassinosteroid action. Plant Biol. 8: 291-296.

Mussig, C., Shin, G., Altmann, T. (2003). Brassinosteroids promote root growth in Arabidopsis. Plant Physiology 133: 1261-1271.

Mussig, D. (2005). Brassinosteroid-Promoted Growth. Plant Biol. 7:110-117.

Nakamoto, D., Ikeura, A., Asami, T., Yamamoto, K. (2006). Inhibition of brassinosteroid biosynthesis by either a dwarf4 mutation or a brassinosteroid biosynthesis inhibitor rescues defects in tropic responses of hypocotyls in the Arabidopsis mutant *nonphototropic hyposotyl 4.* Plant Physiology141: 456-464.

Nemhauser, J., Mochler, T., Chory, J. (2004). Interdependency of brassinosteroid and auxin signaling in Arabidopsis. PloS Biology.2: (9) 1460-1471.

Noguchi, T., Fujioka, S., Choe, S., Takatsuto, S., Yoshida, S., Yuan, H., Feldmann, K., Tax, F. (1999). Brassinosteroid-intensive dwarf mutants of Arabidopsis accumulate brassinosteroids. Plant Physiology121: 743-752.

Park SK, Howden R, Twell D (1998) The Arabidopsis thaliana gametophytic mutation gemini pollen1 disrupts microspore polarity, division asymmetry and pollen cell fate. Development 125: 3789-3799.

Park SK, Twell D (2001) Novel patterns of ectopic cell plate growth and lipid body distribution in the Arabidopsis gemini pollen1 mutant. Plant Physiol 126: 899-909.

Refregier, G., Pelletier, S., Jailland, D., Hofte, H. (2004). Interaction between wall deposition and cell elongation in dark-grown hypocotyl cells in Arabidopsis. Plant Physiology 135: 959-968.

Ruzicka, K., Ljung, K., Vanneste, S., Podhorska, R., Beeckman, T., Friml. J., Benkova, E. (2007). Ethylene regulates root growth through effects on auxin biosynthesis and transport-dependent auxin distribution. Plant Cell 19: 2197-2212.

Salvaldi-Goldstein, S., Peto, D., Chory, J. (2007). The epidermis both drives and restricts plant shoot growth. Nature Vol. 446, 8 March 2007, pp. 199-202.

Scheible, W., Eshed, R., Richmond, T., Delmer, D., Somerville, C. (2001). Modifications of cellulose synthase confer resistance to isoxaben and thiazolidinone herbicides in Arabidopsis 1xr1 mutants. PNAS 98: (18) 10079-10084.

Symons, G., Reid, J. (2004). Brassinosteroids do not undergo long-distance transport in Pea. implications for the regulation of endogenous brassinosteroids levels. Plant Physiology 135: 2196-2206.

Symons, G., Ross, J., Jager, C., and Reid, J. (2008). Brassinosteriod transport. Journal of Experimental Botany 59(1):17-24.

Synek, L., Schlager, N., Eliáš, M., Quentin, M., Hauser, M.T., and Žárský, V. (2006). AtEXO70A1, a member of a family of putative exocyst subunits specifically expanded in land plants, is important for polar growth and plant development. Plant Journal 48: 54 - 72.

Szekeres, M., Nemeth, K., Koncz-Kalman, A., Mathur, J., Kauschmann, A., Altmann, T., Redei, G., Nagy, N., Schell, J., Koncz, C. (1996). Brassinosteroids rescue the deficiency of CYP90, a cytochrome P450, controlling cell elongation and de-etiolation in Arabidopsis. Cell 85: 171-182.

TerBush, D.R., Maurice, T., Roth, D., and Novick, P. (1996). The Exocyst is a multiprotein complex required for exocytosis in Saccharomyces cerevisiae. EMBO J 15: 6483-6494.

Wang, Z., Nakano, T., Gendron, J., He, J., Chen, M., Vafeados, D., Yang, Y., Fujioka, S., Yoshida, S., Asami, T., Chory, J. (2002). Nuclear-localized BZR1 mediates brassinosteroid-induced growth and feedback suppression of brassinosteroid biosynthesis. Developmental Cell.2: 505-513.

Wen, T.J., Hochholdinger, F., Sauer, M., Bruce, W., and Schnable, P.S. (2005). The roothairless1 gene of maize encodes a homolog of sec3, which is involved in polar exocytosis. Plant Physiol 138: 1637-1643.

Werner, T., Motyka, V., Laucou, V., Smets, R., Van Onckelen, H., Schmulling, T. (2003). Cytokinin-deficient transgenic Arabidopsis plants show multiple developmental alterations indicating opposite functions of cytokinins in the regulation of shoot and root meristem activity. (2003). Plant Cell 15: 2532-2550.

Xu, W., Campbell, P., Vargheese, A., and Braam, J. (1996). The Arabidopsis XET-related gene family: environmental and hormonal regulation of expression. Plant J. 9(6):879-889.

4.7 FIGURES

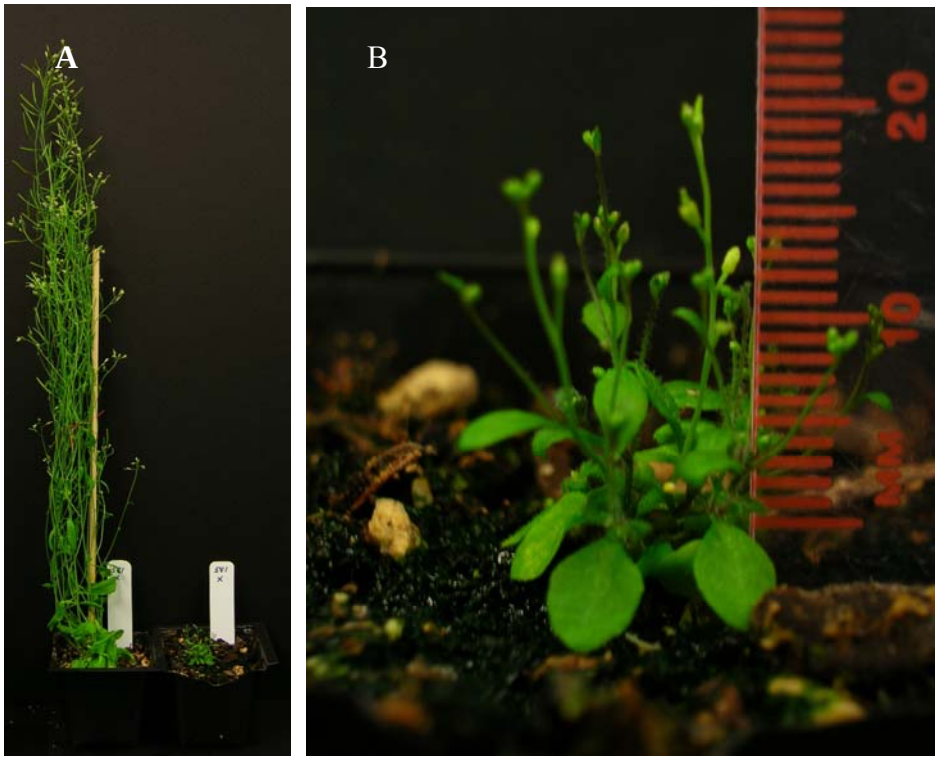

Figure 4.1. Exocyst mutants are dwarfs.
(A) *sec8-3* homozygote (left) and wild-type sibling (right), progeny of *sec8-3* heterozygote containing *LAT52:SEC8* construct. (B) Close-up of the *sec8-3* dwarf.

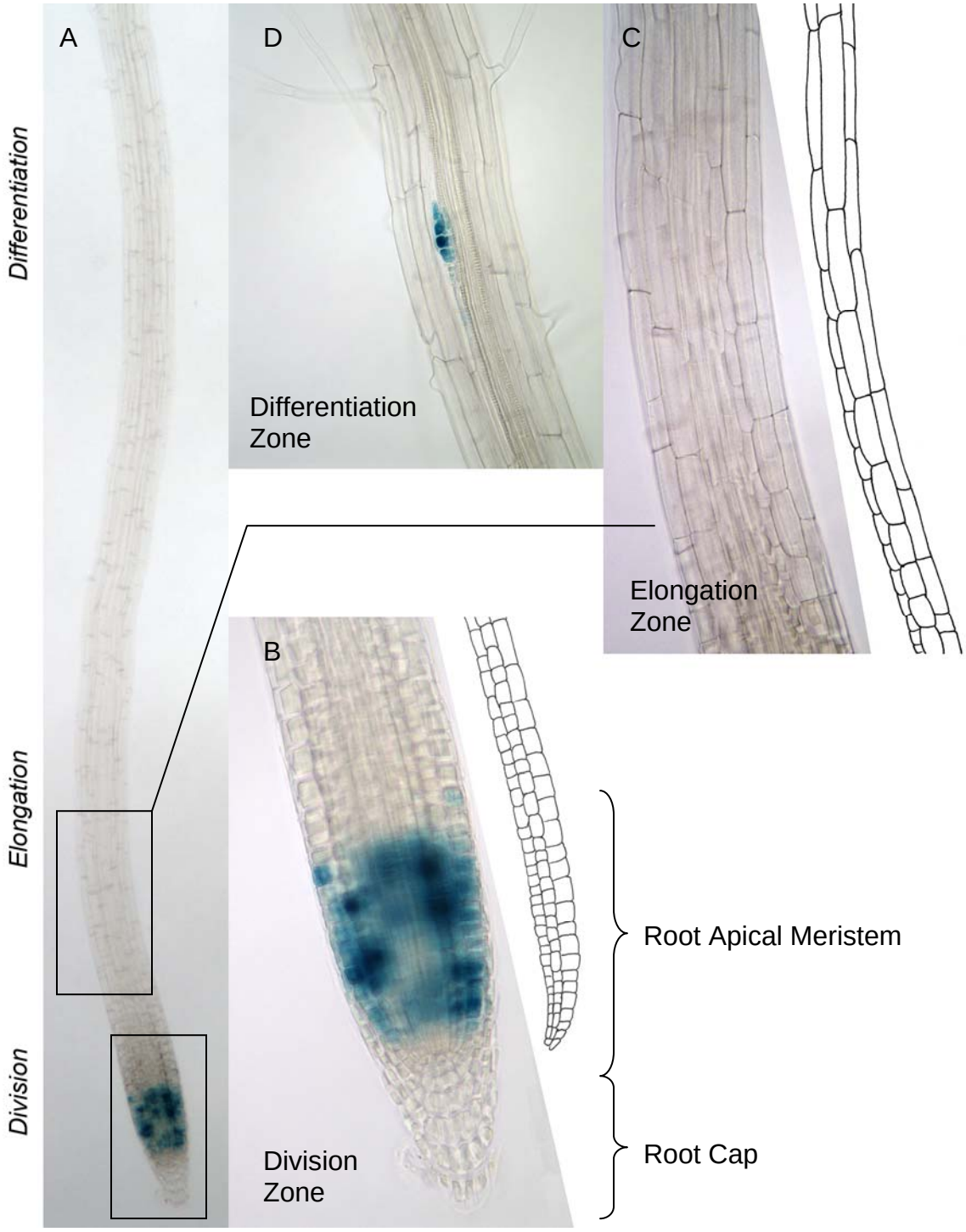

Figure 4.2 Root growth zones in Arabidopsis. *CYCB:GUS* staining dividing cells blue. B. Cells divide without elongating >2-fold in division zone. C. In elongation zone progression of cell elongation is evident in each cell file. D. In the differentiation zone cells develop root hairs, and lateral roots form as evidenced by patches of dividing cells.

Figure 4.3. (next page) Severe exocyst mutants demonstrate delayed development of a root elongation zone, resulting in a region of near isotropic growth near the collet. (A) Wild-type root with cell elongation occurring within a few cells of collet; collet marked by dark DR5-GUS staining at top of image. (B) *sec8-1* root with region of near isotropic growth extending from collet (top) until just before a lateral root branches to the right. (C) Wild-type root demonstrating elongating cells shortly after germination (after 30 hours incubation), stained with Toluidine blue (D) *sec8-1* root at same time point. (E) Fully elongated cortical cells (second layer from surface) in wild-type root. (F) Non-elongated root cells in region near collet of *sec8-1*. (G) Cross-section of wild-type root, and (H) or sec8-1 root. (I) 7 day old *sec8-6 exo70A1-2* root with CYCB:GUS construct stained for GUS, demonstrating active meristem and aberrant elongation zone. Bar = 100 μm for A (applies also to B), C, D, and I. Bar = 50 μm for E (applies also to F), G and H.

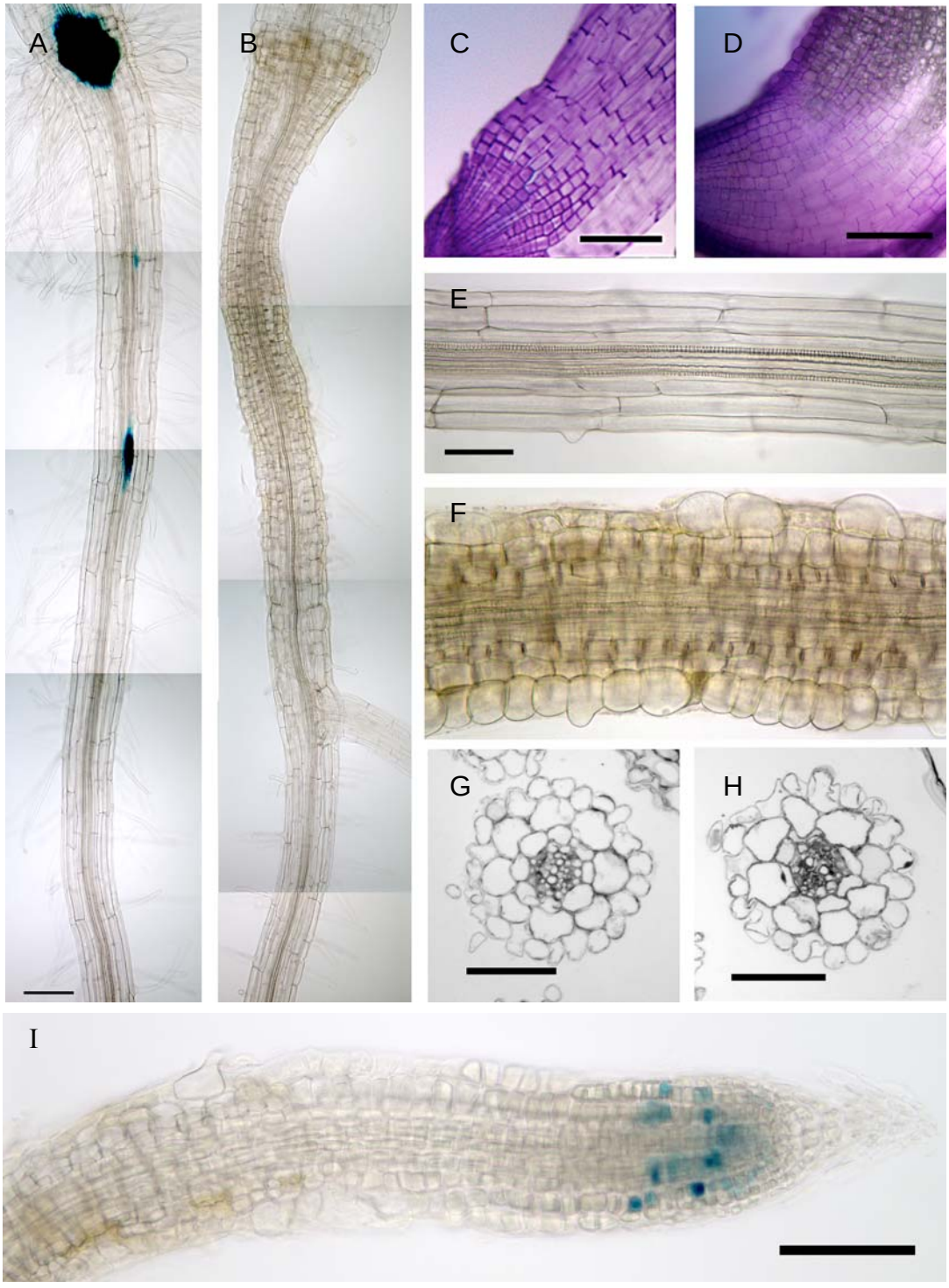

Figure 4.3. Severe exocyst mutants demonstrate delayed development of a root elongation zone, resulting in a region of near isotropic growth near the collet.

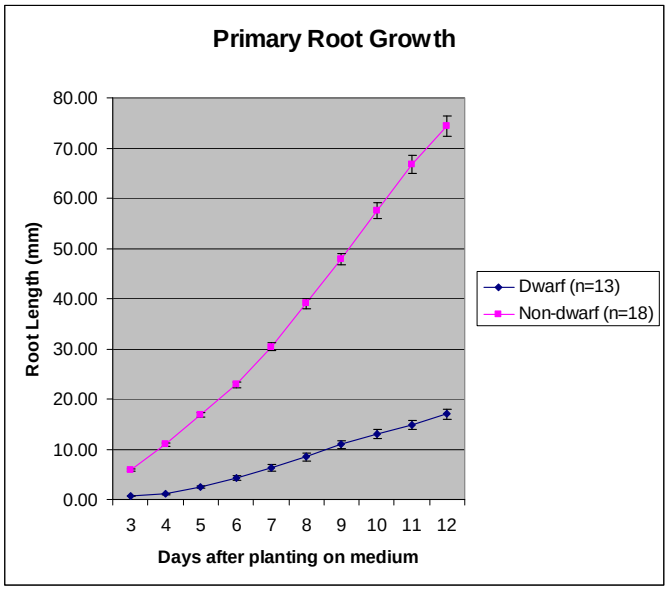

Figure 4.4. Primary roots of *sec8-3* mutant dwarfs grow slower than those of wild-type non-dwarf siblings.

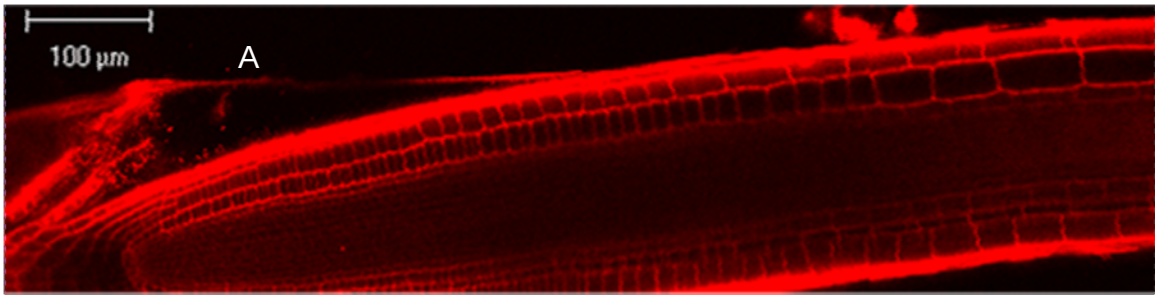

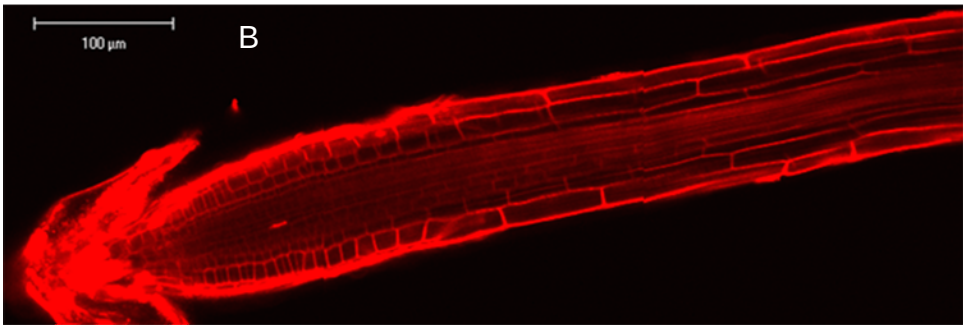

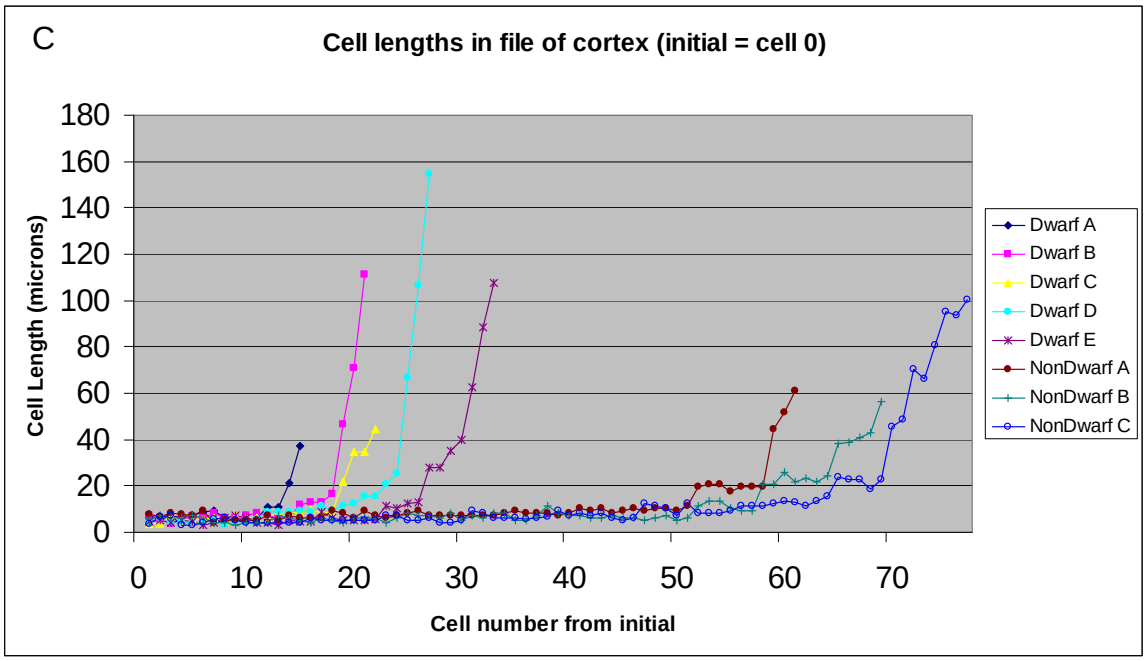

Figure 4.5. Roots of *sec8-3* mutants have shorter meristems and elongation zones than wild-type. Propridium iodine staining of wild-type (A) and *sec8-3* (B) root tips. (C) Graph of cell length as a function of cell position counted along cell file from meristematic initials.

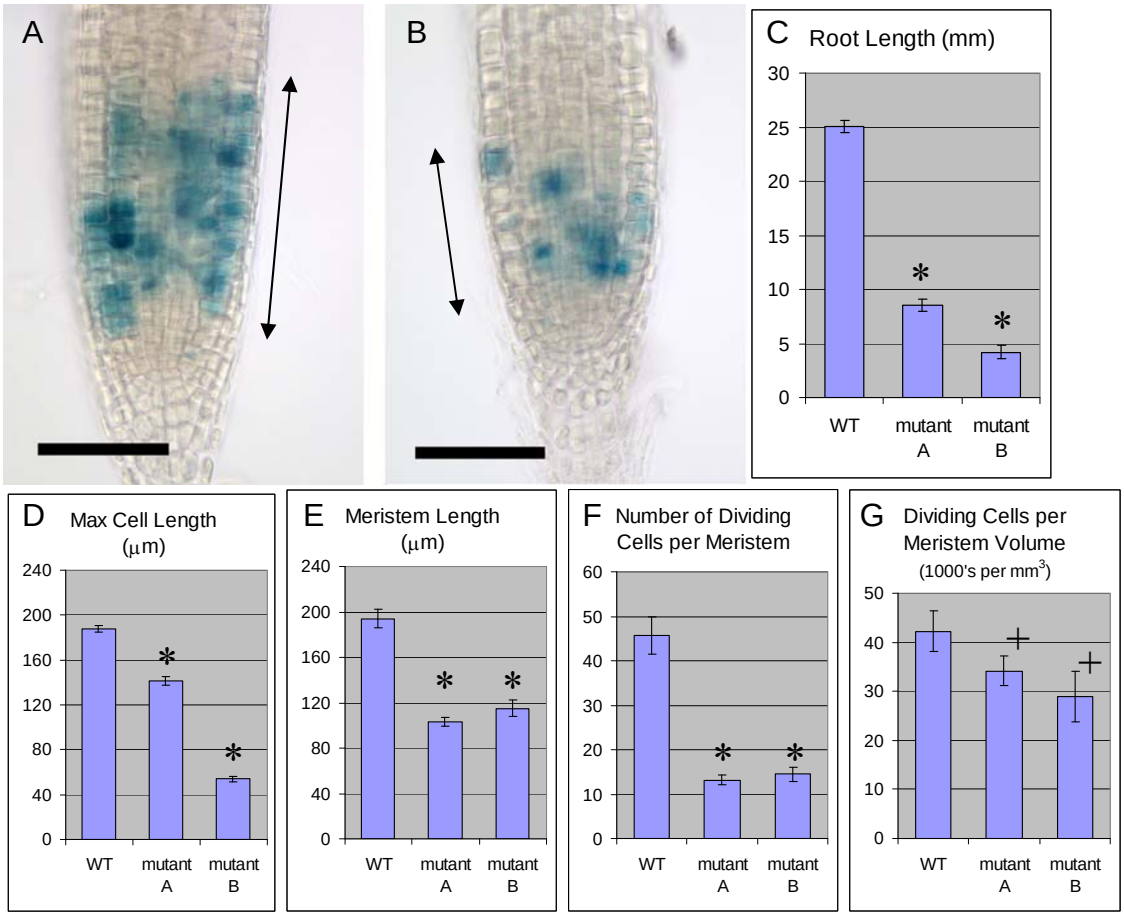

Figure 4.6. *CYCB:GUS* analysis of meristem size and cell division in *sec8-3* roots. Wild-type and *sec8-3* mutant roots with *CYCB:GUS* construct were stained for GUS expression. A. Wild-type (WT) root tip (meristem size marked with arrow, bar = 50 μm). B. *sec8-3* root tip. C-G. Graphs of root parameters for wild-type roots (n=23) and *sec8-3* roots [mutant Group A (n=19) and mutant Group B (n=8), see text]. Mutant A refers to roots that developed an elongation zone, whereas mutant B refers to those roots without an elongation zone from the collet to the meristem. Root Length corresponds to length of entire primary root; Max Cell Length corresponds to maximum cortical cell length within the entire root; Meristem Length corresponds the length of the region identified by GUS staining to contain dividing cells; Number of Dividing Cells per Meristem is based on counting GUS-positive stained cells; Dividing Cells per Meristem Volume is based on calculations using the measurement of length and two widths of each meristem (see methods). Asterisk indicates significantly different from WT, $p<0.001$, t-test. Plus sign indicates significantly different from WT, $p<0.05$, t-test.

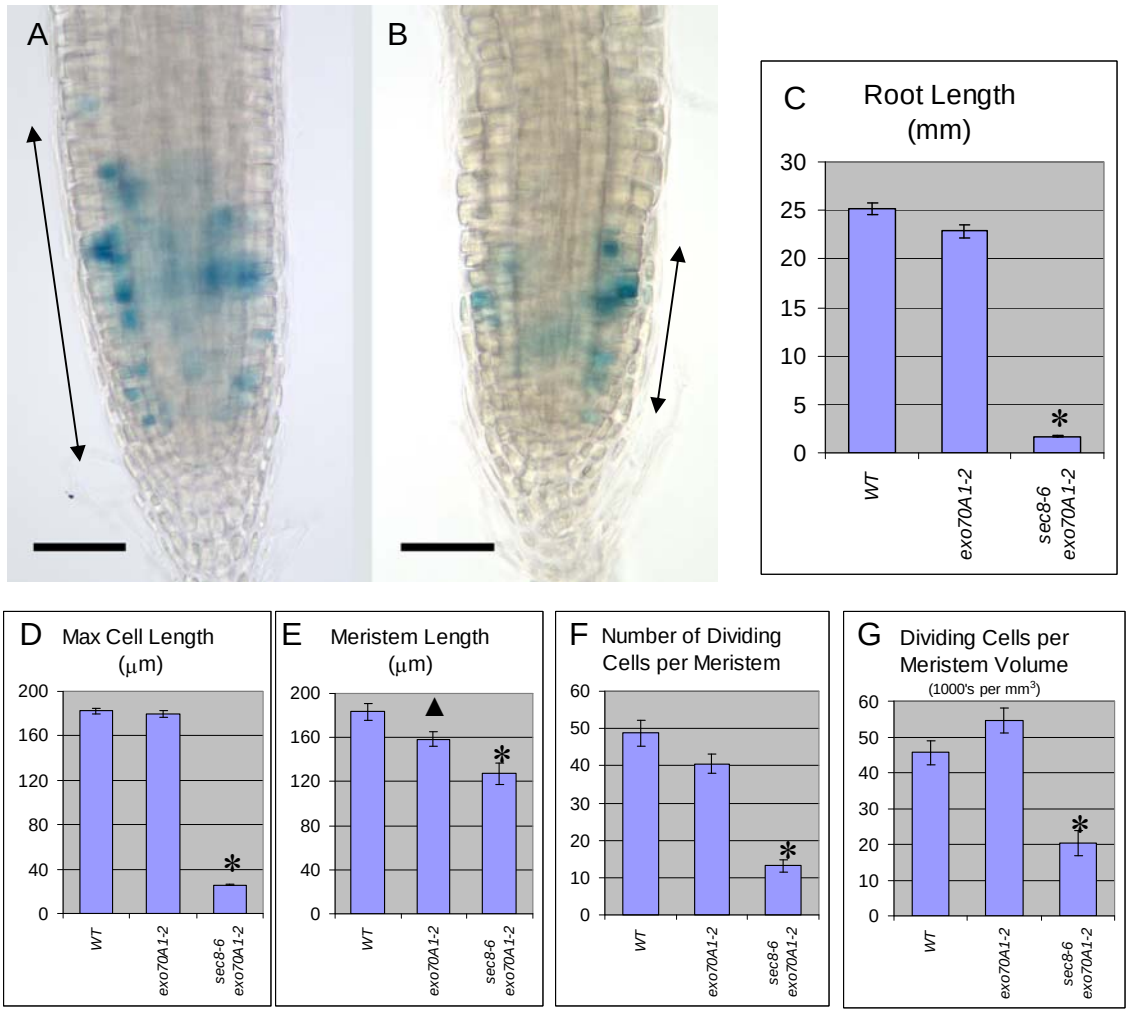

Figure 4.7. *CYCB:GUS* analysis of meristem size and cell-division in roots of *exo70A1-2, and exo70A1-2 sec8-6* mutants, compared to wild-type siblings. Wild-type and mutant roots with *CYCB:GUS* construct were stained for GUS expression. (A) *exo70A1-2* root tip (meristem size marked with arrow). (B) *exo70A1-2 sec8-6* mutant root tip. (C-G). Graphs of measured parameters for wild-type (n=30) and mutant roots [*exo70A1-2*, n=30; *exo70A1-2 sec8-6*, n=15] (see Figure 4.6 for definitions). Asterisk: significantly different from wild-type, $p<0.001$, t-test. Triangle: significantly different from wild-type, $p<0.01$, t-test.

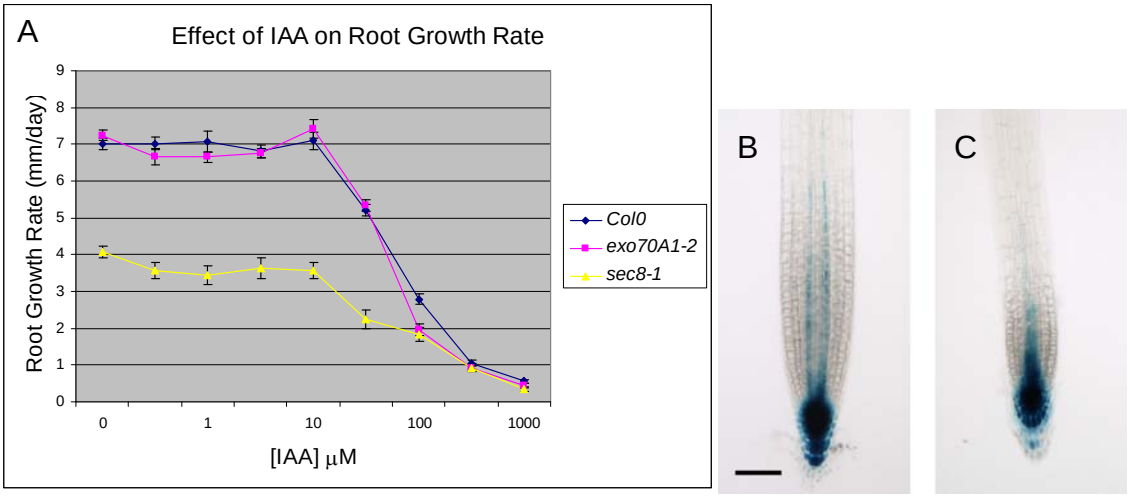

Figure 4.8. Indicators of auxin signaling in exocyst mutants. (A) Growth rate response to exogenous IAA. For each IAA concentration Columbia 0: n=23-24; *exo70A1-2*: n=23-30; *sec8-1*: n=16-30. Standard error bars shown. (B) GUS staining of wild-type root tip harboring the *DR5:GUS* construct. Bar = 50 μm. (C) GUS staining of *sec8-1* mutant harboring the *DR5:GUS* construct.

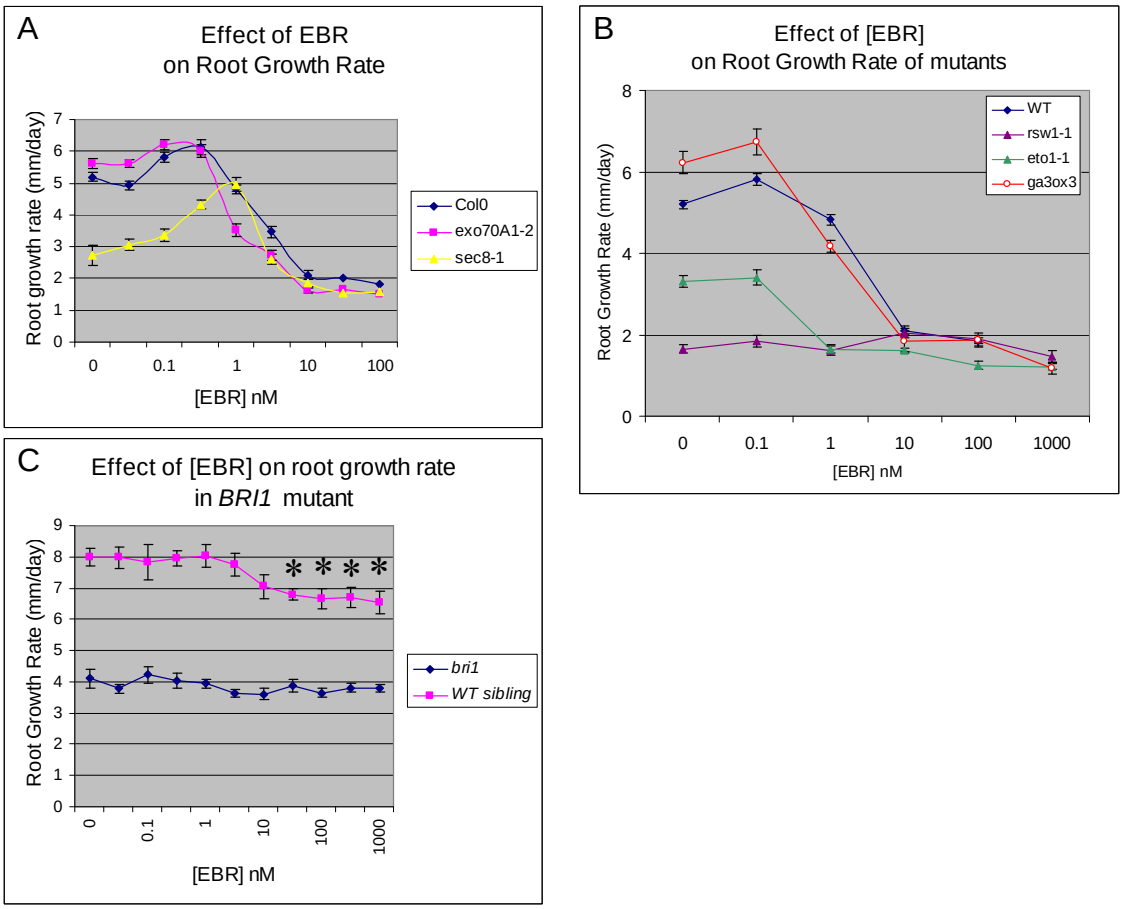

Figure 4.9. Response of exocyst mutants to exogenous 24-epibrassinolide (EBR). (A) Dose – root growth rate response of exocyst mutants. For each EBR concentration Columbia 0: n=17-33; *exo70A1-2*: n=17-32; *sec8-1*: n=11-32. (B) Root growth rate response of other mutants with short root phenotypes. For each EBR concentration Columbia 0: n=17-33; *rsw1-1*: n=29-31; *eto1-1*: n=25-31; *ga3ox1-3*: n=13-34. (C) Root growth rate response of *bri1* (brassinosteroid receptor) mutant (SALK_03371) (n=12-15) compared to wild-type sibling (n=13-15). Asterisk indicates significantly less than growth rate at exogenous [EBR] = 0, $p<0.01$, t-test. Standard error bars shown.

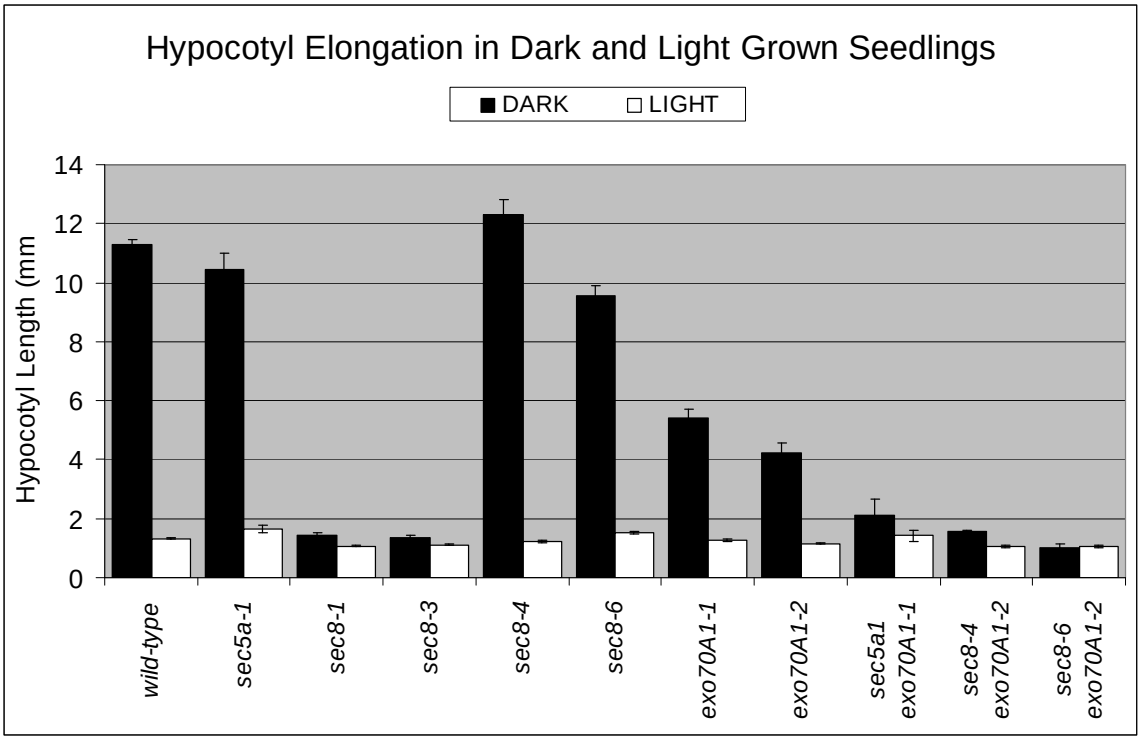

Figure 4.10. Hypocotyl elongation observed after 5 days of growth in the dark or the light.
Wild-type (dark n=240, light n=184); *sec5a-1* (n=25, 12); *sec8-1* (n=16, 27); *sec8-3* (n=21, 34); *sec8-4* (n=35, 19); *sec8-6* (n=18, 9); *exo70A1-1* (n=74, 53); *exo70A1-2* (n=96, 57); *sec5a-1 exo70A1-1* (n=8, 5); *sec8-4 exo70A1-2* (n=21, 13); *sec8-6 exo70A1-2* (n=10, 16). For each genotype, light and dark grown lengths are significantly different ($p < 0.001$, t test), with the exception of the *sec5a1 exo70A1-1* double mutant, and the *sec8-6 exo70A1-2* double mutant, for which sample sizes were small. Standard error bars shown.

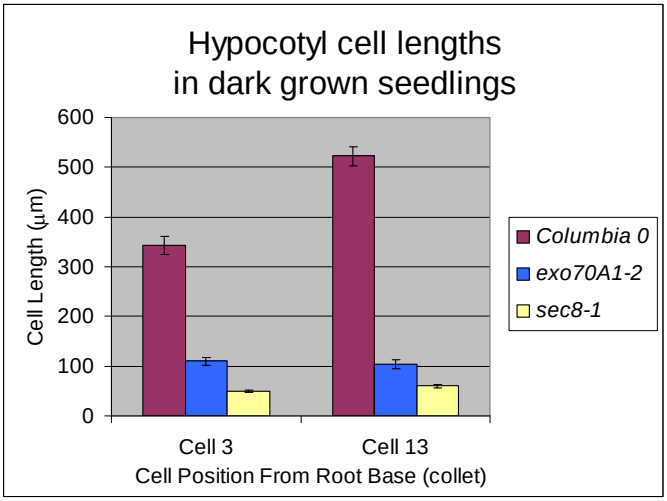

Figure 4.11. Hypocotyl cells are shorter in dark grown exocyst mutants compared to wild-type. Cell lengths were measured at two positions in the hypocotyls of seedlings grown 5 days in the dark. (n=30 for each cell type; standard error bars shown)

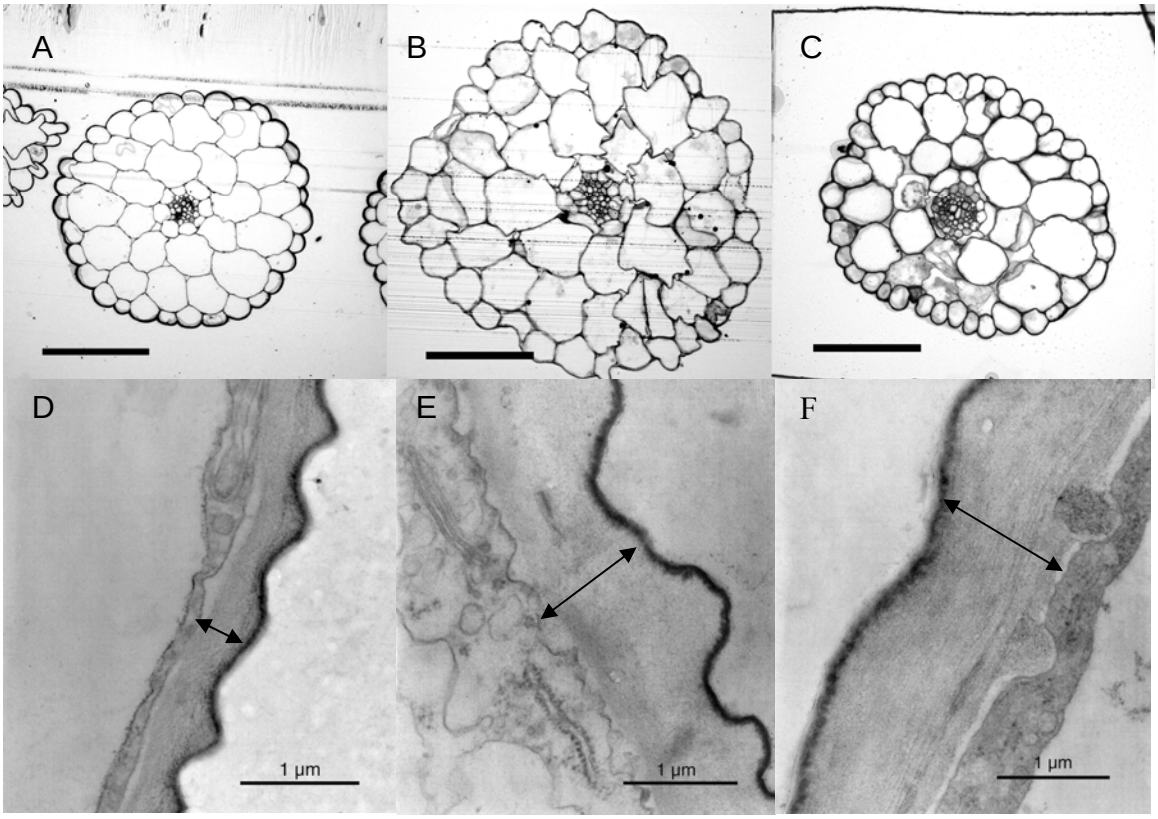

Location of Section	Cell Wall Measured	Average Cell Wall Thickness (microns)					
		n	Col0	n	sec8-1	n	exo70A1-2
Mid Hypocotyl	Outer Epidermal	3	0.356	3	0.607	2	0.666
Mid Hypocotyl	Cortical	4	0.126	2	0.344	1	0.447
Cotyledon End	Outer Epidermal	2	1.019	1	0.655	0	na
Cotyledon End	Cortical	2	0.261	1	0.226	0	na

Figure 4.12 Cross sections and TEM of hypocotyls.
Mid-hypocotyl cross sections of (A,D) *Columbia-O*, (B,E) *exo70A1-2*, and (C,F) *sec8-1* five day old dark grown seedlings. (A,B,C) optical microscopy, bar=100 microns (D,E,F) Transmission electron microscopy, arrows show thickness of cell wall, bar=1 micron. Lower table provides data on cell wall thicknesses obtained from TEM.

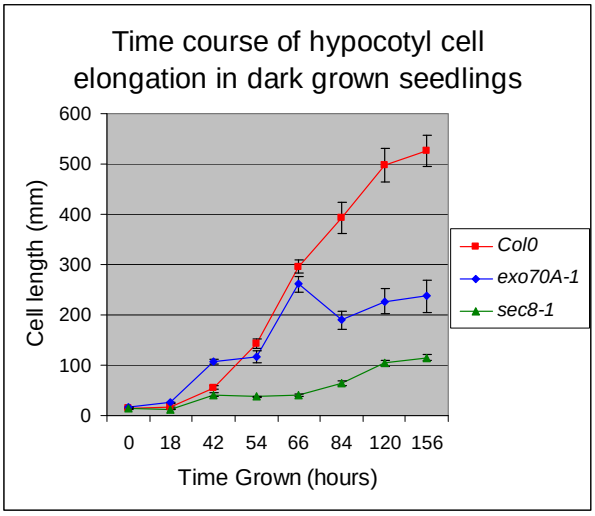

Figure 4.13. Dark grown exocyst mutants fail to develop an exponential rate of cell elongation. Mid-hypocotyl cell lengths were measured after specified duration of growth in the dark (n=20-35 cells; 4-7 hypocotyls for each data point). Standard error bars shown.

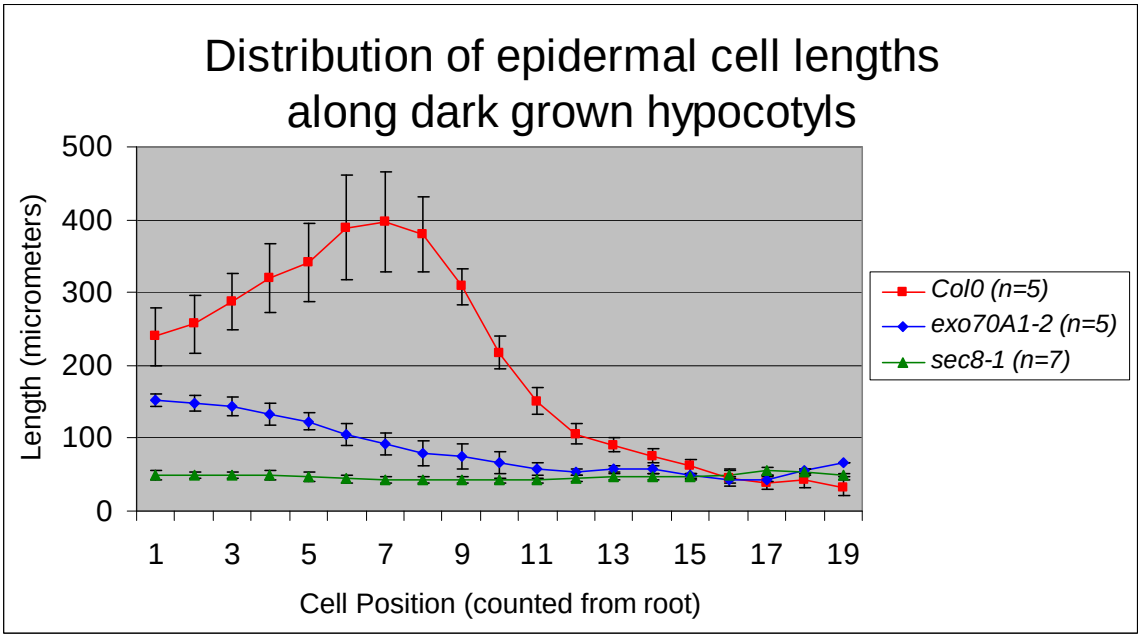

Figure 4.14. Cell elongation is more uniform along the length of the hypocotyl in exocyst mutants. Average cell lengths at each cell position along the hypocotyl were measured in *Columbia 0*, *exo70A1-2*, and *sec8-1* seedlings grown in the dark for 84 hours. Standard error bars shown.

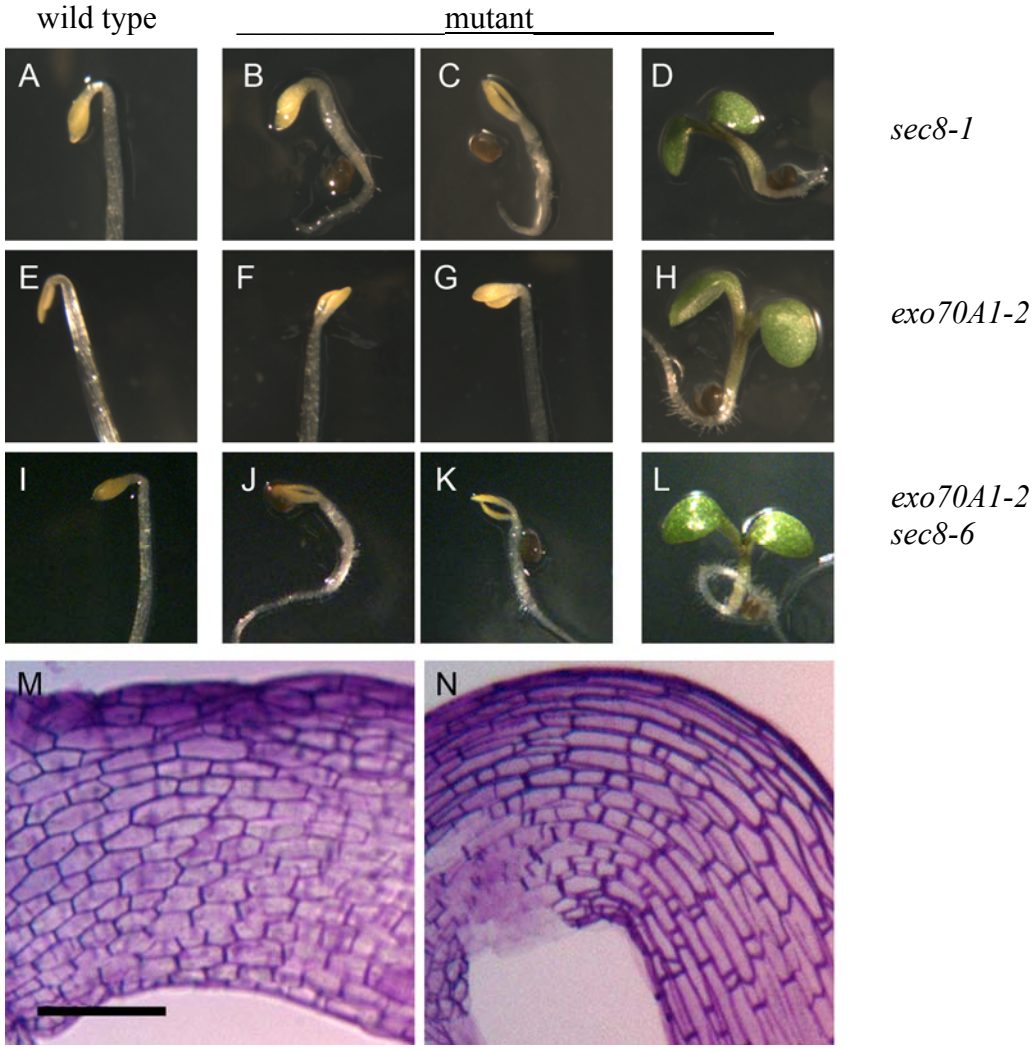

Figure 4.15. Partially de-etiolated apical hook phenotype in exocyst mutants grown in the dark. Note the absence of fully elongated cells at the upper side of the hook region (M), compared to Columbia-0 (N).
(A-C, E-G, I-K) dark grown and (D, H, L) Light grown for 5 days. (A,E,I) wild-type siblings of mutants to the right: (B,C,D) *sec8-1*; (F,G,H) *exo70A1-2*; (J,K,L) *exo70A1-2 sec8-6*. (M) Apical hook region of *sec8-1* hypocotyl stained with toluidine blue.
(N) Apical hook of Columbia-0. Bar=100 μm.

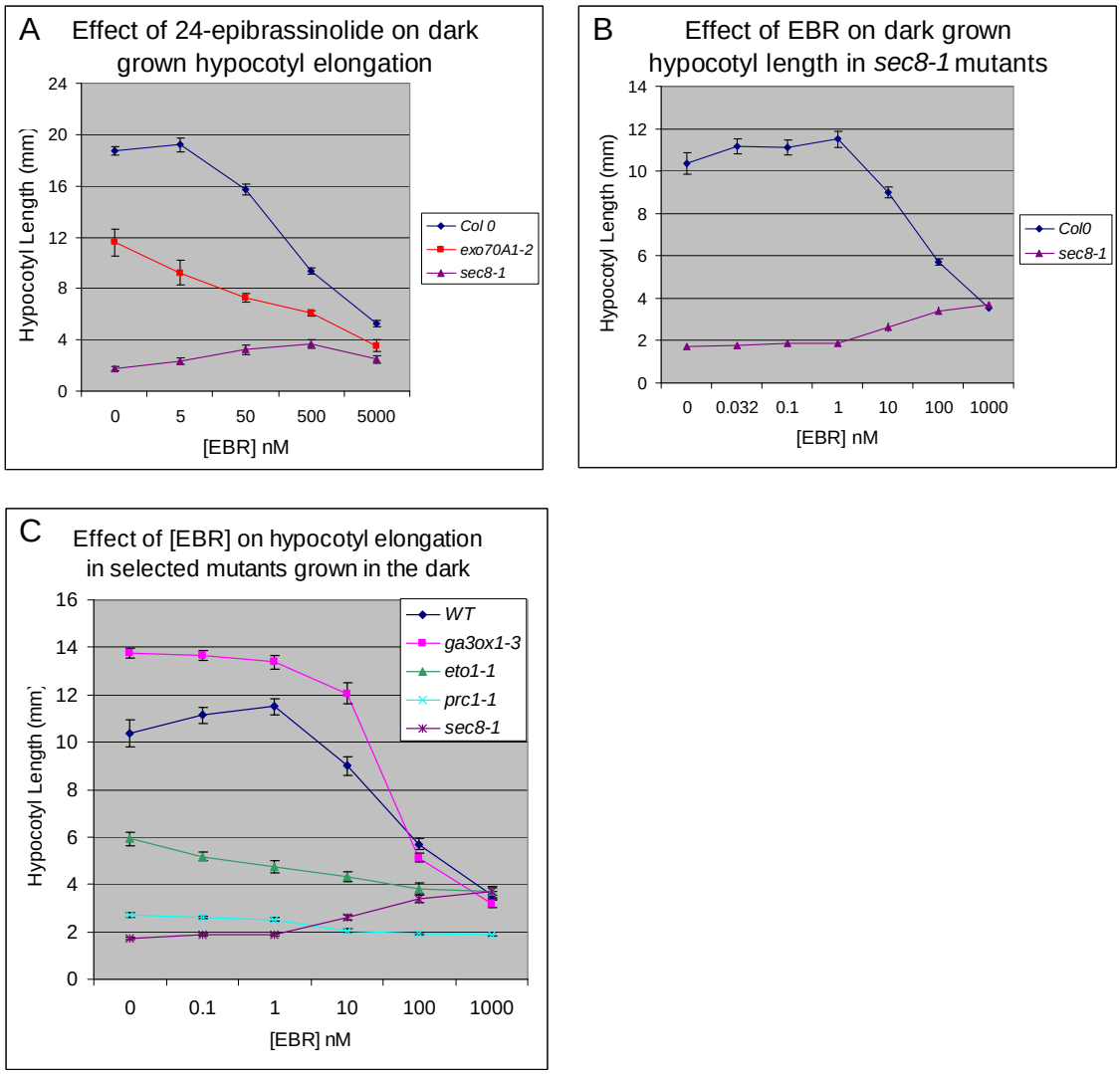

Figure 4.16. 24-epibrassinolide dose-response curves for mutants and wild-type seedlings grown in the dark. (A) Trial 1. (n=7-12 for each data point); (B) Trial 2. (n=32-36 for each data point); (C) Other mutants as indicated (n=21-36 for each data point). Standard errors shown.

CHAPTER 5

Conclusions

In 1996 Terbush et al. identified a multiprotein complex in *Saccharomyces cerevisiae* that was involved in vesicular transport from the Golgi apparatus to the plasma membrane. This complex was specifically required for exocytosis, and so they named it the exocyst. Since that time the exocyst has been identified and studied in a host of eukaryotes. These studies have linked the exocyst to a wide range of vital physiological and developmental processes (see Introduction). The existence of the exocyst complex in plants was anticipated by the discovery that genes orthologous to those encoding the eight exocyst components in yeast and mammals are present in several plant genomes and expressed in Arabidopsis and rice. At the onset of the research described in this dissertation, however, there was no known function of the exocyst in plants. The work reported here establishes and explores the function of the exocyst in plants, and demonstrates that the exocyst plays an important role in plant cell morphogenesis in several different developmental contexts.

Based upon the evidence in *S. cerevisiae*, I initially formed the general hypothesis that the exocyst is involved in polarized plant cell growth. Research investigating the exocyst component SEC8 (Chapter 2) and subsequently, investigations of other exocyst components (SEC6, SEC5a, SEC5b and SEC15a) (Chapter 3), firmly established a role for the exocyst in the premier example of polarized plant cell growth, the tip-growth in pollen tubes. Mutations in these exocyst components result in defects in pollen germination and pollen tube growth. As a consequence, the most severe alleles result in an absolute male-specific transmission defect, such that the mutant allele is never transmitted through the pollen. It was suspected from the *SEC8* work that the absolute transmission defect observed for the most severe alleles arose from the absolute inability of the pollen to germinate. However, expression of the mutant alleles in a *quartet1* background demonstrated that this was not the case. Rarely, one or two of the mutant pollen grains in a quartet did germinate. The pollen tube that was produced had twice the diameter of wild-type, was extremely short, and occasionally misshapen. Polarized growth was evident, but it was occurring in a less focused and perhaps a less efficient manner. The initial hypothesis can now be refined, and I can now hypothesize that one function of the plant exocyst complex is to facilitate the initiation and maintenance of

efficient and focused tip growth in pollen tubes, although the exocyst is not strictly essential for establishing the polarity in that growth.

In a related hypothesis, others have suggested that the exocyst plays a role in plant cytokinesis (Segui-Simarro et al., 2004), and particularly in cytokinesis during early pollen development (Otegui and Staehelin, 2004). Cytokinesis in plants can be envisioned as a polarization of the exocytic pathway towards the division plane (reviewed in Bednarek and Falbel, 2002). Other mutations affecting early pollen development (e.g., those in *SCP1* - Chen and McCormick, 1996; *GEM1* - Park et al., 1998; and *MAD1* - Grini et al., 1999) display aberrant cell plate formation or abnormal cell division that is readily evident under microscopic examination. However, I observed no cell division defect in *sec8* mutant pollen examined at several stages during development. Additionally, I examined mature quartet pollen from heterozygotes possessing mutant alleles for one of four different exocyst components using DAPI staining. In each case, the two sperm nuclei and the vegetative nucleus appeared indistinguishable in size and location from wild-type in all four pollen grains in each quartet. This suggests that the pollen had undergone meiosis and subsequent mitotic divisions without gross defect. Overall, I found no evidence to support a role for the exocyst in cytokinesis during early pollen development. However, the possibility remains that exocyst component mRNAs or proteins generated prior to meiosis may act in the male gametophytic mitoses, obscuring any gametophytic mutant defect. Evaluation of pollen from the severe *sec8* dwarfs, which are fertile, would help address this possibility.

The work with *SEC8* had revealed a role for a single exocyst component in plants, and others had demonstrated roles for the exocyst components EXO70 (Synek et al., 2006) and SEC3 (Wen et al. 2005), but it was still not known if the putative plant exocyst functioned as a complex. Using genetic analysis, phenotypic analysis, and cell biological experiments, I provided functional evidence for the existence of a plant exocyst complex. Combined with the co-localization data and biochemistry results obtained by my collaborators, we can now make a strong argument that the exocyst does indeed function as a complex in plants. It is important to recognize that we did not determine the exact composition of the complex. Given the multiple copies of some exocyst components

(e.g., 23 copies of *EXO70* in Arabidopsis) it is quite possible that the composition of the complex changes depending on cell type or developmental context. In yeast, six of the eight exocyst subunits travel with the secretory vesicles to the site of exocytosis, where the remaining two, Sec3p and Exo70p, arrive independently to serve as spatial landmarks (Finger et al., 1998; Guo et al., 1999a; Matern et al., 2001; Boyd et al., 2004). This suggests that the structure of exocyst complex may be dynamic, and that the assembly and disassembly of the complex at the exocytic site may be integral to its tethering function. With the existence of an exocyst complex in plants now firmly established, we can begin to ask some interesting questions about its assembly, function, and regulation.

The identification of an interaction between the exocyst and brassinosteroid signaling was unexpected, and offers a new avenue of research to better understand both exocyst function and brassinosteroid signaling. This connection was most clearly identified in primary root growth, but was also detected in hypocotyl elongation of etiolated seedlings. I hypothesize that the exocyst is required for the plasma membrane placement of the brassinosteroid BRI1 receptor in the epidermal cells of the primary root and in the hypocotyl. Such a role is consistent with roles the exocyst has had in non-plant organisms (see Introduction) in which exocytosis must be controlled, both spatially and temporally, to regulate the localized placement of a specific plasma membrane protein. The hypothesized role of the exocyst in BRI1 trafficking is testable; a GFP-tagged BRI1 is available and has been used to study BRI1 cycling to the plasma membrane of root cells (Geldner, et al. 2007). An alternative hypothesis, that the exocyst is involved in the trafficking of brassinosteroids to the plasma membrane for delivery to the exterior of the cell is equally attractive, and might explain why the severe exocyst mutants have a root phenotype that is similar to that of BRX mutants, presumed to have lower BR levels secondary to decreased brassinosteroid synthesis. If this second hypothesis proves to be correct, the exocyst research will help to answer one of the remaining mysteries of brassinosteroid signalling – how the brassinosteroids get from their site of synthesis inside the cell to the cell's exterior.

The interaction of the exocyst with brassinosteroid signaling in the hypocotyl might be further explored by monitoring BZR1 expression. BZR1 is a transcription

factor that functions downstream of BRI1 in hypocotyl cells to mediate their dark-grown elongation response. Intriguingly, BZR1 is expressed in a pattern that coincides with the pattern of elongation seen in wild-type plants (Wang et al., 2002; Gendreau, 1997; and Figure 14). The expression of a native promoter-driven BRZ1-CFP is initially strongest at the base of the hypocotyl, but over time this diminishes as expression becomes stronger higher in the hypocotyl (Wang et al., 2002). BRZ1 does not appear to move intercellularly (Salvaldi-Goldstein et al., 2007), and brassinosteroids are not believed to undergo long distance transport (Symons and Reid, 2004, Symons et al., 2008). This raises the possibility that brassinosteroid signaling is responsible for the pattern of elongation in etiolated hypocotyls. For example, the region of elongation could spread up the hypocotyl in a positive feedback loop of localized production and diffusion of brassinosteroid, carrying the signal to neighboring cells. According to such a model, exocyst mutants did not demonstrate the regionally enhanced and spatial progression of elongation in their hypocotyls either because their hypocotyl cells could not transport sufficient brassinosteriod to the extracellular space, or because hypocotyl cells did not have sufficient receptors in place to receive the signal and generate the feedback loop. To test this model, it would be valuable to know how the expression of BRZ1 varies along the length of dark-grown hypocotyls in exocyst mutants over the time course of hypocotyl elongation.

There is no reason to suggest that the exocyst acts by a single mechanism (e.g., by facilitating BRI1 transport) to assist in hypocotyl elongation or primary root growth. The lack of complete rescue of hypocotyl elongation with exogenous BR in the exocyst mutants may be indicative of multiple sites of action for the exocyst. For example, downstream in brassinosteroid signaling is expression of TCH4, a xyloglucan endotransglycolase, whose expression is stimulated by darkness or exogenous 1 mM 24-epibrassinolide (Xu, 1996). TCH4 is secreted to act on the major hemicellulose of the plant cell wall, potentially influencing hypocotyl cell elongation. Part of the effect of exocyst mutations could conceivably be the altered secretion of cell wall modifying enyzmes, such as TCH4, thus reducing the capacity of hypocotyl cells to expand. Additionally, the exocyst could be involved in the signaling pathways of other

phytohormones, although none of my initial tests with auxin, cytokinin or ethylene strongly support such a conclusion. Significant interdependency of brassinosteroid and auxin signaling (Hardtke, 2007; Hardtke et al., 2007; Nemhauser et al., 2004), predicts that if exocyst mutations do affect brassinosteroid signalling, they could also, perhaps indirectly, affect auxin singaling. Indicators of auxin signaling more sensitive than the application of exogenous hormone will need to be employed to evaluate this possibility.

The observation of the aberrant root cell elongation phenotype in seedlings in exocyst mutants bearing strong mutant alleles is a particularly exciting discovery. Significantly, in the *sec8-1* and *sec8-3* mutants the region of the root with near-isotropic expansion extends from the collet towards the root tip for a length that varies from root to root. In each root however, at the point that this region ends, a wild-type cell elongation pattern emerges and extends all the way up to the meristem. In wild-type or *exo70A1* mutants (which have a minimal defect in root growth), this near-isotropic region near the collet extends for only a few cells before cell elongation becomes obvious. In the *sec8-6 exo70A1-2* double mutant, the near-isotropic region extends from the collet all the way to the meristem, i.e. there is no distinguishable elongation zone evident. This appears to be an unprecedented phenotype. The pattern could be explained by the existence of a developmental switch that must be turned on (or off) for an elongation zone to develop. One can envision that in wild-type plants the switch has occurred by the time of germination, and an elongation zone is defined such that elongated cells are generated immediately. In *sec8-6 exo70A1-2* mutants, the switch is never turned on; therefore, an elongation zone is never defined and the cells produced by the root meristem do not adopt an elongated morphology. However, in *sec8-1* and *sec8-3* mutants, root growth starts with the switch in the off position, although perhaps poised on the edge of being turned on. In these mutants the root initially grows primarily by cell division with near-isotropic cell expansion until at some point, perhaps in a purely stochastic manner, the developmental switch is flipped on, and the wild-type elongation zone develops behind the meristem. If there is such a developmental switch, the exocyst appears to be part of it. Future plant exocyst research to explore this phenotype may provide new insights into

the meristem-elongation zone interaction and the regulatory system that dictates the development of the elongation zone.

In conclusion, it seems safe to predict that the plant exocyst will attract significant attention in the plant development research community in the near future.

Figure 5.1 Plant Morphogenesis. Oil Painting on canvas by Mary Cole

BIBLIOGRAPHY

Alabadi, D., Gallego-Bartolome, J., Orlando, L., Garcia-Carcel, L., Rubio, V., Martinez, C., Frigerio, M., Iglesias-Pedraz, J., Espinosa, A., Deng, X., Blazquez, M. (2008). Gibberellins modulate light signaling pathways to prevent Arabidopsis seedling de-etiolation in darkness. Plant Journal 53: 324-335.

Alexander M (1969) Differential staining of aborted and nonaborted pollen. Stain Technol 44: 117-122.

Alonso, J.M., Stepanova, A.N., Leisse, T.J., Kim, C.J., Chen, H., Shinn, P., Stevenson, D.K., Zimmerman, J., Barajas, P., Cheuk, R., Gadrinab, C., Heller, C., Jeske, A., Koesema, E., Meyers, C.C., Parker, H., Prednis, L., Ansari, Y., Choy, N., Deen, H., Geralt, M., Hazari, N., Hom, E., Karnes, M., Mulholland, C., Ndubaku, R., Schmidt, I., Guzman, P., Aguilar-Henonin, L., Schmid, M., Weigel, D., Carter, D.E., Marchand, T., Risseeuw, E., Brogden, D., Zeko, A., Crosby, W.L., Berry, C.C., and Ecker, J.R. (2003). Genome-wide insertional mutagenesis of Arabidopsis thaliana. Science 301: 653-657.

Altschul SF, Madden TL, Schaffer AA, Zhang J, Zhang Z, Miller W, Lipman DJ (1997) Gapped BLAST and PSI-BLAST: a new generation of protein database search programs. Nucleic Acids Res 25: 3389-3402.

Anitei, M., Ifrim, M., Ewart, M.A., Cowan, A.E., Carson, J.H., Bansal, R., and Pfeiffer, S.E. (2006). A role for Sec8 in oligodendrocyte morphological differentiation. J. Cell Sci. 119: 807-818.

Arthur KM, Vejlupkova Z, Meeley RB, Fowler JE (2003) Maize ROP2 GTPase provides a competitive advantage to the male gametophyte. Genetics 165: 2137-2151
Bednarek SY, Falbel TG (2002) Membrane trafficking during plant cytokinesis. Traffic 3: 621-629.

Berghöfer, J., and Klösgen, R.B. (1999). Two distinct translocation intermediates can be distinguished during protein transport by the TAT (Deltaph) pathway across the thylakoid membrane. FEBS Lett. 460: 328-332.

Blilou, I., Xu, J., Wildwater, M., Willemsen,V., Paponov, I., Frimi, J., Heidstra, R., Aida, M., Palme, K., Scheres, B. (2005) The PIN auxin efflux facilitator network controls growth and patterning in Arabidopsis roots. Nature 433: 39-44.

Blankenship, J.T., Fuller, M.T., and Zallen, J.A. (2007). The Drosophila homolog of the Exo84 exocyst subunit promotes apical epithelial identity. J. Cell Sci. 120: 3099-3110.

Boutte,Y., Crosnier, M., Carraro, N., Traas, J, Satiat-Jeunemaitre, B. (2006). The plasma membrane recycling pathway and cell polarity in plants: studies on PIN proteins. Journal of Cell Science 119:1255-1265.

Boutte, Y., Ikeda, Y., Grebe, M. (2007). Mechanisms of auxin-dependent cell and tissue polarity. Current Opinion in Plant Biology 10: 616-623.

Boyd, C., Hughes, T., Pypaert, M., and Novick, P. (2004). Vesicles carry most exocyst subunits to exocytic sites marked by the remaining two subunits, Sec3p and Exo70p. J Cell Biol 167: 889-901.

Cai, H., Reinisch, K., and Ferro-Novick, S. (2007). Coats, tethers, Rabs, and SNAREs work together to mediate the intracellular destination of a transport vesicle. Dev Cell. 12: 671-82.

Camacho L, Malhó R (2003) Endo/exocytosis in the pollen tube apex is differentially regulated by Ca^{2+} and GTPases. J Exp Bot 54: 83-92.

Chen, X.W., Inoue, M., Hsu, S.C., and Saltiel, A.R. (2006). RalA-exocyst dependent recycling endosome trafficking is required for the completion of cytokinesis. J. Biol. Chem. 281(51):38609-38616.

Chen, X.W., Leto, D., Chiang, S.H., Wang, Q. and Saltiel, A.R. (2007). Activation of RalA is required for insulin-stimulated Glut4 trafficking to the plasma membrane via the exocyst and the motor protein Myo1c. Dev. Cell 13(3):391-404.

Chen YC, McCormick S (1996) sidecar pollen, an Arabidopsis thaliana male gametophytic mutant with aberrant cell divisions during pollen development. Development 122: 3243-3253.

Clough SJ, Bent AF (1998) Floral dip: a simplified method for Agrobacterium-mediated transformation of Arabidopsis thaliana. Plant J 16: 735-743.

Clouse, S. (2001). Integration of light and brassinosteroid signals in etiolated seedling growth. TRENDS in Plant Science 6:(10) 443-445.

Clouse, S., Langford, M., McMorris, T. (1996). A brassinosteroid-insensitive mutant in *Arabidopsis thaliana* exhibits multiple defects in growth and development. Plant Physiology 111:671-678.

Cole, R.A., and Fowler, J.E. (2006). Polarized growth: maintaining focus on the tip. Curr. Opin. Plant Biol. 9: 579-588.

Cole, R.A., Synek, L., Žárský, V., and Fowler, J.E. (2005). SEC8, a subunit of the putative Arabidopsis exocyst complex, facilitates pollen germination and competitive pollen tube growth. Plant Physiology 138: 2005-2018.

Collett, C., Harberd, N., Leyse, O. (2000). Hormonal interactions in the control of Arabidopsis hypocotyl elongation. Plant Physiology 124: 553-561.

Colon-Carmona, A., You, R., Haimovitdh-Gal, T., and Doerner, P. (1999). Spatio-temporal analysis of mitotic activity with a labile cyclin-GUS fusion. Plant J. 20: 503-508.

Cowling, R.,Harberd, N. (1999). Gibberellins control Arabidopsis hypocotyl growth via regulation of cellular elongation. J. of Experimental Botany 50 (337): 1351-1357.

Cvrčková, F., Eliáš, M., Hála, M., Obermeyer, G., and Žárský, V. (2001). Small GTPases and conserved signalling pathways in plant cell morphogenesis: From exocytosis to Exocyst. In A. Geitmann, M. Cresti, eds, Cell Biology of Plant and Fungal Tip Growth, IOS Press, Amsterdam, pp 105-122.

De Grauwe, L., Vandenbusssch, F., Tietz, O., Palme, L.,Van Der Straeten, D. (2005). Auxin, ethylene and brassinosteroids: triparitite control of growth in the Arabidopsis hypocotyl. Plant Cell Physiol. 46(6):827-836.

de Lucas, M., Daviere, J., Rogriguez-Falcon, M., Pontin, M., Iglesias-Pedraz, J., Lorrain, S., Fankhauser, C., Blazquez, M., Titarenke, E., Prat, S. (2008) A molecular framework for light and gibberellin control of cell elongation. Nature 451: 480-484.

Desnos, T., Orbovic, V., Bellini, C., Kronenberger, J., Caboche, M., Traas, J., Hofte, H. (1996). Procuste1 mutants identify two distinct genetic pathways controlling hypocotyl cell elongation, respectively in dare-and light-grown Arabidopsis seedlings. Development 122: 683-693.

Desprez, T., Vernhettes, S., Fagard, M., Refregier, G., Desnos, T., Aletti, E., Py, N., Pelletier, S., Hofte, H. (2002). Resistance against herbicide isoxaben and cellulose deficiency mutations in same cellulose synthase isoform CEXA6. Plant Physiology 128: 482-490.

Dong, G., Hutagalung, A.H., Fu, C., Novick, P., and Reinisch, K.M. (2005). The structures of exocyst subunit Exo70p and the Exo84p C-terminal domains reveal a common motif. Nat Struct Mol Biol 12: 1094-1100.

Edlund AF, Swanson R, Preuss D (2004) Pollen and stigma structure and function: the role of diversity in pollination. Plant Cell 16 Suppl: S84-97.

Eliáš, M., Drdová, E., Ziak, D., Bavlnka, B., Hála, M., Cvrčková, F., Soukupová, H., and Žárský, V. (2003). The exocyst complex in plants. Cell Biol Int 27: 199-201.

Eubel, H., Braun, H.P., and Millar, A.H. (2005). Blue-native PAGE in plants: a tool in analysis of protein-protein interactions. Plant Methods 1: 11.

Feijó JA, Costa SS, Prado AM, Becker JD, Certal AC (2004) Signalling by tips. Curr Opin Plant Biol 7: 589-598.

Finger, F.P., Hughes, T.E., and Novick, P. (1998). Sec3p is a spatial landmark for polarized secretion in budding yeast. Cell 92: 559-571.

Fowler JE, Quatrano RS (1997) Plant cell morphogenesis: plasma membrane interactions with the cytoskeleton and cell wall. Annu Rev Cell Dev Biol 13: 697-743.

Friedrichsen,D., Joazeiro, C., Li, J., Hunter,T., Chory, J. (2000). Brassinosteroid-insensitive-1 is a ubiquitously expressed leucine-rich repeat receptor serine/threonine kinase. (2000). Plant Physiology 123: 1247-1255.

Fu Y, Yang Z (2001) Rop GTPase: a master switch of cell polarity development in plants. Trends Plant Sci 6: 545-547.

Garrick, M.D., and Garrick, L.M. (2007). Loss of rapid transferrin receptor recycling due to a mutation in Sec15l1 in hbd mice. Biochim. Biophys. Acta. 1773: 105-108.

Geldner, N., Frimi, J., Stierhof, Y., Jurgens, G., Palme, K. (2001). Auxin transport inhibitors block PIN1 cycling and vescicle trafficking. Nature 413: 425-428.

Geldner, N., Hyman, D., Wang, X., Schumacher, K., Chory, J. (2007). Endosomal signaling of plant steroid redeptor kinase BR11. Genes & Development 21: 1598-1602.

Gendreau, E., Traas, J., Desnos, T., Grandjean, O., Caboche, M., Hofte, H. (1997). Cellular basis of hypocotyl growth in *Arabadopsis thaliana.* Plant Physiol. 114: 295-305.

Gengron, J., Wang, Z. (2007). Multiple mechanisms modulate brassinosteroid signaling. Current Opinion in Plant Biology 10:436-441.

Gerges, N.Z., Backos, D.S., Rupasinghe, C.N., Spaller, M.R., and Esteban, J.A. (2006). Dual role of the exocyst in AMPA receptor targeting and insertion into the postsynaptic membrane. EMBO J. 25: 1623-1634.

Golovkin M, Reddy AS (2003) A calmodulin-binding protein from Arabidopsis has an essential role in pollen germination. Proc Natl Acad Sci U S A 100: 10558-10563.

Goubet F, Misrahi A, Park SK, Zhang Z, Twell D, Dupree P (2003) AtCSLA7, a cellulose synthase-like putative glycosyltransferase, is important for pollen tube growth and embryogenesis in Arabidopsis. Plant Physiol 131: 547-557.

Grindstaff KK, Yeaman C, Anandasabapathy N, Hsu SC, Rodriguez-Boulan E, Scheller RH, Nelson WJ (1998) Sec6/8 complex is recruited to cell-cell contacts and specifies transport vesicle delivery to the basal-lateral membrane in epithelial cells. Cell 93: 731-740.

Grini PE, Schnittger A, Schwarz H, Zimmermann I, Schwab B, Jurgens G, Hulskamp M (1999) Isolation of ethyl methanesulfonate-induced gametophytic mutants in Arabidopsis thaliana by a segregation distortion assay using the multimarker chromosome 1. Genetics 151: 849-863.

Gu Y, Wang Z, Yang Z (2004) ROP/RAC GTPase: an old new master regulator for plant signaling. Curr Opin Plant Biol 7: 527-536.

Guo, H., Echer, J. (2004). The ethylene signaling pathway: new insights. Current Opinion in Plant Biology 7: 40-49.

Guo W, Grant A, Novick P (1999) Exo84p is an exocyst protein essential for secretion. J Biol Chem 274: 23558-23564

Guo, W., Novick, P. (2004). The exocyst meets the translocon: a regulatory circuit for secretion and protein syntheis? TRENDS in Cell Biology 14(2): 61-63.

Guo, W., Roth, D., Walch-Solimena, C., and Novick, P. (1999a). The exocyst is an effector for Sec4p, targeting secretory vesicles to sites of exocytosis. EMBO J. 4: 71-80.

Haizel, T., Merkle, T., Turck, F., and Nagy, F. (1995). Characterization of membrane-bound small GTP-binding proteins from Nicotiana tabacum. Plant Physiol. 108: 59-67.

Hamburger, Z.A., Hamburger, A.E., West, A.P., and Weis, W.I. (2006). Crystal structure of the S. cerevisiae exocyst component Exo70p. J Mol Biol 356: 9-21.

Hala, M., Cole, R., Synek, L., Drodova, E., Pecenkova, T., Nordheim, A., Lamkemeyer, T., Madlung, J., Hochholdinger, F., Fowler, J., and Zarsky, V. (2008) An exocyst complex functions in plant cell growth. Submitted to Plant Cell. February 28, 2008.

Hardtke, C. (2007). Transcriptional auxin-brassinosteroid crosstalk:who's talking? Bioessays 29:1115-1123.

Hardtke, C., Dorcey, E., Osmont, K., Sibout. (2007). Phytohormone collaboration: zooming in on auxin-brassinosteroid interactions. TRENDS in Cell Biology, 17 (10): 485-492.

Hazuka CD, Foletti DL, Hsu SC, Kee Y, Hopf FW, Scheller RH (1999) The sec6/8 complex is located at neurite outgrowth and axonal synapse-assembly domains. J Neurosci 19 (4): 1324-1334.

Hepler, PK, Vidali L, Cheung AY (2001) Polarized cell growth in higher plants. Annu Rev Cell Dev Biol 17: 159-187.

Hicks GR, Rojo E, Hong S, Carter DG, Raikhel NV (2004) Geminating pollen has tubular vacuoles, displays highly dynamic vacuole biogenesis, and requires VACUOLESS1 for proper function. Plant Physiol 134: 1227-1239.

Honys D, Twell D (2003) Comparative analysis of the Arabidopsis pollen transcriptome. Plant Physiol 132: 640-652.

Honys D, Twell D (2004) Transcriptome analysis of haploid male gametophyte development in Arabidopsis. Genome Biol 5: R85

Howell, W., Keller III, G., Kirkpatrick, J., Jenkins, R., Hunsinger, R., McLaughlin, E. (2007). Effects of the plant steroidal hormone, 24-epibrassinolide, on the mitotic index and growth of onion (*Allium cepa)* root tips. Genet. Mol. Res. 6 (1):50-58.

Hsu, S.C., Ting, A.E., Hazuka, C.D., Davanger, S., Kenny, J.W., Kee, Y., and Scheller, R.H. (1996). The mammalian brain rsec6/8 complex. Neuron 6: 209-219.

Hsu, S.C., Hazuka, C.D., Foletti, D.L., Heuser, J., and Scheller, R.H. (1998). Subunit composition, protein interactions and structures of the mammalian brain sec6/8 complex and septin filaments. Neuron 20: 1111-1122.

Hsu, S.C., TerBush, D., Abraham, M., and Guo, W. (2004). The exocyst complex in polarized exocytosis. Int Rev Cytol 233: 243-265.

Inoue, M., Chang, L., Hwang, J., Chiang, S.H., and Saltiel, A.R. (2003). The exocyst complex is required for targeting of Glut4 to the plasma membrane by insulin. Nature 422: 629-633.

Ioio, R., Linhares, F., Scacchi, E., Casamitjana-Martinez, E., Heidstra, R., Costantino, P., Sabatini, S. (2007). Cytokinins determine Arabidopsis root-meristem size by controlling cell differentiation. Current Biology 17: 678-682.

Ivanchenko, M., Coffeen, W., Lomax, T., and Dubrovsky, J. (2006) Mutations in the Digeotropica (Dgt) gene uncouple patterned cell division during lateral root initiation form proliferative cell division in the pericycle. Plant J. 46: 436-447.

Iwano M, Shiba H, Miwa T, Che FS, Takayama S, Nagai T, Miyawaki A, Isogai A (2004) Ca^{2+} dynamics in a pollen grain and papilla cell during pollination of Arabidopsis. Plant Physiol 136: 3562-3571.

Johnson MA, von Besser K, Zhou Q, Smith E, Aux G, Patton D, Levin JZ, Preuss D (2004) Arabidopsis hapless mutations define essential gametophytic functions. Genetics 168: 971-982.

Johnson-Brousseau, S. and McCormick, S. (2004) A compendium of methods useful for characterizing Arabidopsis pollen mutants and gametophytically expressed Genes. The Plant Journal 39, 761–775.

Jurgens, G., and Geldner, N. (2002). Protein secretion in plants: from the trans-Golgi network to the outer space. Traffic 3: 605-613.

Kandasamy MK, Nasrallah JB, Nasrallah ME (1994) Pollon-pistil interactions and developmental regulation of pollon tube growth in Arabidopsis. Development 120: 3405-3418.

Kauschmann, A., Jessop, A., Koncz, C., Szekeres, M., Willmitzer, L., Altmann, T. (1996). Genetic evidence for an essential role of brassinosteroids in plant development. Plant Journal 9 (5) 701-713.

Kee, Y., Yoo, J.S., Hazuka, C.D., Peterson, K.E., Hsu, S.C., and Scheller, R.H. (1997). Subunit structure of the mammalian exocyst complex. Proc Natl Acad Sci USA 94: 14438-14443.

Kim, T., Lee, S., Joo, S., Yun, H., Lee, Y., Kaufman, P., Kirakosyan, A., Kim S., Nam, K., Lee, J., Chang, S., Kim., S. (2007). Elongation and gravitropic responses of Arabidopsis roots are regulated by brassinolide and IAA. Plant, Cell, and Environment 30: 679-689.

Knee, E., Hangarter, R., Knee, M. (2000). Interactions of light and ethylene in hypocotyl hook maintenance in *Arabidopsis thaliana* seedlings. Physiologia Plantarum 108:208-215.

Koumandou, V.L., Dacks, J.B., Coulson, R.M., and Field, M.C. (2007). Control systems for membrane fusion in the ancestral eukaryote; evolution of tethering complexes and SM proteins. BMC Evol. Biol. 7: 29.

Krasinska, L., de Bettignies, G., Fisher, D., Abrieu, A., Fesquet, D., and Morin, N. (2007). Regulation of multiple cell cycle events by Cdc14 homologues in vertebrates. Exp Cell Res. 313: 1225-1239.

Lalanne E, Honys D, Johnson A, Borner GH, Lilley KS, Dupree P, Grossniklaus U, Twell D (2004a) SETH1 and SETH2, Two components of the glycosylphosphatidylinositol anchor biosynthetic pathway, are required for pollen germination and tube growth in Arabidopsis. Plant Cell 16: 229-240.

Lavy, M., Bloch, D., Hazak, O., Gutman, I., Poraty, L., Sorek, N., Sternberg, H., and Yalovsky, S.A. (2007). Novel ROP/RAC Effector Links Cell Polarity, Root-Meristem Maintenance, and Vesicle Trafficking. Curr. Biol. 17: 947-952.

Li, C.R., Lee, R.T., Wang, Y.M., Zheng, X.D., and Wang, Y. (2007) Candida albicans hyphal morphogenesis occurs in Sec3p-independent and Sec3p-dependent phases separated by septin ring formation. J. Cell Sci. 120(11):1898-1907.

Li H, Lin Y, Heath RM, Zhu MX, Yang Z (1999) Control of pollen tube tip growth by a Rop GTPase-dependent pathway that leads to tip-localized calcium influx. Plant Cell 11: 1731-1742.

Li, J., Johnson, P., Stepanova, A., Alonso, J., Echer, J. (2004). Convergence of signaling pathways in the control of differential cell growth in Arabadopsis. Developmental Cell 7: 193-204.

Li, L., Xu, J., Xu, Z., Xue, H. (2005). Brassinosteroids stimulate plant tropism through modulation of polar auxin transport in brassica and Arabidopsis. Plant Cell17: 2783-2753.

Liscum, E., Hangarter, R. (1993). Light-stimulated apical hook opening in wild-type *Arabidopsis thaliana* seedlings. Plant Physiol. 101: 567-572.

Malamy, J. and Benfey, P. (1997) Orcanization and cell differentiation in lateral roots of Arabidopsis thaliana. Development 124: 33-44.

Matern, H.T., Yeaman, C., Nelson, W.J., and Scheller, R.H. (2001). The Sec6/8 complex in mammalian cells: characterization of mammalian Sec3, subunit interactions, and expression of subunits in polarized cells. Proc Natl Acad Sci USA 98: 9648-9653.

McCormick S (2004) Control of male gametophyte development. Plant Cell 16 Suppl: S142-153.

Mitchum, M., Yamaguchi, S., Hanada, A., Kuwahara, A., Yoshioka, Y., Kato, T., Tobata, S., Kamiya, Y., Sun, T. (2006). Distinct and overlapping roles of two gibberellin 3-oxidases in Arabidopsis development. Plant Journal 445: 804-818.

Moskalenko, S., Tong, C., Rosse, C., Mirey, G., Formstecher, E., Daviet, L., Camonis, J., and White, M.A. (2003). Ral GTPases regulate exocyst assembly through dual subunit interactions. J. Biol. Chem. 278: 51743-48.

Mouchel, C., Briggs, G., Hardtke, C. (2004). Natural genetic variation in Arabidopsis identifies *Brevis radix,* a novel regulator of cell proliferation and elongation in the root. Genes & Development 18: 700-714.

Mouchel, C., Osmont, K., Hardtke, C. (2006). *BRX* mediates feedback between brassinosteroid levels and auxin signalling in root growth. Nature 443:458-461.

Munson M., and Novick P. (2006). The exocyst defrocked, a framework of rods revealed. Nat. Struct. Mol. Biol. 13: 577-581.

Murthy, M., Garza, D., Scheller, R.H., and Schwarz, T.L. (2003). Mutations in the exocyst component Sec5 disrupt neuronal membrane traffic, but neurotransmitter release persists. Neuron 37: 433-447.

Mussig, C., Lisso, J., Coll-Garcia, D., Altmann, T. (2006). Molecular analysis of brassinosteroid action. Plant Biol. 8: 291-296.

Mussig, C., Shin, G., Altmann, T. (2003). Brassinosteroids promote root growth in Arabidopsis. Plant Physiology 133: 1261-1271.

Mussig, D. (2005). Brassinosteroid-Promoted Growth. Plant Biol. 7:110-117.

Nakamoto, D., Ikeura, A., Asami, T., Yamamoto, K. (2006). Inhibition of brassinosteroid biosynthesis by either a dwarf4 mutation or a brassinosteroid biosynthesis inhibitor rescues defects in tropic responses of hyposotyls in the Arabidopsis mutant *nonphototropic hyposotyl 4.* Plant Physiology141: 456-464.

Nakazawa M, Matsui M (2003) Selection of hygromycin-resistant Arabidopsis seedlings. Biotechniques 34: 28-30.

Nemhauser, J., Mochler, T., Chory, J. (2004). Interdependency of brassinosteroid and auxin signaling in Arabidopsis. PloS Biology.2: (9) 1460-1471.

Noguchi, T., Fujioka, S., Choe, S., Takatsuto, S., Yoshida, S., Yuan, H., Feldmann, K., Tax, F. (1999). Brassinosteroid-intensive dwarf mutants of Arabidopsis accumulate brassinosteroids. Plant Physiology121: 743-752.

Novick P, Guo W (2002) Ras family therapy: Rab, Rho and Ral talk to the exocyst. Trends Cell Biol 12: 247-249.

Otegui, M.S., and Staehelin, L.A. (2004). Electron tomographic analysis of post-meiotic cytokinesis during pollen development in Arabidopsis thaliana. Planta 218: 501-515.

Oztan, A., Silvis, M., Weisz, O.A., Bradbury, N.A., Hsu, S.C., Goldenring, J.R., Yeaman, C., and Apodaca, G. (2007). Exocyst requirement for endocytic traffic directed toward the apical and basolateral poles of polarized MDCK cells. Mol. Biol. Cell 18: 3978-3992.

Palanivelu R, Preuss D (2000) Pollen tube targeting and axon guidance: parallels in tip growth mechanisms. Trends Cell Biol 10: 517-524.

Park SK, Howden R, Twell D (1998) The Arabidopsis thaliana gametophytic mutation gemini pollen1 disrupts microspore polarity, division asymmetry and pollen cell fate. Development 125: 3789-3799.

Park SK, Twell D (2001) Novel patterns of ectopic cell plate growth and lipid body distribution in the Arabidopsis gemini pollen1 mutant. Plant Physiol 126: 899-909.

Pfeffer SR (1999) Transport-vesicle targeting: tethers before SNAREs. Nat Cell Biol 1: E17-22.

Pommereit, D., and Wouters, F.S. (2007). An NGF-induced Exo70-TC10 complex locally antagonises Cdc42-mediated activation of N-WASP to modulate neurite outgrowth. J. Cell Sci. 120: 2694-2705.

Preuss, D., Rhee, S.Y., and Davis, R.W. (1994). Tetrad analysis possible in Arabidopsis with mutation of the QUARTET (QRT) genes. Science 264: 1458-1460.

Procissi A, de Laissardiere S, Ferault M, Vezon D, Pelletier G, Bonhomme S (2001) Five gametophytic mutations affecting pollen development and pollen tube growth in Arabidopsis thaliana. Genetics 158: 1773-1783.

Refregier, G., Pelletier, S., Jailland, D., Hofte, H. (2004). Interaction between wall deposition and cell elongation in dark-grown hypocotyl cells in Arabidopsis. Plant Physiology 135: 959-968.

Riefler GM, Balasingam G, Lucas KG, Wang S, Hsu SC, Firestein BL (2003) Exocyst complex subunit sec8 binds to postsynaptic density protein-95 (PSD-95): a novel interaction regulated by cypin (cytosolic PSD-95 interactor). Biochem J 373: 49-55.

Rosso, M.G., Li, Y., Strizhov, N., Reiss, B., Dekker, K., and Weisshaar, B. (2003). An Arabidopsis thaliana T-DNA mutagenized population (GABI-Kat) for flanking sequence tag-based reverse genetics. Plant Mol. Biol. 53: 247-259.

Roth, D., Guo, W., and Novick, P. (1998). Dominant-negative alleles of SEC10 reveal distinct domains involved in secretion and morphogenesis in yeast. Mol. Biol. Cell 7: 725-739.

Ruzicka, K., Ljung, K., Vanneste, S., Podhorska, R., Beeckman, T., Friml. J., Benkova, E. (2007). Ethylene regulates root growth through effects on auxin biosynthesis and transport-dependent auxin distribution. Plant Cell 19: 2197-2212.

Salvaldi-Goldstein, S., Peto, D., Chory, J. (2007). The epidermis both drives and restricts plant shoot growth. Nature Vol. 446, 8 March 2007, pp. 199-202.

Sans N, Prybylowski K, Petralia RS, Chang K, Wang YX, Racca C, Vicini S, Wenthold RJ (2003) NMDA receptor trafficking through an interaction between PDZ proteins and the exocyst complex. Nat Cell Biol 5: 520-530.

Schägger, H., and von Jagow, G. (1991). Blue native electrophoresis for isolation of membrane protein complexes in enzymatically active form. Anal. Biochem. 199: 223-31.

Scheible, W., Eshed, R., Richmond, T., Delmer, D., Somerville, C. (2001). Modifications of cellulose synthase confer resistance to isoxaben and thiazolidinone herbicides in Arabidopsis 1xr1 mutants. PNAS 98: (18) 10079-10084.

Schekman R, Novick P (2004) 23 genes, 23 years later. Cell S116: S13-15.

Seguí-Simarro, J.M., Austin J.R 2nd, White, E.A., and Staehelin, L.A. (2004). Electron tomographic analysis of somatic cell plate formation in meristematic cells of Arabidopsis preserved by high-pressure freezing. Plant Cell 16: 836-856.

Segui-Simarro JM, Austin JR, 2nd, White EA, Staehelin LA (2004) Electron tomographic analysis of somatic cell plate formation in meristematic cells of Arabidopsis preserved by high-pressure freezing. Plant Cell 16: 836-856.

Sivaram, M.V., Furgason, M.L., Brewer, D.N., and Munson, M. (2006). The structure of the exocyst subunit Sec6p defines a conserved architecture with diverse roles. Nat. Struct. Mol. Biol. 13: 555-556.

Steinebrunner I, Wu J, Sun Y, Corbett A, Roux SJ (2003) Disruption of apyrases inhibits pollen germination in Arabidopsis. Plant Physiol 131: 1638-1647.

Sugihara K, Asano S, Tanaka K, Iwamatsu A, Okawa K, Ohta Y (2002) The exocyst complex binds the small GTPase RalA to mediate filopodia formation. Nat Cell Biol 4: 73-78.

Symons, G., Reid, J. (2004). Brassinosteroids do not undergo long-distance transport in Pea. implications for the regulation of endogenous brassinosteroids levels. Plant Physiology 135: 2196-2206.

Symons, G., Ross, J., Jager, C., and Reid, J. (2008). Brassinosteriod transport. Journal of Experimental Botany 59(1):17-24.

Synek, L., Schlager, N., Eliáš, M., Quentin, M., Hauser, M.T., and Žárský, V. (2006). AtEXO70A1, a member of a family of putative exocyst subunits specifically expanded in land plants, is important for polar growth and plant development. Plant Journal 48: 54 - 72.

Szekeres, M., Nemeth, K., Koncz-Kalman, A., Mathur, J., Kauschmann, A., Altmann, T., Redei, G., Nagy, N., Schell, J., Koncz, C. (1996). Brassinosteroids rescue the deficiency of CYP90, a cytochrome P450, controlling cell elongation and de-etiolation in Arabidopsis. Cell 85: 171-182.

Tang W, Ezcurra I, Muschietti J, McCormick S (2002) A cysteine-rich extracellular protein, LAT52, interacts with the extracellular domain of the pollen receptor kinase LePRK2. Plant Cell 14: 2277-2287.

TerBush DR, Maurice T, Roth D, Novick P (1996) The Exocyst is a multiprotein complex required for exocytosis in Saccharomyces cerevisiae. EMBO J. 15: 6483-6494.

TerBush, D.R., and Novick, P. (1995). Sec6, Sec8, and Sec15 are components of a multisubunit complex which localizes to small bud tips in Saccharomyces cerevisiae. J Cell Biol 130: 299-312.

TerBush, D.R., Maurice, T., Roth, D., and Novick, P. (1996). The Exocyst is a multiprotein complex required for exocytosis in Saccharomyces cerevisiae. EMBO J 15: 6483-6494.

Terbush, D.R., Guo, W., Dunkelbarger, S., and Novick P. (2001). Purification and characterization of yeast exocyst complex.Methods Enzymol. 329:100-10.

Twell D, Yamaguchi J, Wing RA, Ushiba J, McCormick S (1991) Promoter analysis of genes that are coordinately expressed during pollen development reveals pollen-specific enhancer sequences and shared regulatory elements. Genes Dev 5: 496-507.

Vega, I.E., and Hsu, S.C. (2001). The exocyst complex associates with microtubules to mediate vesicle targeting and neurite outgrowth. J Neurosci 21: 3839-3848.

Wang, H., Tang, X., Liu, J., Trautmann, S., Balasundaram, D., McCollum, D., and Balasubramanian, M.K. (2002). The multiprotein exocyst complex is essential for cell separation in Schizosaccharomyces pombe. Mol. Biol. Cell 13: 515-529.

Wang, Z., Nakano, T., Gendron, J., He, J., Chen, M., Vafeados, D., Yang, Y., Fujioka, S., Yoshida, S., Asami, T., Chory, J. (2002). Nuclear-localized BZR1 mediates brassinosteroid-induced growth and feedback suppression of brassinosteroid biosynthesis. Developmental Cell.2: 505-513.

Wen, T.J., Hochholdinger, F., Sauer, M., Bruce, W., and Schnable, P.S. (2005). The roothairless1 gene of maize encodes a homolog of sec3, which is involved in polar exocytosis. Plant Physiol 138: 1637-1643.

Wengier D, Valsecchi I, Cabanas ML, Tang WH, McCormick S, Muschietti J (2003) The receptor kinases LePRK1 and LePRK2 associate in pollen and when expressed in yeast, but dissociate in the presence of style extract. Proc Natl Acad Sci U S A 100: 6860-6865.

Werhahn, W., and Braun, H.P. (2002). Biochemical dissection of the mitochondrial proteome from Arabidopsis thaliana by three-dimensional gel electrophoresis. Electrophoresis 23: 640-646.

Werner, T., Motyka, V., Laucou, V., Smets, R., Van Onckelen, H., Schmulling, T. (2003). Cytokinin-deficient transgenic Arabidopsis plants show multiple developmental alterations indicating opposite functions of cytokinins in the regulation of shoot and root meristem activity. (2003). Plant Cell 15: 2532-2550.

Whyte J.R., and Munro S. (2001). The Sec34/35 Golgi transport complex is related to the exocyst, defining a family of complexes involved in multiple steps of membrane traffic. Dev. Cell 1: 527-37.

Whyte JR, Munro S (2002) Vesicle tethering complexes in membrane traffic. J Cell Sci 115: 2627-2637.

Wisniewska, J., Xu, J., Seifertova, D., Brewer, P., Ruzicka, K., Blilou, I., Rouquie, D., Benkova, E., Scheres, B., and Friml, J. (2006) Polar PIN localization directs auxin flow in plants. Science. 312:883.

Wu, S., Mehta, S.Q., Pichaud, F., Bellen, H.J., and Quiocho, F.A. (2005). Sec15 interacts with Rab11 via a novel domain and affects Rab11 localization in vivo. Nat. Struct. Mol. Biol. 12: 879-885.

Xu, W., Campbell, P., Vargheese, A., and Braam, J. (1996). The Arabidopsis XET-related gene family: environmental and hormonal regulation of expression. Plant J. 9(6):879-889.

Yamada K, Lim J, Dale JM, Chen H, Shinn P, Palm CJ, Southwick AM, Wu HC, Kim C, Nguyen M, Pham P, Cheuk R, Karlin-Newmann G, Liu SX, Lam B, Sakano H, Wu T, Yu G, Miranda M, Quach HL, Tripp M, Chang CH, Lee JM, Toriumi M, Chan MM, Tang CC, Onodera CS, Deng JM, Akiyama K, Ansari Y, Arakawa T, Banh J, Banno F, Bowser L, Brooks S, Carninci P, Chao Q, Choy N, Enju A, Goldsmith AD, Gurjal M, Hansen NF, Hayashizaki Y, Johnson-Hopson C, Hsuan VW, Iida K, Karnes M, Khan S, Koesema E, Ishida J, Jiang PX, Jones T, Kawai J, Kamiya A, Meyers C, Nakajima M, Narusaka M, Seki M, Sakurai T, Satou M, Tamse R, Vaysberg M, Wallender EK, Wong C, Yamamura Y, Yuan S, Shinozaki K, Davis RW, Theologis A, Ecker JR (2003) Empirical analysis of transcriptional activity in the Arabidopsis genome. Science 302: 842-846.

Yamamoto Y, Nishimura M, Hara-Nishimura I, Noguchi T (2003) Behavior of vacuoles during microspore and pollen development in Arabidopsis thaliana. Plant Cell Physiol 44: 1192-1201.

Yang , Z. (2002) Small GTPases: versatile signaling switches in plants. Plant Cell 14 Suppl: S375-388.

Yeaman C, Grindstaff KK, Nelson WJ (2004) Mechanism of recruiting Sec6/8 (exocyst) complex to the apical junctional complex during polarization of epithelial cells. J Cell Sci 117: 559-570.

Yeaman C., Grindstaff, K.K., Wright, J.R., and Nelson, W.J. (2001). Sec6/8 complexes on trans-Golgi network and plasma membrane regulate late stages of exocytosis in mammalian cells. J. Cell Biol. 155: 593-604.

Zhou, X., Liu, Q., Xie, F., Wen, C. (2007). RTE1 is a golgi-associated and ETR1-dependent negative regulator of ethylene responses. Plant Physiology 145: 75-86.

Zuo, X., Zhang, J., Zhang, Y., Hsu, S.C., Zhou, D., and Guo, W. (2006). Exo70 interacts with the Arp2/3 complex and regulates cell migration. Nat Cell Biol 8: 1383-1388.